THREE DIMENSIONAL MODELING OF THE KNEE JOINT: PREDICTION OF LIGAMENT RELATED GAIT ABNORMALITIES

by

N. Ekin Akalan

B.Sc. in Division of Physical Therapy and Rehabilitation, Istanbul Medical Faculty, 1995
M.S. in Division of the Developmental Child Neurology, Istanbul Medical Faculty, 1999

Submitted to the Institute of Biomedical Engineering
in partial fulfillment of the requirements
for the degree of
Doctor of
Philosphy
in
Biomedical Engineering
Boğaziçi University

31.10. 2007

THREE DIMENSIONAL MODELING OF THE KNEE JOINT: PREDICTION OF LIGAMENT RELATED GAIT ABNORMALITIES

APPROVED BY:

Prof. Dr. Mehmed Özkan .....
(Thesis Advisor)

Prof. Dr. Yener Temelli ……

Assoc. Prof. Dr. Halil Özcan Gülçür ……

Prof. Dr. Ahmet Ademoğlu ……

Assistant. Prof. Dr. Can A. Yücesoy ……

DATE OF APPROVAL: 31.10.2007

ACKNOWLEDGEMENTS

I would like to gratefully thank to my thesis advisor Professor Dr. Mehmed Özkan for his patiently supervision and insightful manner throughout this work. He always motivates me whenever I have hard times with research. Therefore, it was impossible to progress in this project without his encouragements and great efforts.

I would like to express my sincere gratitude and special thanks to Professor Yener Temelli for his continuous guidance on my clinical and scientific life. I was not be able to improve my knowledge about gait analysis and biomechanical knowledge without his grateful help.

I would like to special thanks to Professor Meral Özmen to encourage me to progress in our work and to motivate me for permitting to spend my official time in Boğaziçi University to complete my doctoral education.

I am deeply grateful to Prof. Dr. Yorgo Istafanopulos for encouraging me to begin the doctoral education in Biomedical Institute of Boğaziçi University.

I am indebt to my colleagues: Shavkat, Sanem, Sibel, Saadet, Feride, Gönül, Fadile in Motion Analysis Laboratory and Division of Physical Therapy in Istanbul Medical Faculty. They are my companions who were always ready to help.

I would like to address special thanks to my family for their continuous support, encouragement. They give me moral help and patience. I also thanks my fiancé for tolerating me in sleepless days and for insightful approach.

I would like to thank Assoc. Prof. Dr. Halil Özcan Gülçür, Professor Ahmet Usta for their contribution to participate in my thesis presentation as Committee member.

This project is consequence of efforts and patience of all those great people. I would like to devote this project to all of them.

This project is supported in part by TUBITAK (The Scientific and Technological Research Council of Turkey) grant number 104S508. The project has been coordinated at the Institute of Biomedical Engineering in Boğaziçi University.

ABSTRACT

THREE DIMENSIONAL MODELING OF THE KNEE JOINT: PREDICTION OF LIGAMENT RELATED GAIT ABNORMALITIES

The purpose of this study is to investigate the affect of anterior bundle of ACL (aACL), anterior portion of posterior cruciate ligament PCL (aPCL), anterior and deep portions of MCL (aMCL, dMCL) and the tibiofemoral articular contacts on to passive knee motion.

A well accepted reference model for a normal tibio-femoral joint was reconstructed from the literature in which attachments of the bundles of the ligaments and the articular surfaces in medial and the lateral components were carefully defined.

Another three dimensional dynamic tibiofemoral model which includes the isometric fascicles, aACL, aPCL, aMCL, dMCL, and the medial-lateral articular surfaces were represented as the constraints to predict the trajectory of the tibia on the femur during flexion.

The tibiofemoral model was also integrated in to the dynamic patella-tibio-femoral model. The behavior of the knee model was also tested by simulating dynamic and static clinical tests such as knee extension exercise and drawing test. The patello- tibio-femoral model was integrated into full-body model to simulate people walk with normal and ACL deficient patterns.

The predictions were closely agreed with the literatures and correspond well to measurements of the model which represents natural patello-tibio-femoral joint. The aACL, aPCL, aMCL, dMCL bundles and the medial-lateral articular surfaces might play a primary role to give the nature of distal femoral sphere like shape. The clinical significance of the work is that anything which changes the lengths and locations of the related ligaments may demolish natural constraints and force the articular structures in to unnatural shape which may make the knee to change contact behavior on the articular surface and may cause pain. The surgical treatments must be accurate enough to provide both ligament bundle geometries and articular geometry to achieve a problem free knee kinematics after the surgery.

***Keywords*:** Knee, Kinematics, Geometry, Three-dimensional model, Ligament surgery.

ÖZET

DİZ EKLEMNİNİN ÜÇ BOYUTLU MODELLENMESİ: BAĞ MENŞEYLİ YÜRÜME BOZUKLUKLARININ TAHMİNİ

Bu çalışmanın amacı ön çapraz bağın ön parçasının (aÖÇB), arka çapraz bağın ön parçasının (aAÇB), iç yan bağın ön ve derin kısımlarının (aİYB, dİYB) ve kaval keimiği ile uyluk kemiği arasındaki temasın pasif diz bükülmesine olan etkisini araştrmaktır.

Çalışmamızda normal bir uyluk-kaval kemik ekleminin üç boyutlu dinamik hereketlerini tahmin etmek için bağ parçalırının kemiğe tutunduğu noktaları, uyluk-kaval kemik eklemin iç ve dış tarafındaki yüzeylerini içeren 3 boyutlu anatomik dinamik bir model kullanıldı.

Hareketleri, boyu diz bükülmesi sırasında değişmeyen bağ kısımları (aÖÇB, aAÇB, aİYB, dİYB) ve iç-dış taraf eklem yüzeyleri ile sınırlanmış bir başka üç boyutlu dinamik uyluk-kaval kemik modeli kaval kemiğinin uyluk kemiği üzerinde oluşturduğu izleri belirlemek için kullnıldı. Kaval kemiğinin diz eklmeinin bükülmesi sırasındaki dönme hareketleri her iki modelle ve literatürle karşılaştırıldı.

Çalışmamızda oluşturduğumuz uyluk–kaval eklemi, diz kapağı-kaval-uyluk eklem modeline eklenmiş ve yeni oluşturulan modelin doğruluğu, klinikte ÖÇB yırtığı tespiti için kullanılan çekmece testi ve diz düzeltme egzersizi simüle edilerek test edildi. Bu model tüm vücut modeline yerleştirilerek normal ve ÖÇB yaralanması olan hastaların yürümesini simüle etmek için kullanıldı.

Alınan sonuçlar literatüre ve doğal diz kapağı- uyluk–kaval kemik eklem modeli ile yakın bir uyumluluk gösterdi.

Çalışmamızda kullanılan diz modeli, ÖÇB yaralanmalı hastalara uygulanan klinik testlerde ve bu hastaların yürüyüşünü simüle edebilmiştir. Bu çalışmada yukarıda bahsi geçen bağ parçalının yerini veya uzunluğunu değiştirecek herhengi bir girişimin dizin doğal sınırlarını oluşturan yapıları bozabileceği ve ağrıya neden olabileceğidir. Cerrahi tedavi, bağ kısımlarının geometrisinin ve eklem geometrisinin doğruluğunu sağlanması gerekmektedir.

Anahtar Kelimeler: Diz, Kinematik, Geometri, 3 boyutlu model, Bağ cerrahisi.

TABLE OF CONTENTS

ACKNOWLEDGEMENTS iii

ABSTRACT iv

THREE DIMENSIONAL MODELING OF THE KNEE JOINT: PREDICTION OF LIGAMENT RELATED GAIT ABNORMALITIES iv

ÖZET v

TABLE OF CONTENTS vi

LIST OF TABLES viii

LIST OF FIGURES ix

LIST OF ABBREVIATIONS xv

1. INTRODUCTION 1

2. THEORETICAL BACKGROUND 5

2.1. An Overview of the Knee 5

2.1.1. Bones and Joints of the Knee 6

2.1.2. Ligaments and Tendons of the Knee 7

2.1.3 Articular Cartilage 17

2.1.4 Meniscus 18

2.1.5 Muscles 19

2.1.6 Tendons 20

2.1.7 Nerves 21

2.1.8 Blood Vessels 21

2.1.9 The Movements of the Knee Joint 21

2.1.10 Arthrokinematics at the Tibiofemoral Joint 25

2.1.11 Patello-Femoral Joint 28

2.2 Conventional Modeling of the Knee 30

2.2.1 Experimental Knee Models 31

2.2.2 Mathematical Models of the Knee 32
2.3 Theory of Motion Analysis 43
2.3.1. Kinematics 44
2.3.2 Kinetics 46
2.3.3 Gait Analysis 48
2.3.4 Gait Abnormalities 52
2.3.5 The Simulation Tool 57
3. MATERIALS AND METHODS 60
3.1 Constraint Based Model 60
3.2 Validation of Tibiofemoral Model 70
3.3 Patello-Tibio-Femoral Model 71
3.3.1. Modeling Femoral Geometric Shape 71
3.3.2 Modeling Patello-Tibio-Femoral Joint 73
3.4 Implementing the Knee Model into the Full Body Model 79
4. RESULTS 83
4.1 Constraint Based Tibiofemoral Joint Model 83
4.2 Patello-Tibio-Femoral Joint Model 85
4.3 Simulation of Drawer Test 90
4.4 Full Body Model 92
5. DISCUSSION AND CONCLUSION 97
6. REFERENCES 106

LIST OF TABLES

Table 3.1 Medial and lateral contact points on tibial plateau for flexion range of 0 to 110°. Adapted from [3]……... 65

LIST OF FIGURES

Figure 2.1 The bones and joints of the knee. Adapted from [16]. 6

Figure 2.2 The knee joint is a synovial joint. Adapted from [16]..... 6

Figure 2.3 The ligaments of the knee. Adapted from [16] 8

Figure 2.4 Medial view of the right knee shows many muscles and connective tissues. The tendons of the sartorius and gracilis are ct to better expose the anterior and posterior parts of the MCL. Adapted from [17]..... 9

Figure 2.5 Lateral view of the right knee shows muscles and connective tissues. The ilitibial band, lateral head of the gastrocnemius, and biceps femoris are cut to better expose the LCL and leteral meniscus. Adapted from [17]. 10

Figure 2.6 Posterior view of the deep structures of the right knee after all muscles and posterior capsule are removed. Observe the menisci, collateral ligaments, and cruciate ligaments. Adapted from [17]. 11

Figure 2.7 Medial view of the knee shows the elongation of the medial collateral ligament and the posterior capsule and oblique popliteal ligament during active femoral-on-tibial extension. In the knee flexion these ligaments are relatively slackened (A). The structures are pulled taut as the knee actively extends by contraction of quadriceps (B). Adapted from [17]. 12

Figure 2.8 The anterior and posterior cruciate ligaments. A, Lateral view. B, Anterior view. Adapted from [17]..... 14

Figure 2.9 The interaction between muscle contractions and tension changes in the cruciate ligaments is shown. A) Contraction of quadriceps muscle extends the knee and slides the tibia anterior relatively to the femur. Knee extension also elongates most of the ACL, Poterior capsule, hamstring muscles, and collateral ligaments. B) The anterior drawer test evaluates the integrity of the ACL. C, Contraction of hamstring muscles flexes the knee and slides the tibia posteriorly. Knee flexion elongates the quadriceps muscle and most of the fibers in PCL. D, the posterior drawer test checks the integrity of the PCL. Adapted from [17]. 16

Figure 2.10. Articular Cartilage of the knee [15]. 18

Figure 2.11 An overview of meniscus. Adapted from [15]. 19

Figure 2.12 The view of the quadriceps and hamstring muscles. Adapted from [16]..... 20

Figure 2.13 The illustration of the knee flexion and extension in sugittal plane. Adapted from [17]. 22

Figure 2.14 The flexing knee generates a migrating medial-lateral axis of rotation. This migration is described as “the evolute”. Adapted from [17]. 23

Figure 2.15 The illustration of the knee internal rotation and external rotation transvers plane. 24

Figure 2.16 The illustration of Valgus (Abduction) and Varus (Adduction) rotation of the knee joint. 24

Figure 2.17 The active arthrokinematics of knee extension (Tibia-on-Femur perspective). Adapted from [17]. 25

Figure 2.18 “Screw-home” locking mechanism of the knee. A, during terminal tibia-on-femoral extension, three contribute to the locking mechanism of the knee. Each factor contributes bias to external rotation of the tibia. Adapted from [17] 27

Figure 2.19 The kinematics at the patello-femoral joint during active tibial-onfemoral extension. The circle depict in A-C indicates the point of maximal contact between the patella and femur. As the knee is extended, the contact point on the patella migrates from its superior pole to its inferior pole. Adapted from [17]. 28

Figure 2.20 The path (A) and contact areas of the patella (B) on intercondylar groove of the femur. The values 135, 90, 60, 20 degrees indicate flexed positions of the knee. Adapted from [17]. 29

Figure 2.21 Patellar motion in terms of patellar body fixed axes 30

Figure 2.22 Joint rotation and translations. Adapted from [10] 34

Figure 2.23 Link segment model representation 44

Figure 2.24 Link-segment modelling and free body diagram. Adapted from [54]. 48

Figure 2.25 Time dimensions of the gait cycle. Adapted from [56]. 49

Figure 2.26 Illustration of setting reflective markers (a) and gait analysis (b). 50

Figure 2.27 Normal kinematics of the pelvis, hip, knee, ankle during walking. Adapted from [58]. 51

Figure 2.28 Kinetics of the joints during normal walking. Adapted from [58]. 52

Figure 2.29 (a) Combined ground reaction force (GRF) vectors from walking. (b) Same

GRF from force palteforms under rear and forefoot. The line segments indicate direction and relative magnitudes of GRFs. The lower end of the segments correspond to the location of the COP in the antero-posterior direction. Adapted from [59]. 53

Figure 2.30 (a and b), The gait cycle divided into four phases (HA, WA, TE and SW). The extrema of intersegmental anterior–posterior force (Fant, Fpost) were in the same direction as the corresponding displacements (APant and APte) during stance phase. The extrema of intersegmental internal–external moment (Tqext and Tqint) were in the same direction as the corresponding rotations (IEext and IEint) during stance phase. The arrow_ indicates the direction of significant changes for the ACL deficient knee. Adapted from [60]..... 54

Figure 2.31 Mean values of the ground reaction forces (——— normal subjects, ····· ACL-deficient subjects, – – – ACL-reconstructed subjects). The amplitude of the force is indicated in relation to the phases of the gait cycle beginning with heel strike. Values are normalized to subject's weight. Adapted from [61]... 55

Figure 2.32 The illustration of anterior drawer test. Adapted from [17]. 57

Figure 2.33 Illustration of ADAMS (a) and LIFEMOD (b) software Adapted from [62]. 59

Figure 3.1 Back-oblique view of three-dimensional model of the knee joint. 61

Figure 3.2 Frontal-oblique view of three-dimensional model of the knee joint. 62

Figure 3.3 Relative ligament length during knee flexion. Closely agreed with literature. The abbreviations in parenthesis state the ligaments in this study correspond to Crowninshield et al.`s representations for each ligament. Adapted from [13]..... 63

Figure 3.4 Assumption of inextensible rigid ligaments. 64

Figure 3.5 Contact points during passive knee flexion Adapted from [3]. 64

Figure 3.6 Seven lateral trajectories of the contact points after tracing the lateral contacts during knee flexion and the constraints of the model in the present study..... 66

Figure 3.7 Three medial trajectories of the contact points after tracing the lateral contacts during knee flexion and the constraints of the model in the present study..... 67

Figure 3.8 The spheres to represent distal femoral geometry in the present study. 70

Figure 3.9 Sulcus angle in 33 cartilaginous and 29 osseous specimens, mean± SD. Error bars are shown in only one direction for clarity: those for cartilage go up, those for bone go down. Adapted from [69]..... 71

Figure 3.10 Diagram of the axial view of the distal femur. A and B = the most anterior projections of the lateral and medial femoral condyles; C and D = the most posterior projections of the lateral and medial femoral condyles; E and F = the most prominent points of the lateral and medial epicondyles; G = the deepest part of the trochlar groove; H = the center of the intercondylar notch; AB = trochlear line; EF = trans epicondylar line; CD = posterior condylar line; GH = anterior-posterior line; AGB = [sigma] = sulcus angle; [epsilon] = AP line-epicondylar line angle; [kappa] = AP line-posterior condylar line angle; [THETA] = epicondylar line-posterior condylar line angle; [tau] = trochlear line-epicondylar line angle; H3 = height of the lateral condyle; H4 = height of the medial condyle; al = anterior lateral cut; pl = posterior lateral cut; am = anterior medial cut; and pm = posterior medial cut. Adapted from [70]. 72

Figure 3.11 Representing distal femoral geometry in the present study. 73

Figure 3.12 The anatomy of patella femur and the tibia. Adapted from.[17] 74

Figure 3.13 Oblique and sagittal view of the patella femoral model in the present study. 75

Figure 3.14 The representation of tendon attachments for patellar tendon and quadriceps. Adapted from [71]. 76

Figure 3.15 Forcing functions applied to the quardriceps tendon to simulate knee extension exercise. Adapted from [11]. 77

Figure 3.16 The sugittal and oblique view of patello-tibio-femoral joint in the present study. 78

Figure 3.17 The simulation of anterior Drawer test in the present study. 79

Figure 3.18 The full body model in LIFEMOD software in the present study. 80

Figure 3.19 Simulation of normal walking in the present study. 81

Figure 4.1 Tibial rotations of the present study (dashed lines) and rotations from Wilson et al, 2000 (Solid lines and gray ranges). 84

Figure 4.2 Medial and lateral contact forces of the tibiofemoral joint Adapted from [10]. 84

Figure 4.3 Medial lateral contact force in the present study. 85

Figure 4.4 The dashed lines indicate constraint based simulation results and the solid lines demonstrate simulation of spherical model. Internal/external rotation (i/e) and abduction / adduction (a/a). 86

Figure 4.5 The dashed lines indicate constraint based simulation results and the solid

lines demonstrate simulation of spherical model . Antero/posterior (p/a), proximo/distal (p/d) and medio/lateral (m/l) translations. Adapted from [72]. 86

Figure 4.6 Comparison of the medial (black lines) and the lateral (red lines) contact forces for constraint based (dashed lines) and Spherical Model (solid lines) with tibio-femoral flexion. 87

Figure 4.7 Illustration of the patellar rotations in the present study. 87

Figure 4.8 The comparison of patellar rotations during knee extension with the literature (dashed black line for plantar flexion) [11]. 88

Figure 4.9 Patellar lateral (solid red line), proximal (dashed pink line), posterior (dashed blue line) translations during knee extension in the present study compared with the literature (solid black line for lateral tilt) [75]. 89

Figure 4.10 Illustration of contacts force on medio-lateral compartments of the tibia during knee extension..... 89

Figure 4.11 Contact forces on medial (Solid blue line) and lateral (Dashed red line) compartments from the literature[11]. 90

Figure 4.12 Anterior displacement of the tibia during drawer test simulation in the present study for intact knee (red spheres) and the literatures (vertical and solid lines) [81]. 91

Figure 4.13 Anterior displacement of the tibia during simulation of drawer test in the present study (blue sphere), for ACL deficient knee and the literatures (vertical and solid lines) [81]. 91

Figure 4.14 The anterior translation of the tibia during anterior drawer test with internal-external rotational force for intact and no-ACL model in the present study. . 92

Figure 4.15 GRF during the muscle driven forward dynamics of normal walking simulation in present study. 92

Figure 4.16 The GRF illustration of muscle driven forward dynamic simulation of normal walking with the patello-tibio-femoral joint in the present study. 93

Figure 4.17 The comparison of GRF for the intact knee model (blue solid line) and model with no ACL (dashed red line) for the right side in the present study..... 94

Figure 4.18 The GRF for the model with no aACL in the present study 94

Figure 4.19 The comparison of the knee model with aACL (solid line) and without aACL (dashed line) in the present study. 95

Figure 4.20 Tibial translation relative to the femur during swing phase of gait for the intact knee model in the present study. 96

Figure 4.21 Tibial translation relative to the femur (dashed line) and tibial internal/external rotation during swing phase of gait for the model with no aACL in the present study 96

LIST OF ABBREVIATIONS

ACL	Anterior Cruciate Ligament
aACL	Anterior portion of Anterior Cruciate Ligament
pACL	Posterior portion of Anterior Cruciate Ligament
PCL	Posterior Cruciate Ligament
aPCL,	Anterior portion of Posterior Cruciate Ligament
pPCL,	Posterior portion of Posterior Cruciate Ligament
LCL	Lateral Colleteral Ligament
MCL	Medial Colleteral Ligament
aMCL,	Anterior portion of Medial Colleteral Ligament
dMCL,	Deep portion of Medial Colleteral Ligament
oMCL	Oblique portion of Medial Colleteral Ligament
COP	Center of pressure
GRF	Ground reaction force
AP	Anterior–posterior
IE	Internal–external

1. INTRODUCTION

There are numerous surgical procedures on treating the injury and disease of the knee joint [1]. A major goal of these procedures is the recreation of a physiologically normal joint loading environment. Many investigators have studied in vivo knee kinematics after total knee arthroplasty and have reported inconsistent in vivo motion data [1, 2]. Previous investigators have suggested that the altered joint kinematics caused by ligament injury may alter the contact patterns within the joint and hence predispose the knee to the long-term development of osteoarthritis [2].

An accurate knowledge of the in vivo articular contact mechanics of the knee is important for understanding of the causes of joint degeneration. For example, previous investigators have suggested that the altered joint kinematics caused by ligament injury may alter the contact patterns within the joint and hence predispose the knee to the long-term development of osteoarthritis [2].

The human knee has a complex anatomical structure and undergoes complicated three-dimensional movements. It has proved challenging to measure and then to depict knee joint motion [3]. Because of the complexity of the joint, not only a faithful description of normal function, but also identification and treatment of dysfunction presents many problems [4, 5].

It is well known that mathematical models play an important role for the understanding of complicated biological structures. The mechanical functions of the structures at the tibiofemoral joint include guiding the relative motion of the tibia and femur and transmitting load between these two bones. It was proposed that; the best way of calculating the displacement of a three-dimensional model of knee mobility can be achieved by using the constraint-based solution [1, 7]. Feikes *et al.*, 2003 [6] concluded that constraint based formulation may be a very useful tool for the design of new joint replacements by allowing examination of different shape surfaces and various ligament arrangements. It helps to achieve more physiological surface shapes in the knee model [2].

The alignments of the ligaments and the geometries and the mechanical properties of

the joint structures are changed in surgical procedures. For instance in ACL reconstruction or total knee arthroplasty, the insertion points of the ACL change by replacing the ACL with the graft, or the shapes, mechanical properties and the ACL locations relative to the ligament attachments are altered [7].

The structures to guide the passive knee motion and influence to change the geometry of the knee was studied by Wilson *et al.*, 1998 [7], Feikes *et al.*, 2003[6]. Wilson *et al.*, 1998 stated that the both internal rotation (Meyer, 1853) and posterior translation (Weber an Weber, 1836) movement of the femur on the tibia in flexion must be guided by anatomical structures of the tibiofemoral joint. However their hypothesis was not supported by sufficiently detailed ligament bundle models. The anterior cruciate ligament (ACL), posterior cruciate ligament (PCL), medial collateral ligament (MCL) and the articular contacts of the medial and lateral compartments alone may not give sufficient information to understand which forces shape the geometries and how geometric changes of the joint structures will affect the three dimensional movement of the knee. Therefore, which part of anatomical structures guide knee in passive flexion and how their geometric arrangement produces the unique path of passive knee motion is not well defined [7].

A three-dimensional model defined by Abdel-Rahman and Hefzy [10] is the only anatomical model available in the literature that predicts the three-dimensional dynamic response of the knee joint [11]. The bundles of the ligaments were also well defined in this model.

Abdel-Rahman and Hefzy, 1998 [10] revealed that the major fibre bundles resisting a posterior forcing action on the tibia are the anterior fibers of the PCL and the anterior and deep fiber of MCL in the knee flexion range of 20 to 90°. A number of studies described that some bundles of the ligaments remain isometric fascicle during passive knee flexion [10, 12, 13, 14]. According to Crowninshield *et al.* [13] anterior bundle of ACL, anterior portion of PCL, anterior and deep portions of MCL displayed only a little or no change in length during knee flexion. Therefore we can deduce that the above mentioned bundles have very strong potential to act as motion constraints between femur and the tibia. As a result, considering the effects of constraint modification, special care is needed during the reconstruction of these bundles in orthopedic surgeries.

However in constraint based formulation, isometric fibers are not the only actors. Articular surfaces work together with the ligaments to guide passive knee motion [7]. Therefore the contacts on articular surfaces must not contradict with the isometric nature of ligaments during the flexion for aACL, aPCL, aMCL, dMCL [13]. The isometric ligaments selected for passive knee motion are ACL, PCL and MCL in Wilson *et al.*1998 [7] However, Crownninshield *et al.* [13] illustrates that only the anterior portions (aACL, aPCL) of ACL and PCL remain isometric. MCL is comprised of three ligaments attached apart on the tibia. Only two of the three MCL ligaments (aMCL, dMCL) are isometric during the passive knee motion [13].

Abdel-Rahman and Hefzy defined an anatomical model of the knee that included aACL, aPCL, aMCL, dMCL along with other ligaments. Their model addresses the correct positioning of the ligament attachments and resulting contact forces. The anatomical components were placed carefully by referring to cadaver studies [10]. In both models, however, [7, 10] they had two contact points, one for each compartment (medial and lateral condyles) on the tibial plateau. This assumption, in need of cooping with the assumed spherical shape of femoral condyles, contradics with the evidence reported by Freeman and Pinskerova [3]. These authors showed several distinct contact points on the tibial plateau for passive knee motion on several cadaver experiments.

In this study we used aACL, aPCL, aMCL, dMCL as the isometric ligaments constraining the knee against tension, while the compression motion is constrained by the contact points on the articular surfaces. To benefit from the anatomical findings we Adapted the tibial contact points from Freeman and Pinskerova`s work [3]. As a result there are 3 contact points on the medial and 6 on the lateral compartments of the tibia for a passive knee flexion between 0-90°. Since we assume the forces on these contact points constrain the motion against compression, one of these points from each compartment is assumed to be in contact with the femur at any given time. In our model, as in the mentioned references, femur is held fixed while moving the tibia. As the knee is flexed the tibial contact points trace the surface of the femoral condyles.

We analyzed tibial rotation, translation and contact forces during passive knee flexion and compared the results to that of reconstructed reference model proposed by Abdel-Rahman

[10], and with the findings reported by Wilson [7]. We showed that the ability to produce a normal knee flexion is higly dependent on the coordination of ligament lengths, attachment points and shapes of the contact surfaces. As a result special care is needed during the reconstruction of the ligament bundles in orthopedic surgeries considering the effects of constraint modification.

The objective of this study is to construct a knee model considering the ligament bundles and contact surfaces. The model simulates passive knee motion. Different from the existing models in the literature we included multiple contact points, without assuming spherical shape for the femur condyles.In addition, behavior of the patella-tibio-femoral model was also tested by simulation of knee extension exercise and clinic tests which are used for diagnosing ACL deficiency. The patello-tibio-femoral model was integrated in to the dynamic full body musculoskeletal model to simulate the walking pattern of normal and ACL deficient patients.

In Chapter I; We summarized the purpose, methods and the findings of the present study in this chapter. The chapter includes also the clinical meanings, limitations, and the future works.

In Chapter II; Some basic explanations and the theories about the anatomical properties of the human knee joint were mentioned in the chapter. It includes the arthrokinemtacis and mathematical models of the knee joint. The clinical tests and specific changes in the gait analysis data for the patients with ACL deficiency were also explained in this chapter.

In Chapter III; The construction of the reference and proposed knee models and inclusion the created model in to the patello-femoral joint were detaily explained in this chapter. The usage of our knee model to simulate the gait characteristics for the patient with ACL deficiency was also mentioned.

In Chapter IV; The comparisons of the findings with the reference model and the literature were explained in this chapter. The vertical GRF, tibial rotation and translation results during the simulation of the walking patterns of the patient with ACL deficiency were also compared with the literature.

In Chapter V; The finding and their clinical and scientific meanings were discussed in this chapter. The conclusion and the clinical significance of the present study were stated and the limitations were criticized in it.

2. THEORETICAL BACKGROUND

2.1. An Overview of the Knee

The human knee has a complicated anatomical structure and complicated three-dimensional movements. It is well known that the mathematical models play an important role for understanding complicated biological structures [4].

To better understand how knee problems occur, it is important to analyze the anatomy of the knee joint and how the parts of the knee work together to maintain normal function in detail [15].

It is common to describe parts of the body using terms that define where the part is in relation to an imaginary line drawn through the middle of the body. For example, medial means closer to the midline. So the medial side of the knee is the side that is closest to the other knee. The lateral side of the knee is the side that is away from the other knee. Structures on the medial side usually have medial as part of their name, (medial meniscus). The term anterior refers to the front of the knee, while the term posterior refers to the back of the knee. So the anterior cruciate ligament is in front of the posterior cruciate ligament [2].

The knee is the largest joint in the body and sometimes has to bear up to four times the weight of the person's body. Even though the analogy to a hinge is often made [8, 9], the knee joint is much more than a simple hinge comprised of the following major structures: bones, muscles, ligaments, cartilages, and tendons..It has also a complex and elaborate network of nerves and vessels that runs throughout the knee. The motions that the knee is capable of consist of bending (flexion) and straightening (extension), with a limited degree of rotation and sliding [15].

2.1.1. Bones and Joints of the Knee

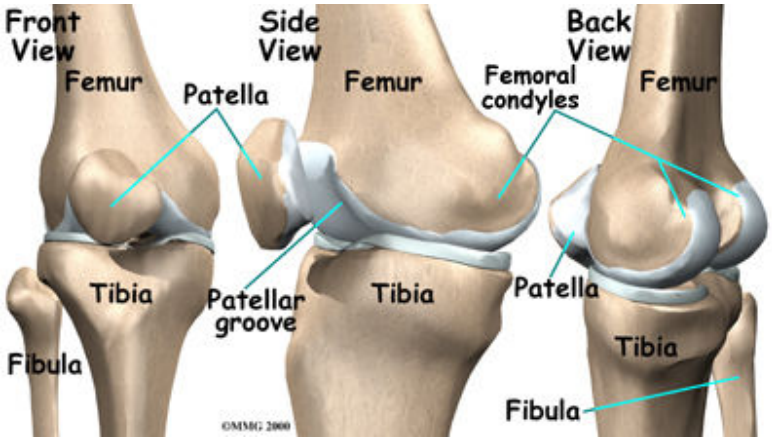

Figure 2.1 The bones and joints of the knee. Adapted from [16].

The knee joint is a synovial joint. Synovial joints are enclosed by a ligament capsule and contain a fluid, called synovium that lubricates the joint [16].

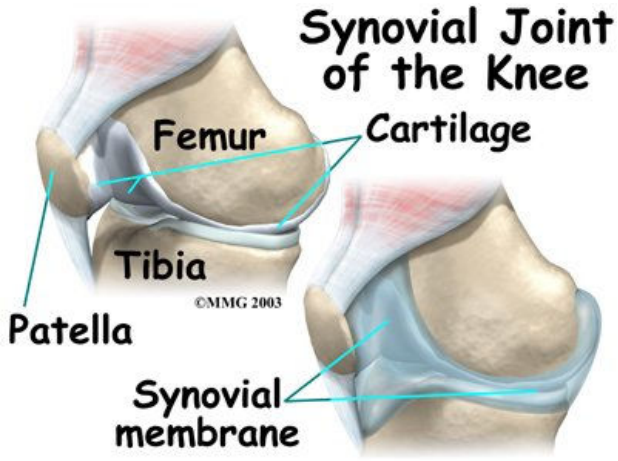

Figure 2.2 The knee joint is a synovial joint. Adapted from [16].

The end of the femur (Thigh bone) joins the top of the tibia (Shin bone) to create the knee joint. Two round knobs called femoral condyles are found on the end of the femur. These condyles rest on the top surface of the tibia. This surface is called the tibial plateau. The outside half (farthest away from the other knee) is called the lateral tibial plateau, and the inside half (closest to the other knee) is called the medial tibial plateau. The patella glides through a special groove formed by the two femoral condyles called the patello-femoral groove [16].

The four bones that meet at the knee joint are the femur, the tibia, the fibula and the patella (kneecap).

Femur: The femur is the thighbone or the bone of the upper leg.

Tibia: The tibia is the shinbone and is the larger bone of the lower leg.

Fibula: The fibula is the smaller bone of the lower leg.

Patella: The kneecap, or patella, is approximately 2-3 inches in width and 3-4 inches in length. Its position in the front of the knee joint allows it to slide when the leg moves, as well as protect the knee and give leverage to the muscles [15].

2.1.2. Ligaments and Tendons of the Knee

Ligaments are bands of connective tissue that connect the bones together (in contrast to the tendons, which connect the muscles to the bones). The Medial Collateral Ligament (MCL), the Lateral Collateral Ligament (LCL), the Anterior Cruiciate Ligament (ACL), and the Posterior Cruciate Ligament (PCL) connect the femur and the tibia at the knee joint. Most of the time when a person suffers a ligament injury, it is to one of these four major ligaments. There are also other ligaments in the knee as part of the knee capsule. The MCL and LCL prevent the knee from moving too far in the side-to-side direction. The ACL and PCL control the front-to-back motion of the knee joint [16].

The ACL keeps the tibia from sliding too far forward in relation to the femur. The PCL keeps the tibia from sliding too far backward in relation to the femur. Working together, the

two cruciate ligaments control the back-and-forth motion of the knee. The ligaments, all taken together, are the most important structures controlling stability of the knee [16].

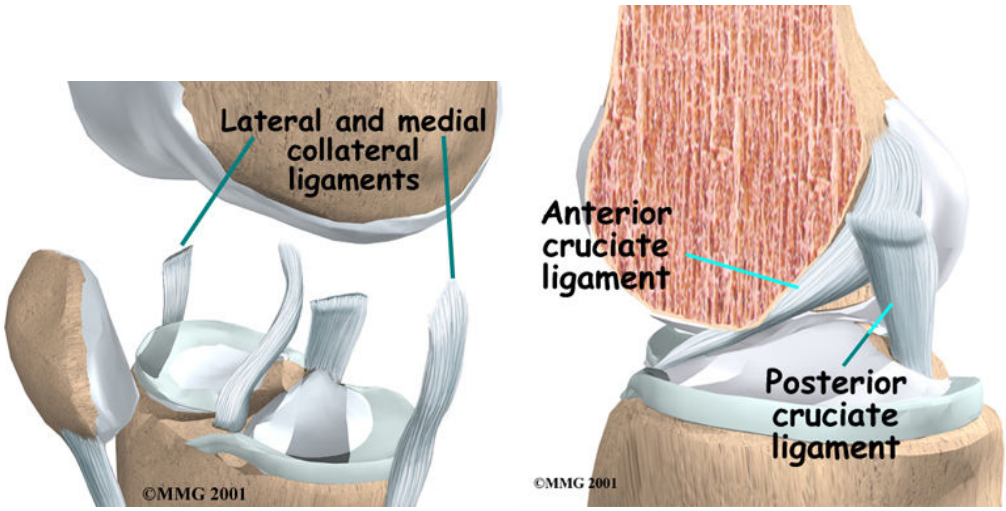

Figure 2.3 The ligaments of the knee. Adapted from [16].

2.1.2.1 Collateral Ligaments

2.1.2.1.1. Anatomic Consideration

The medial collateral ligament (MCL) is a flat, broad structure that spans the medial side of the joint (Figure 2.4). The ligament has anterior and posterior parts.

The larger, anterior part of the MCL blends with medial patellar retinacular fibers before attaching to the medial-proximal aspect of the tibia.

The posterior part of the MCL consists of a short set of fibers, deep to the anterior fibers. These fibers have extensive distal attachments to the posterior-medial joint capsule, medial meniscus, and tendon of the semimembranosus muscle.

The lateral (fibular) collateral ligament consists of a round, strong cord that runs nearly vertical between the lateral epicondyle of the femur to the head of the fibula (Figure 2.5). The

lateral collateral ligament does not attach to the adjacent meniscus (Figure 2.6) [17].

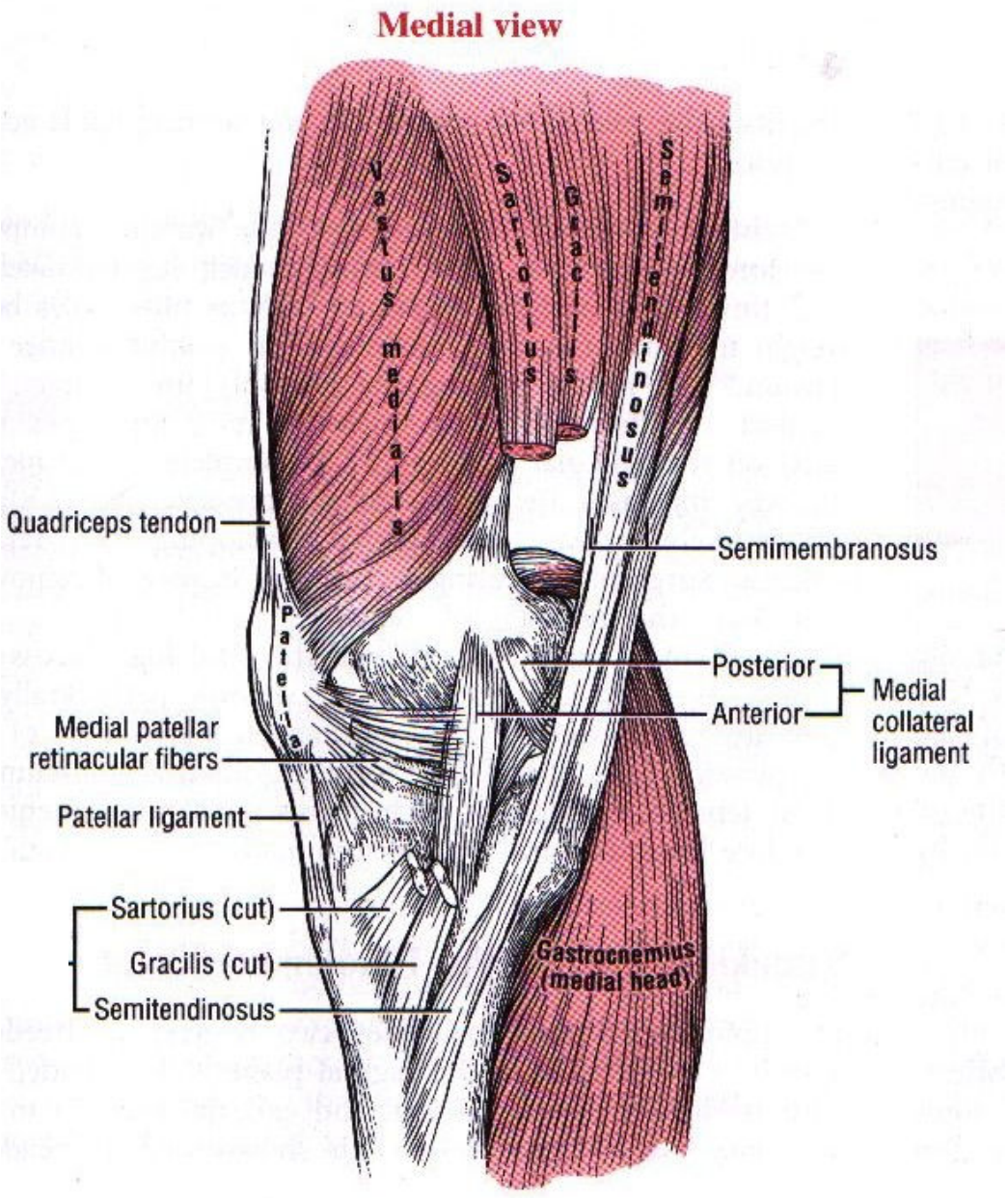

Figure 2.4 Medial view of the right knee shows many muscles and connective tissues. The tendons of the sartorius and gracilis are ct to better expose the anterior and posterior parts of the MCL. Adapted from [17].

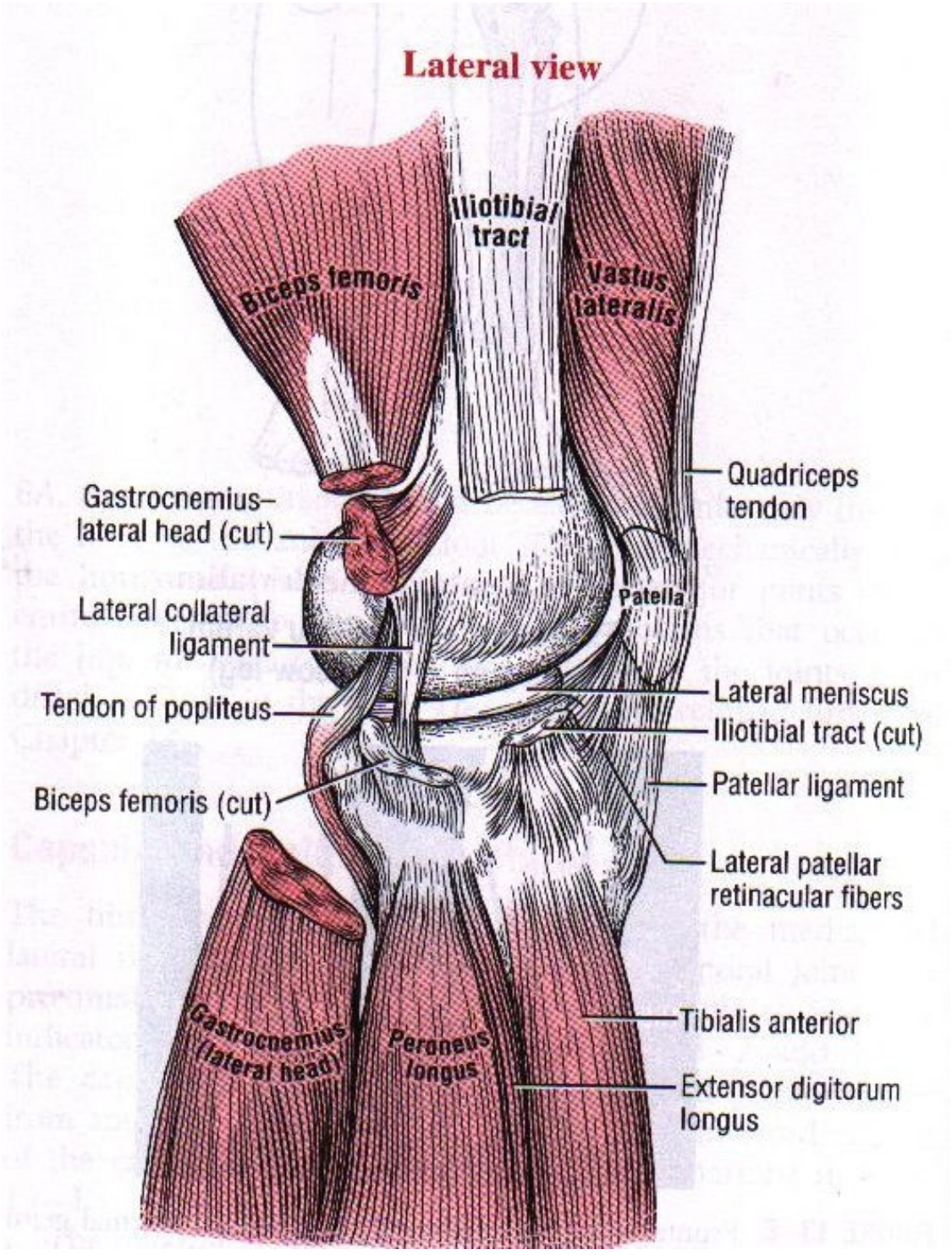

Figure 2.5 Lateral view of the right knee shows muscles and connective tissues. The ilitibial band, lateral head of the gastrocnemius, and biceps femoris are cut to better expose the LCL and leteral meniscus. Adapted from [17].

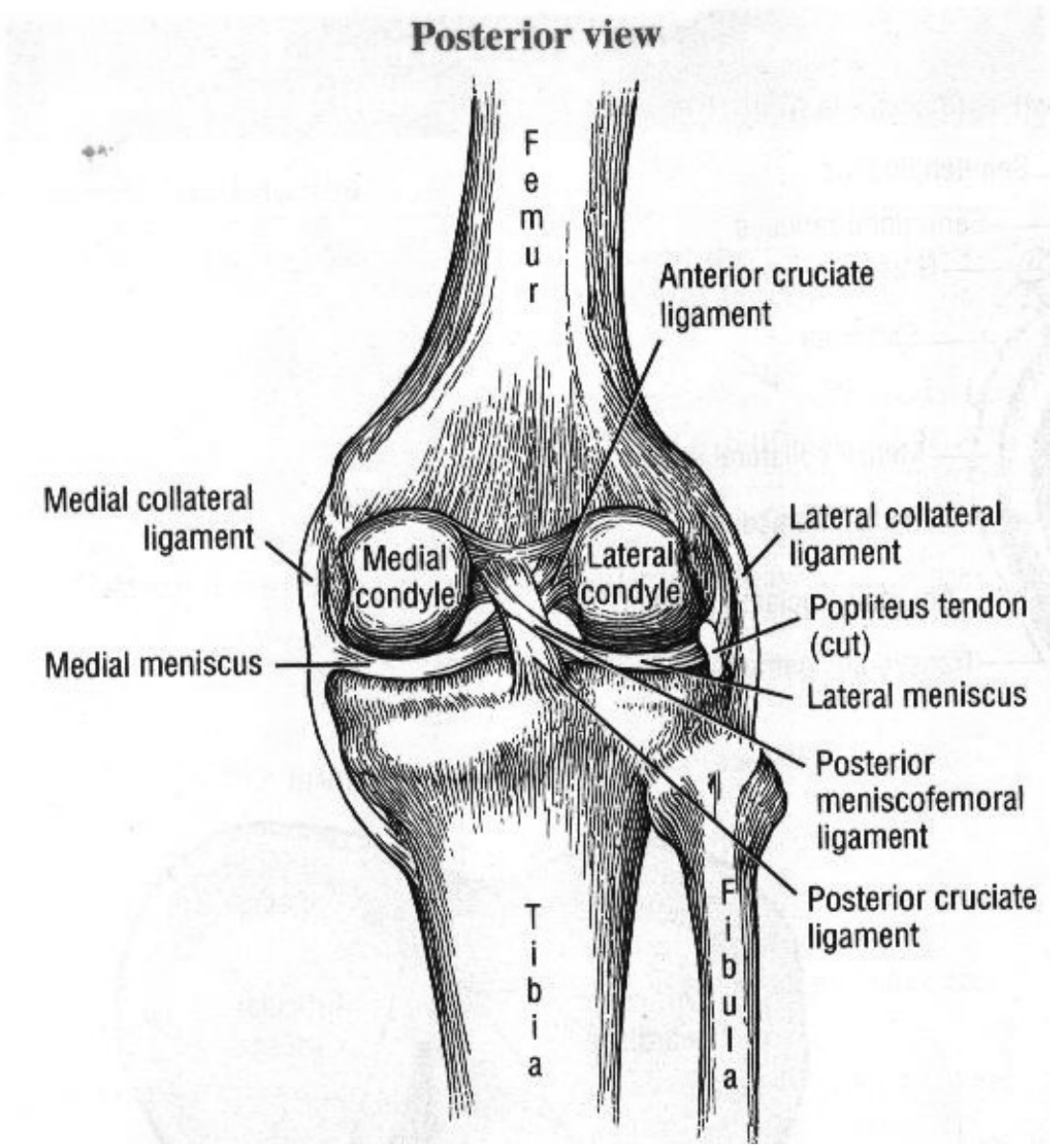

Figure 2.6 Posterior view of the deep structures of the right knee after all muscles and posterior capsule are removed. Observe the menisci, collateral ligaments, and cruciate ligaments. Adapted from [17].

2.1.2.1.2 Functional Considerations

The primary function of the collateral ligaments is to limit excessive motion in the frontal plane. With the knee extended, the anterior part of the MCL provides the primary

resistance against a valgus, or abduction, stress. The lateral collateral ligament, on the other hand, provides the primary resistance against a varus, or adduction, stress.

A secondary function of the collateral ligaments is to limit the extremes of knee extension. This function is shared, however, by the posterior capsule, oblique popliteal ligament, knee flexor muscles, and anterior cruciate ligament (Figure 2.7).

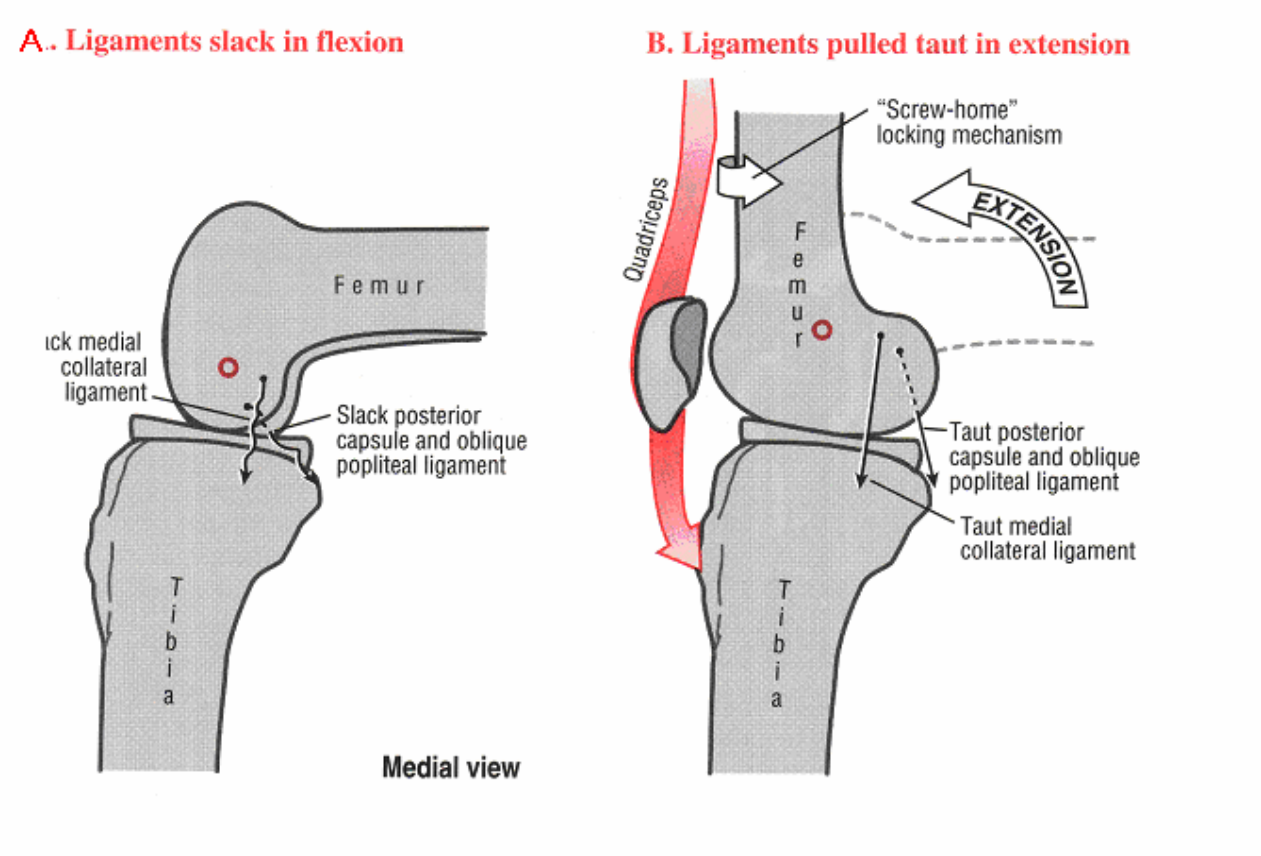

Figure 2.7 Medial view of the knee shows the elongation of the medial collateral ligament and the posterior capsule and oblique popliteal ligament during active femoral-on-tibial extension. In the knee flexion these ligaments are relatively slackened (A). The structures are pulled taut as the knee actively extends by contraction of quadriceps (B). Adapted from [17].

Full extension, which includes the screw-home rotation, elongates the collateral ligaments about 20% beyond their length at full flexion. Although a valuable stabilizer, a taut MCL is especially vulnerable to injury from a valgus (abduction) stress delivered over a

planted foot. This mechanism of injury is part of the classic "clip" in football.

The collateral ligaments also provide limited resistance to the extremes of internal and external rotation while the knee is partially flexed [17].

2.1.2.2 Anterior and Posterior Cruciate Ligaments

2.1.2.2.1 General Consideration

Cruciate, meaning “cross shaped,” describes the spatial relation of the ligaments as they cross within the intercondylar notch of the femur (Figure 2.8). The cruciate ligaments are intracapsular structures that are covered by an extensive synovial lining. The ligaments are supplied with blood from small vessels in the synovial membrane and nearby soft tissue [17].

The cruciate ligaments are named according to their attachment to the tibia. Acting together, the anterior and posterior cruciate ligaments resist the extremes of all knee motions. Perhaps most importantly, however, the cruciate ligaments provide most of the resistance to anterior-posterior shear forces between the tibia and femur.

Injury to the cruciate ligaments can lead to marked instability of the knee. A retrospective review of the literature suggests that the likelihood of gonarthrosis (or arthrosis of the knee) significantly increases following injury to the ACL [17].

2.1.2.2.2 Anterior Cruciate Ligament

From the anterior intercondylar area of the tibial plateau, the anterior cruciate ligament (ACL) runs obliquely in a posterior, slightly superior, and lateral direction to attach on the medial side of the lateral femoral condyle (Figure 2.8). The collagen fibers within the ACL twist upon one another, forming bundles often referred to as posterior-lateral and anterior-medial. The posterior-lateral bundle is the main component of the ACL.

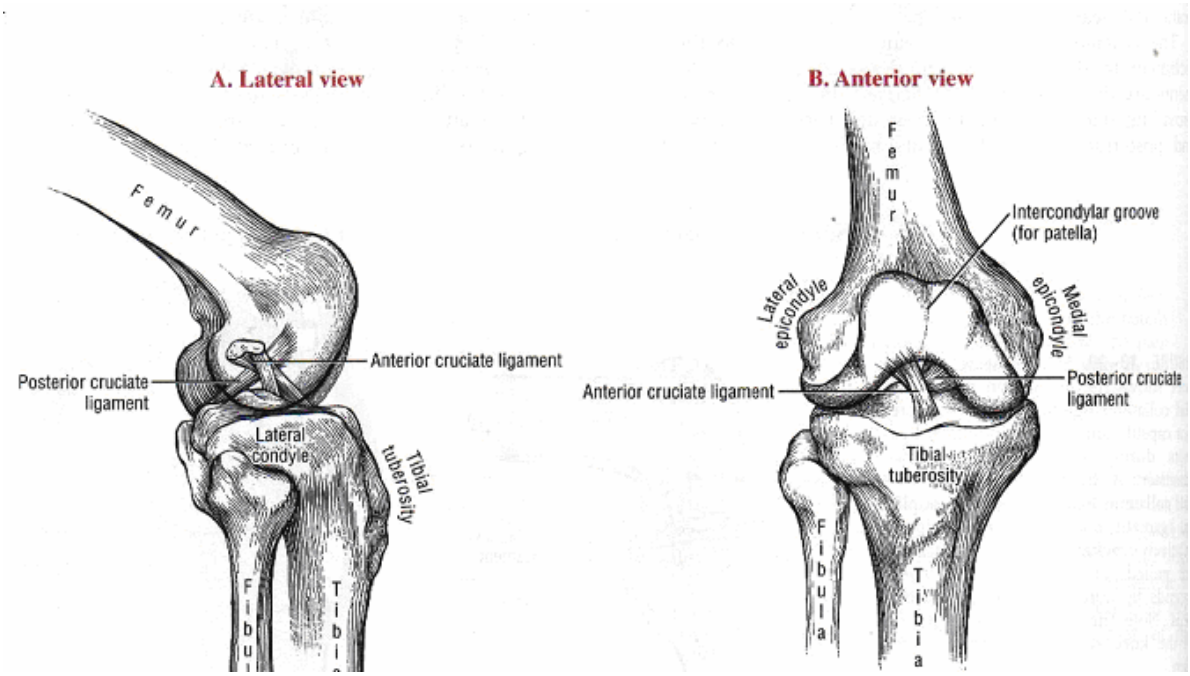

Figure 2.8 The anterior and posterior cruciate ligaments. A, Lateral view. B, Anterior view. Adapted from [17].

Although some fibers of the ACL remain taut throughout the full range of motion, most fibers (especially within the posterior-lateral bundle) become especially taut as the knee approaches full extension (Figure 2.9 A). Along with the posterior capsule, collateral ligaments, and hamstring muscles, the ACL produces useful tension that helps stabilize the extended or near-extended knee. The primer function of the ACL is providing anterior and rotational stability of the knee [17].

2.1.2.2.2.1 Mechanism of Anterior Cruciate Ligament Injury

The ACL is the most frequently injured ligament of the knee. One relatively simple manual test for ACL integrity is the anterior drawer examination (Figure 2.9 A and B). (Although this test may not be the most sensitive to determine ACL injury, it does place

tension in much of the ligament.) With the knee flexed and "unlocked," secondary restraint structures, such as the posterior capsule, collateral ligaments, and flexor muscles, offer less resistance to an anteriorly translating tibia. Spasm in the hamstring muscles may limit anterior translation of the tibia, thereby masking a torn ACL [17].

The oblique manner in which the ACL courses through the knee allows at least part of this structure to resist the extremes of all movements. The ACL is pulled taut as a result of many tibial-on-femoral or femoral-on-tibial movements. A common mechanism for injuring the ACL involves excessive hyperextension of the knee while the foot is planted on the ground. Marked hyperextension frequently involves trauma to the collateral ligaments and the posterior capsule [17].

2.1.2.3 Posterior Cruciate Ligament

2.1.2.3.1 Functional Anatomy

Slightly thicker than the ACL, the posterior cruciate ligament (PCL) attaches from the posterior intercondylar area of the tibia to the lateral side of the medial femoral condyle (Fig 2.6, Fig 2.8). The PCL has two bundles: a larger anterior set (also called anterior-lateral) forming the bulk of the ligament, and smaller posterior set (also called posterior-medial).

Two accessory components of the PCL are often present:

- Anterior meniscofemoral ligament;
- Posterior meniscofemoral ligament (Figure 2.6).

These ligaments play a minor role in stability.

As in the ACL, some fibers in the PCL remain taut throughout the entire range of motion. The majority of the ligament (i.e., the larger anterior fibers), however, becomes taut at the extremes of flexion. As depicted in the Figure 2.9 C, the PCL is pulled taut by hamstring

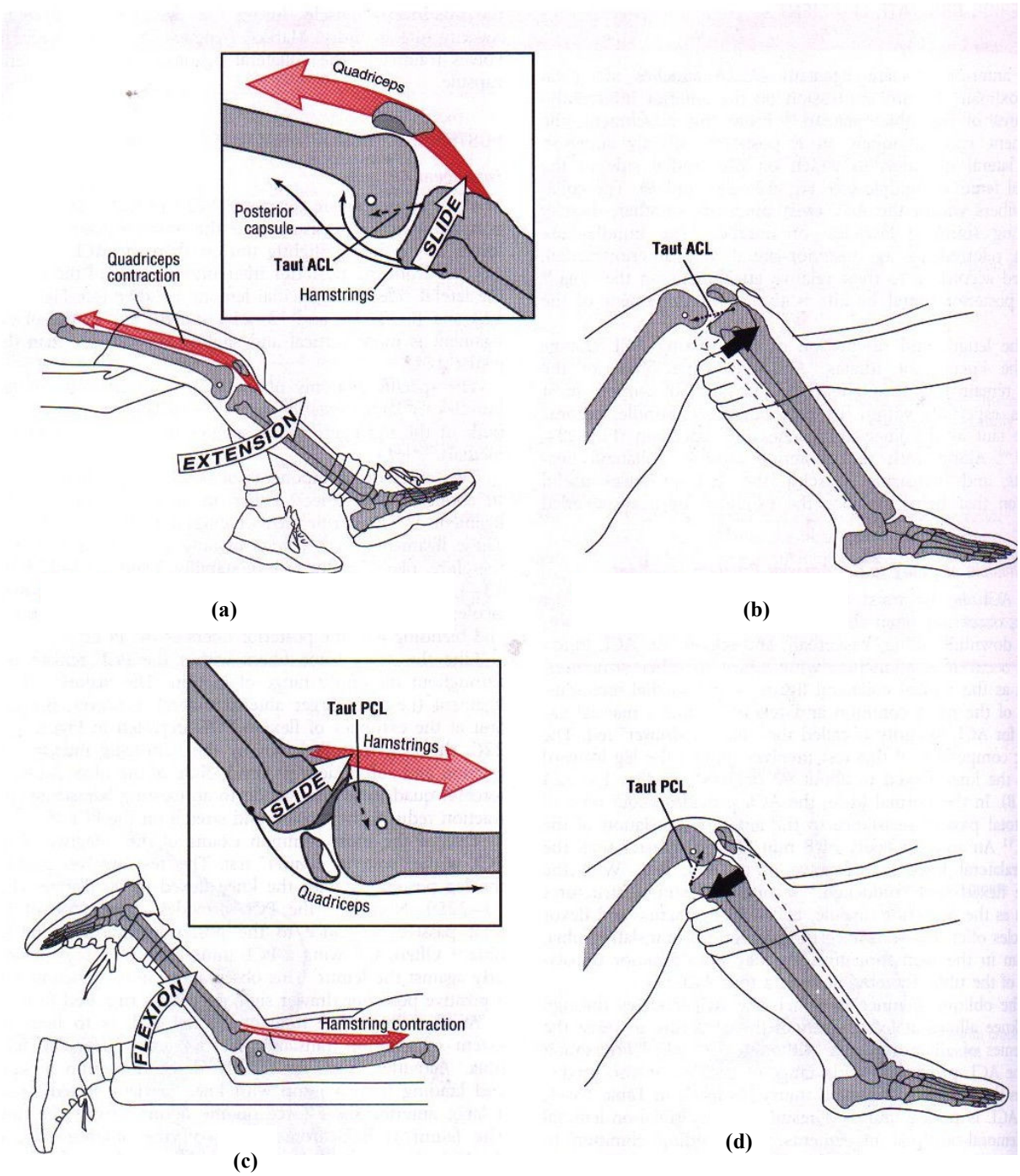

Figure 2.9 The interaction between muscle contractions and tension changes in the cruciate ligaments is shown, a). Contraction of quadriceps muscle extends the knee and slides the tibia anterior relatively to the femur. Knee extension also elongates most of the ACL, Poterior capsule, hamstring muscles, and collateral ligaments, b). Contraction of hamstring muscles flexes the knee and slides the tibia posteriorly. Knee flexion elongates the quadriceps muscle and most of the fibers in PCL, c). The anterior drawer test evaluates the integrity of the ACL, d), the posterior drawer test checks the integrity of the PCL. Adapted from [17].

muscle contraction and the subsequent posterior slide of the tibia. Adding a forceful quadriceps contraction to an existing hamstring contraction reduces the tension and stretch on the PCL [17].

One common test of the integrity of the PCL is the posterior drawer examination (Figure 2.9 D). Normally, the PCL provides about 95% of the total passive resistance to posterior translation of the tibia.

Another important function of the PCL is to limit the extent of anterior translation of the femur over the fixed tibia. Activities such as rapidly descending into a squat and landing from a jump with knee partially flexed create a large anterior shear force on the femur against the tibia [17].

2.1.2.3.1.1 Mechanism of Injury to the Posterior Cruciate Ligament

Injury to the PCL accounts for only 5% to 20% of all ligamentous injuries of the knee. Half of PCL injuries occur with injuries to other knee structures, most often the ACL and posterior-lateral capsule. Three mechanisms are proposed for rupture of the PCL as

- Hyperflexion,
- Pretibial trauma (“dashboard” injury),
- Hyperextension.

2.1.3 Articular Cartilage

The articular cartilage covers the ends of femur, tibia, and fibula, as well as the underside of the patella and provides cushioning and ensures a good fit between the meeting surfaces of the femur and the tibia [15]. This material is about one-quarter of an inch thick in most large joints. It is white and shiny with a rubbery consistency. Articular cartilage is a slippery substance that allows the surfaces to slide against one another without damage to

either surface. The function of articular cartilage is to absorb shock and provide an extremely smooth surface to facilitate motion. We have articular cartilage essentially everywhere that two bony surfaces move against one another, or articulate. In the knee, articular cartilage covers the ends of the femur, the top of the tibia, and the back of the patella [16] (Figure 2.10).

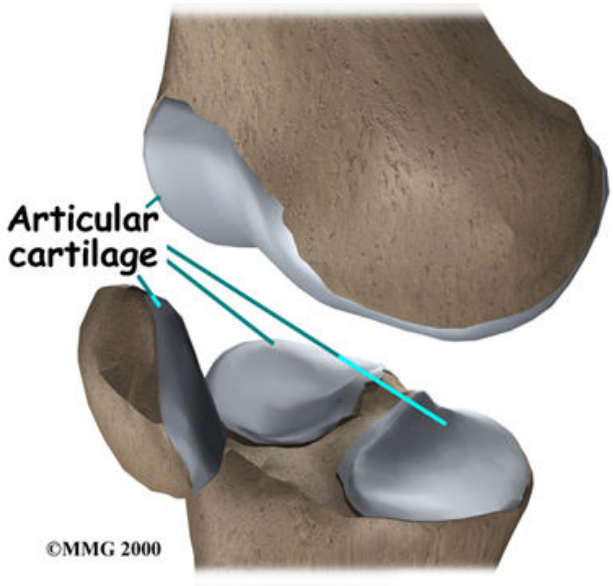

Figure 2.10. Articular Cartilage of the knee [15].

2.1.4 Meniscus

The knee joint is further cushioned by the menisci (lateral and medial), which are the second type of cartilage tissue found in the knee. The menisci act as shock absorbers between the bones and serve to further cushion the knee. These structures are sometimes referred to as the cartilage of the knee, but the menisci differ from the articular cartilage that covers the surface of the joint. The two menisci of the knee are important for two reasons: (1) they work like a gasket to spread the force from the weight of the body over a larger area, and (2) they help the ligaments with stability of the knee. In addition to protecting the articular cartilage, the menisci help the ligaments with stability of the knee [16].

The menisci make the knee joint more stable by acting like a wedge set against the

bottom of a car tire. The menisci are thicker around the outside, and this thickness helps keep the round femur from rolling on the flat tibia. The menisci convert the tibial surface into a shallow socket. A socket is more stable and more efficient at transmitting the weight from the upper body than a round ball on a flat plate. The menisci enhance the stability of the knee and protect the articular cartilage from excessive concentration of force [16] (Figure 2.11).

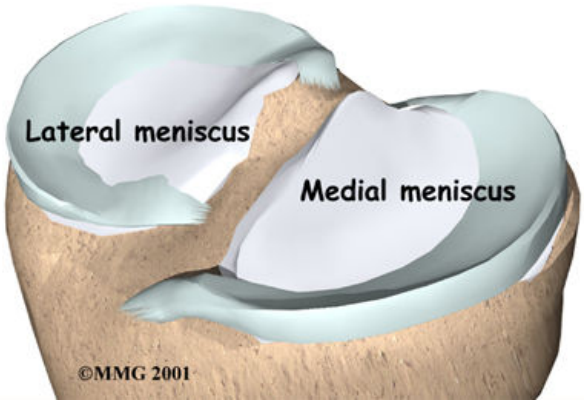

Figure 2.11 An overview of meniscus. Adapted from [15].

2.1.5 Muscles

The extensor mechanism is the motor that drives the knee joint and allows us to walk. It sits in front of the knee joint and is made up of the patella, the patellar tendon, the quadriceps tendon, and the quadriceps muscles. The four quadriceps muscles in front of the thigh are the muscles that attach to the quadriceps tendon. When these muscles contract, they straighten the knee joint, such as when you get up from a squatting position [16]. The way in which the kneecap fits into the patellofemoral groove on the front of the femur and slides as the knee bends can affect the overall function of the knee. The patella works like a fulcrum, increasing the force exerted by the quadriceps muscles as the knee straightens. When these muscles contract, they straighten the knee joint, such as when you get up from a squatting position [15]. Two groups of muscles meet at the knee – the quadriceps and the hamstrings.

Quadriceps; The quadriceps refers to four muscles that are located on the front of the

thigh. Those muscles are responsible for straightening (extending) the knee.

Hamstrings; The muscles that are responsible for the complimentary motion of the knee, or flexion (bending), are called the hamstrings and are located along the back of the thigh from the hip to just below the knee joint (Figure 2.12).

Figure 2.12 The view of the quadriceps and hamstring muscles. Adapted from [16].

2.1.6 Tendons

Tendons are chords of connective tissue that attach the muscles to the bones.

Quadriceps tendon; In the knee joint, the quadriceps tendon joins the quadriceps muscle and the kneecap, also providing power for extension.

Patellar tendon; The patellar tendon (although it is a ligament in nature, it is often

referred to as a tendon) connects the kneecap to the tibia.

2.1.7 Nerves

The most important nerve around the knee is the popliteal nerve in the back of the knee. This large nerve travels to the lower leg and foot, supplying sensation and muscle control. The nerve splits just above the knee to form the tibial nerve and the peroneal nerve. The tibial nerve continues down the back of the leg while the peroneal nerve travels around the outside of the knee and down the front of the leg to the foot. Both of these nerves can be damaged by injuries around the knee [15].

2.1.8 Blood Vessels

The major blood vessels around the knee travel with the popliteal nerve down the back of the leg. The popliteal artery and popliteal vein are the largest blood supply to the leg and foot. If the popliteal artery is damaged beyond repair, it is very likely the leg will not be able to survive. The popliteal artery carries blood to the leg and foot. The popliteal vein carries blood back to the heart.

As a summary the knee has a somewhat unstable design. Yet it must support the body's full weight when standing, and much more than that during walking or running. So it's not surprising that knee problems are a fairly common complaint among people of all ages. Understanding the basic parts of the knee can help you better understand what happens when knee problems occur [15].

2.1.9 The Movements of the Knee Joint

The knee joint consists of tibiofemoral joint and the patellofemoral joint . The knee has important biomechanical functions, many of which are expressed during walking and running.

Running requires that the knee move through a large range of motion, especially in the sagittal plane. Rapidly changing directions (cutting) while running requires additional freedom of movement in the horizontal plane.

With the foot firmly in contact with the ground, the soft tissues stabilizing the knee are often subjected to large forces, both from muscle and external sources. Injuries to ligaments and to cartilage are two common consequences of the large functional demands placed on the knee. Knowledge of the anatomy and kinesiology of the knee is an essential prerequisite to understanding the mechanism of injuries and providing the most effective therapeutic intervention [17].

The tibiofemoral joint or knee possesses two degrees of freedom: (1) flexion and extension in the sagittal plane and (2) provided the knee is slightly flexed, internal and external rotation in the horizontal plane.

2.1.9.1 Flexion and Extension

Flexion and extension at the knee occur about a medial-lateral axis of rotation. In general, the healthy knee rotates from 130 to 140 degrees of flexion to about 5 to 10 degrees of hyperextension (Figure 2.13).

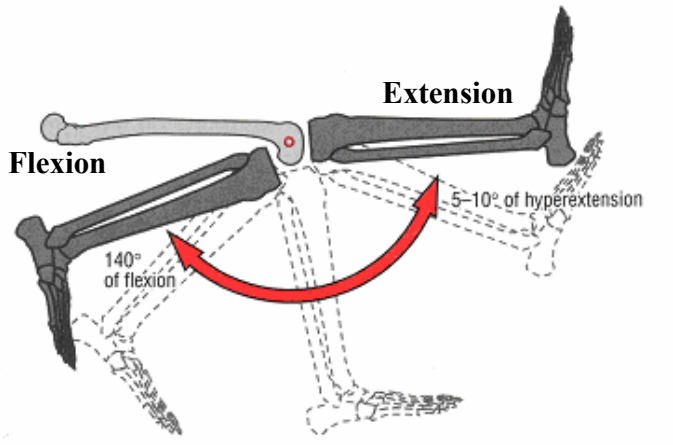

Figure 2.13 The illustration of the knee flexion and extension in sugittal plane. Adapted from [17].

The medial-lateral axis of rotation for flexion and extension is not fixed, but instead migrates within the femoral condyles. The curved path of the axis is known as an "evolute," or instant center of rotation. (Figure 2.14). The migrating axis of rotation has several biomechanical and clinical implications.

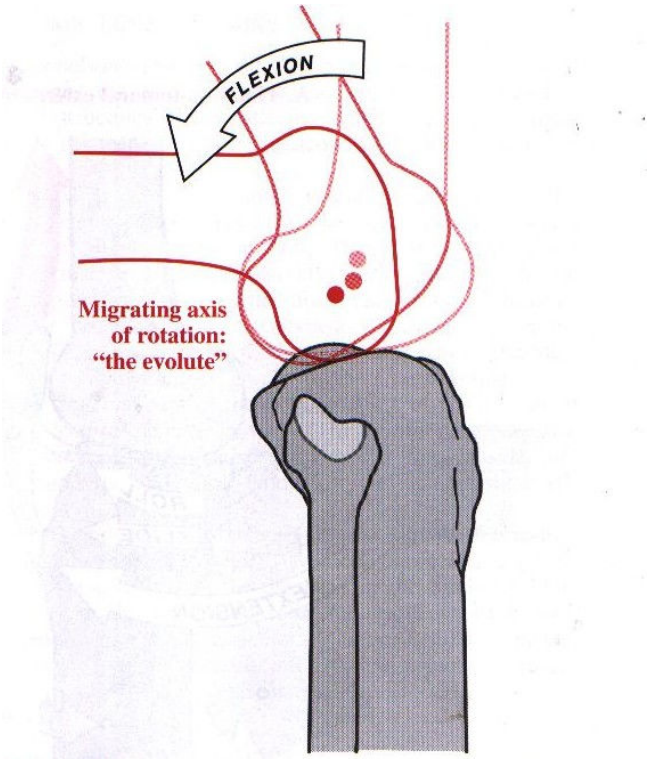

Figure 2.14 The flexing knee generates a migrating medial-lateral axis of rotation. This migration is described as "the evolute". Adapted from [17].

2.1.9.2 Internal and External Rotation

Internal and external rotation of the knee occur in a horizontal plane about a vertical (or longitudinal) axis of rotation (Figure 2.15). External rotation exceeds internal rotation by about 2:1.

In general, axial rotation increases with greater knee flexion. In full extension, axial rotation is essentially absent. The rotation is blocked by passive tension in the stretched

ligaments and the increased bony congruity within the joint.

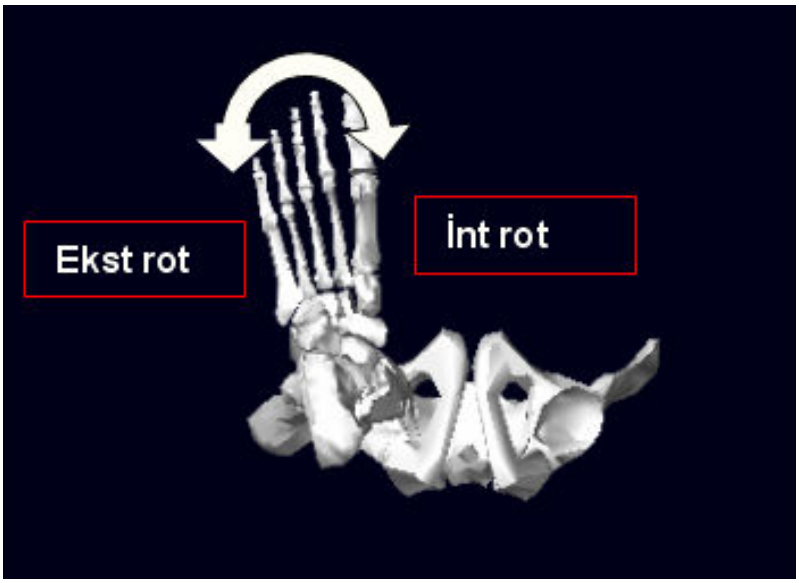

Figure 2.15 The illustration of the knee internal rotation and external rotation transvers plane.

2.1.9.3 Valgus (Abduction) and Varus (Adduction) Rotation

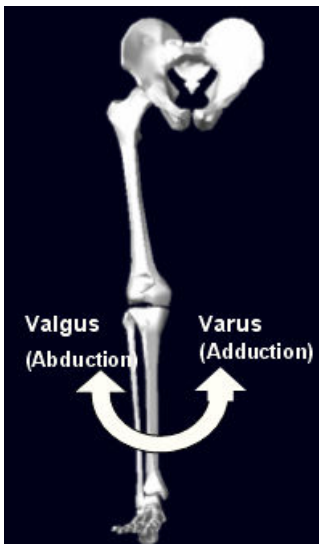

Figure 2.16 The illustration of Valgus (Abduction) and Varus (Adduction) rotation of the knee joint.

The range of varus valgus rotation is only about 5°. The abduction-adduction movement of the knee joint is illustrated in Figure 2.16.

2.1.10 Arthrokinematics at the Tibiofemoral Joint

2.1.10.1 Active Extension of the Knee

Figure 2.17 depicts the arthrokinematics of the last 90 degrees of active knee extension.

During tibial-on-femoral extension, the articular surface of the tibia rolls and slides anteriorly on the femoral condyles (Figure2.17).

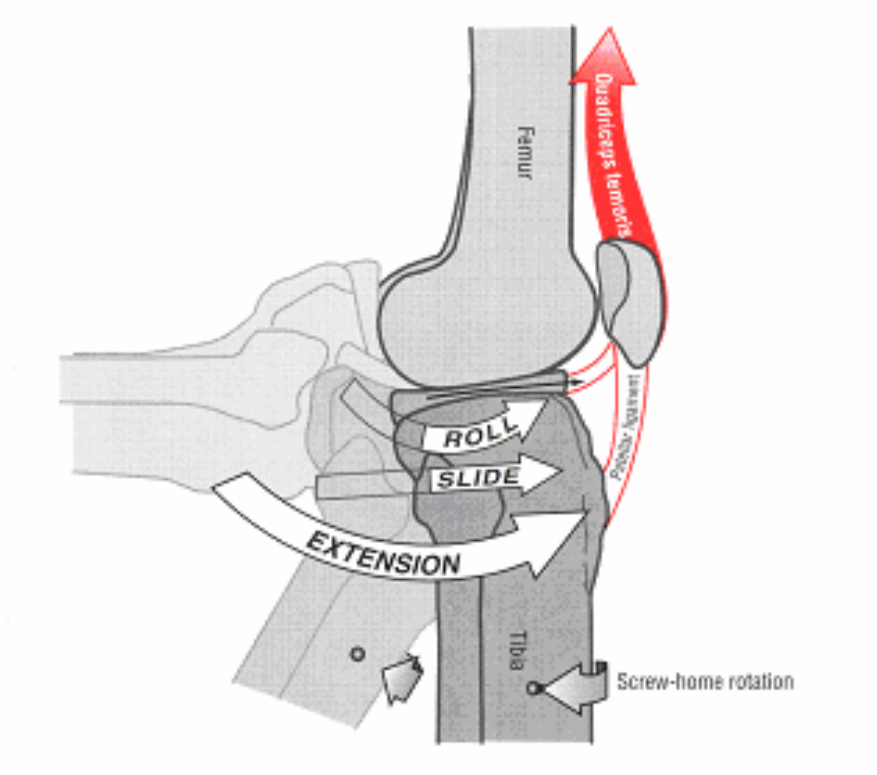

Figure 2.17 The active arthrokinematics of knee extension (Tibia-on-Femur perspective). Adapted from [17].

2.1.10.2 "Screw-Home" Rotation of the Knee

Locking the knee in full extension requires an important 10 degrees of external rotation. The rotary locking action is called "screw-home" rotation based on the observable twisting of the knee during the last 30 degrees of extension. This type of rotation is mechanically linked to the flexion and extension kinematics and cannot be performed independently.

Regardless of whether the thigh or leg is the moving segment, both knee extension movements depicted in Figure 2.10 show a knee joint that is externally rotating when approaching full extension. Note the difference in rotation direction of the femur versus the tibia.

The screw-home rotation mechanics are driven by at least three factors (Figure 2.18):

1. Shape of the medial femoral condyle (most important factor)

2. Passive tension in the anterior cruciate ligament

3. Lateral pull of the quadriceps muscle

Because the articular surface on the medial condyle extends farther anteriorly on the lateral condyle, the tibia "follows" this laterally curved path during full tibial-on-femoral extension. During femoral-on-tibial extension, the femur follows a medially curved path on the tibia. In either case, the result is external rotation of the knee at full extension [17].

2.1.10.3 Active Flexion of the Knee

The arthrokinematics of active knee flexion occur by reverse fashion, depicted in Figure 2.10. To unlock a knee that is fully extended, the joint must first internally rotate, an action driven primarily by the popliteus muscle. The muscle can rotate the femur externally to initiate femoral-on-tibial flexion, or rotate the tibia internally to initiate tibial-on-femoral flexion [17].

2.1.10.4 Internal and External (Axial) Rotation of the Knee

Once flexed, the arthrokinematics of internal and external rotation involve a spin between the menisci and the articular surfaces of the tibia and femur. Horizontal plane rotation of the femur over the tibia causes the menisci to deform slightly as they are compressed between the spinning femoral condyles. The menisci are stabilized by connections from active musculature, such as the popliteus and semimembranosus [17].

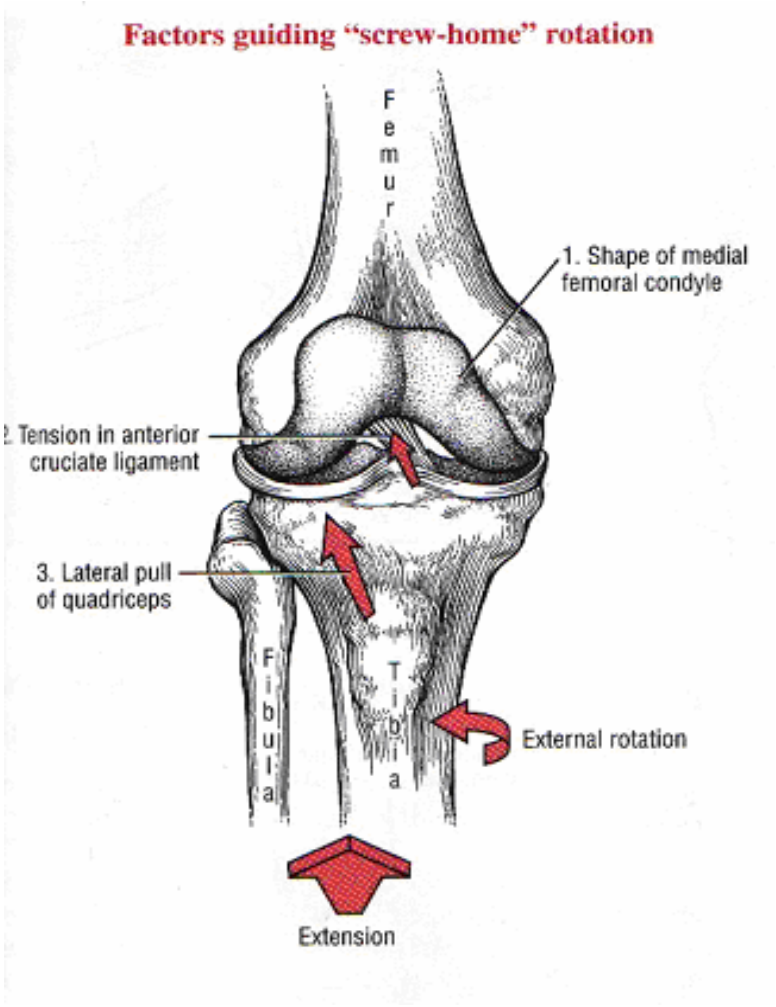

Figure 2.18 "Screw-home" locking mechanism of the knee. A, during terminal tibia-on-femoral extension, three contribute to the locking mechanism of the knee. Each factor contributes bias to external rotation of the tibia. Adapted from [17]

2.1.11 Patello-Femoral Joint

The patellofemoral joint is the interface between the articular side of the patella and the intercondylar groove on the femur. The quadriceps muscle, the articular joint surfaces, and the retinacular fibers stabilize the joint (Figure 2.20).

2.1.11.1 Patello-femoral Kinematics (Path and Area of Patellar Contact on the Femur)

Data from selected studies and cineradiographic observations were used to construct the model in Figure 2.19.

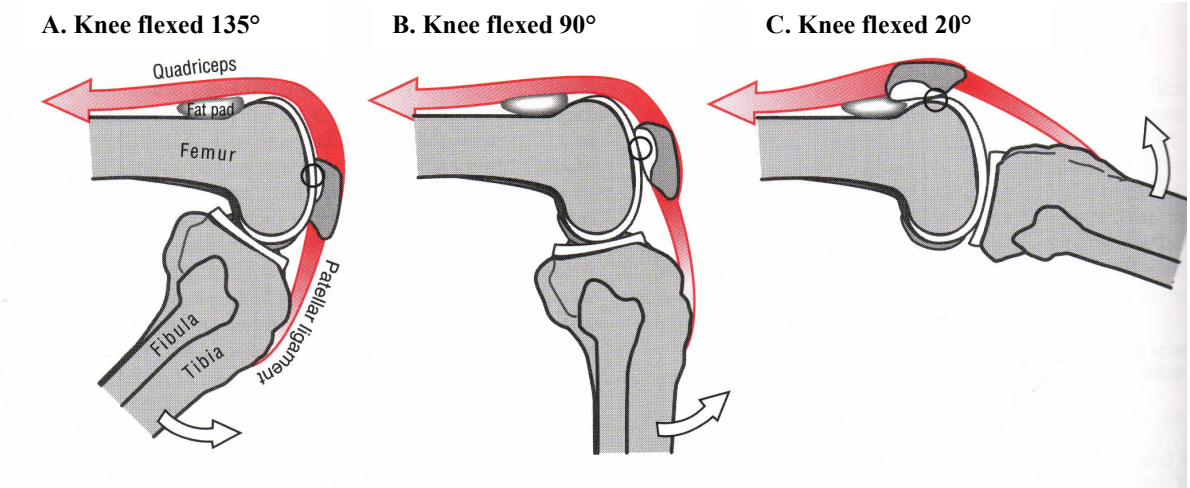

Figure 2.19 The kinematics at the patello-femoral joint during active tibial-onfemoral extension. The circle depict in A-C indicates the point of maximal contact between the patella and femur. As the knee is extended, the contact point on the patella migrates from its superior pole to its inferior pole. Adapted from [17].

• At 135 degrees of flexion:

1. The patella contacts the femur near its superior pole (Figure2.17).

2. The patella bridges the intercondylar notch of the femur (Figure 2.19).

3. The lateral edge of the lateral facet and the "odd" facet of the patella share articular contact with the femur (Figure 2.19) [17].

As the knee extends toward 90 degrees of flexion, the contact region on the patella starts to migrate inferiorly (Figure 2.11). Between 90 and 60 degrees of flexion, the patellofemoral joint occupies its greatest contact area with the femur (Figure 2.12). At its maximum, however, this contact area is only about 30% of the total surface area of the patella.

As the knee extends through the last 20 degrees of flexion, the primary contact point on the patella migrates to the inferior pole (Figure 2.11). In full extension the patella rests completely above the intercondylar groove, against the suprapatellar fat pad [17].

A. Path of Sliding Patella on the Femur **B. Posterior Articular Surface of Patella**

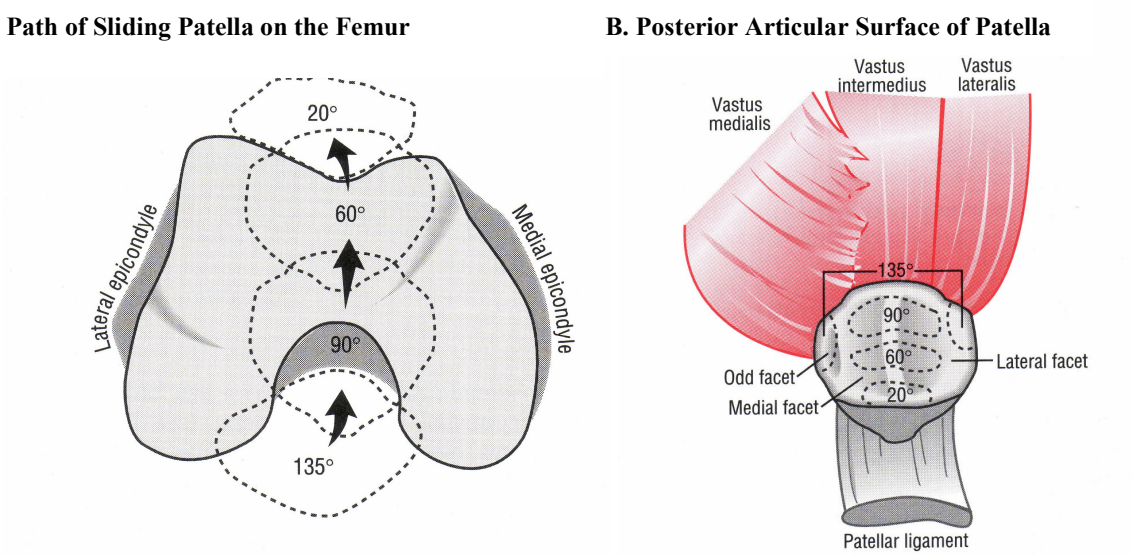

Figure 2.20 The path (A) and contact areas of the patella (B) on intercondylar groove of the femur. The values 135, 90, 60, 20 degrees indicate flexed positions of the knee. Adapted from [17].

2.1.11.2 Terminology of the Patellar Motion

Patellar shift is defined as the movement of the patella parallel to (i.e. along) the

femoral medial-lateral axis.

Patellar rotation is described as the rotation of the patella about a floating axis parallel to the patellar anterior-posterior axis and perpendicular to both the femoral medial-lateral axis and the patellar long axis.

Patellar tilt is defined as the rotation of the patella about the patellar long axis and patellar flexion as the rotation of the patella about the femoral medial-lateral axis (Figure 2.21) [17].

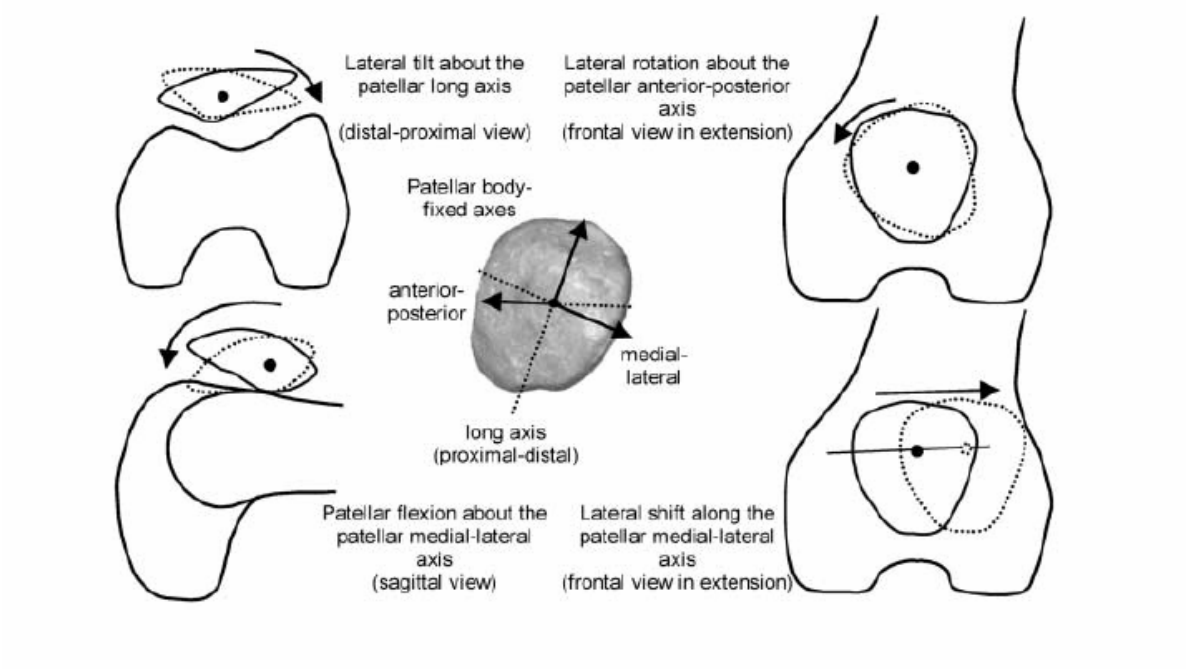

Figure 2.21 Patellar motion in terms of patellar body fixed axes

2.2 Conventional Modeling of the Knee

The models can be c1assified into two types: experimental and mathematical models. Experimental models are mechanical constructions which are designed to simulate certain aspects of the real system. Experimental studies are conducted on the mechanical response of the experimental constructions. Mathematical models are derived from physical laws that

generate a set of mathematical relations of the system. Then a numerical solution method is used to solve the system. There are only a few experimental models. These are briefly discussed before considering the more numerous mathematical models [18].

2.2.1 Experimental Knee Models

One of the first models of the knee joint was the crossed four-bar linkage that is briefly described in [19]. The tibia (lower leg) and the femur (upper leg) were represented by two connecting bars and the Anterior Cruciate Ligament (ACL) and Posterior Cruciate Ligament (PCL) were represented by two crossed rods.

Length ratio of the two crossed rods were equal to that of ACL and PCL. This model could explain the approximate location of the flexion-extension axis, the shape of the femoral condyles and the posterior movement of tibio-femoral contact during knee flexion. Huson [20] extended this mechanism by constructing a 3-dimensional model to investigate tibial rotation.

An experimental model which consisted of the contact force in the patello- femoral joint was the model developed by Bandi [21]. To represent tibia, femur and patella, he used planar wooden models. To model the patellar and quadriceps tendons Iinen tape was used. Contact force of the patello-femoral joint was measured using a piezoelectric force transducer which was attached to the patella.

Chand *et al.* [22] combined mathematical and experimental models to investigate tibio-femoral contact stresses. Formulation of the contact problem between bones was a quadratic programming problem. Analytical results were compared with the results *of* a 2-dimensional photoelastic model. The femur and tibia were made from epoxy resin, and separated by a 1 /8 in. thick layer of foam rubber in order to include the menisci.

Experimental models can be helpful to predict the real behavior of the knee. But it is difficult to construct these kinds of models [18].

2.2.2 Mathematical Models of the Knee

Mathematical models of knee can be classified as phenomenological and anatomical models. The phenomenological models are used to investigate the behavior of the knee without considering its real structures. On the other hand, the anatomical models require accurate geometric description of the real anatomy in order to study the behavior of it.

There are two types of anatomically based knee, those describing knee kinematics and kinetics. Kinetic models include static or quasistatic models and dynamic models [19].

2.2.2.1 Phenomenological Models

The phenomenological knee models can be divided into two models: simple hinged models and rheological models which consist of masses, springs and dashpots.

2.2.2.1.1 Simple Hinged Models

For predicting human body dynamics this model of the knee has been used as part of larger models. In these models, the body segments were represented as rigid links and their positions are actively controlled at their connecting joints, and geometry, or ligament function was not included. Most of these models have been used to predict muscle load sharing and joint reaction. In the development of these models the equilibrium equations are written at each joint. Using the force equilibrium equations at each joint, joint forces are calculated [18].

Hight *et al.* [23] developed a phenomenological model for the lower limb to analyze the mechanism of injury during skiing. The model consisted of a number of elastic bodies joined by relatively soft, nonlinear springs. Model is used to predict large 3-dimensional displacements and rotations of these bodies, and the nonlinear stiffness characteristics of the knee.

2.2.2.1.2 Rheological Models

Modeling the knee joint as viscoelastic hinge is in the scope of second type of the phenomenological knee models. Rheological models determine the dynamic behavior of the knee, accounting for the velocity-dependent dissipative property of muscles and tendons, as well as the feedback control of the stretch reflex. No specific information concerning muscle, tendons and joint capsule structures can be obtained from these models because the effect of these structures is accounted for. In other words, the rheological models depict the dynamic behavior of the articulating which is modeled as an idealized stick figure.

In an experiment carried out by Moffat *et al.* [24], a sinusoidal oscillation of knee was produced by a moment about the knee. In order to obtain "Material properties" of the viscoelastic hinge authors performed experimental measurements. Pope *et al.* [25] also made similar tests where a sinusoidal displacement generator stimulated the knee-Lower limb system in the varus-valgus plane.

2.2.2.2 Kinematic Models

Flexion motion of the knee is a combination of rolling and sliding motion between the tibia and the femur and it is not within a single plane but there is also axial rotation of the tibia [18].

Relative motion of bones has been described using either Euler angles or screw axis methods. Euler angles express joint rotation in terms familiar to the clinicians: flexion/extension, abduction/adduction, and tibial internal/extemal rotation. The screw axis method describes both planar motion (Instant Center) and 3-dimensional motion of the knee joint. The translation and the rotation of the joint are assured in terms of rotation about and a translation along a rotatian axis [18].

2.2.2.2.1 Methods Describing Knee Kinematics

2.2.2.2.1.1 Euler Angles

The 3-dimensional movement of the joint is represented by six independent coordinates. These are three translations and three rotations.

Eulerian angles described in the joint co-ordinate system are as follows: Flexion-extension is about the femoral body fixed axis. Extemal-intemal tibial rotation is about the tibial fixed axis and abduction-adduction is about the floating axis which is perpendicular to both body-fixed axes and is oriented in the direction of their cross product (Figure 2.22).

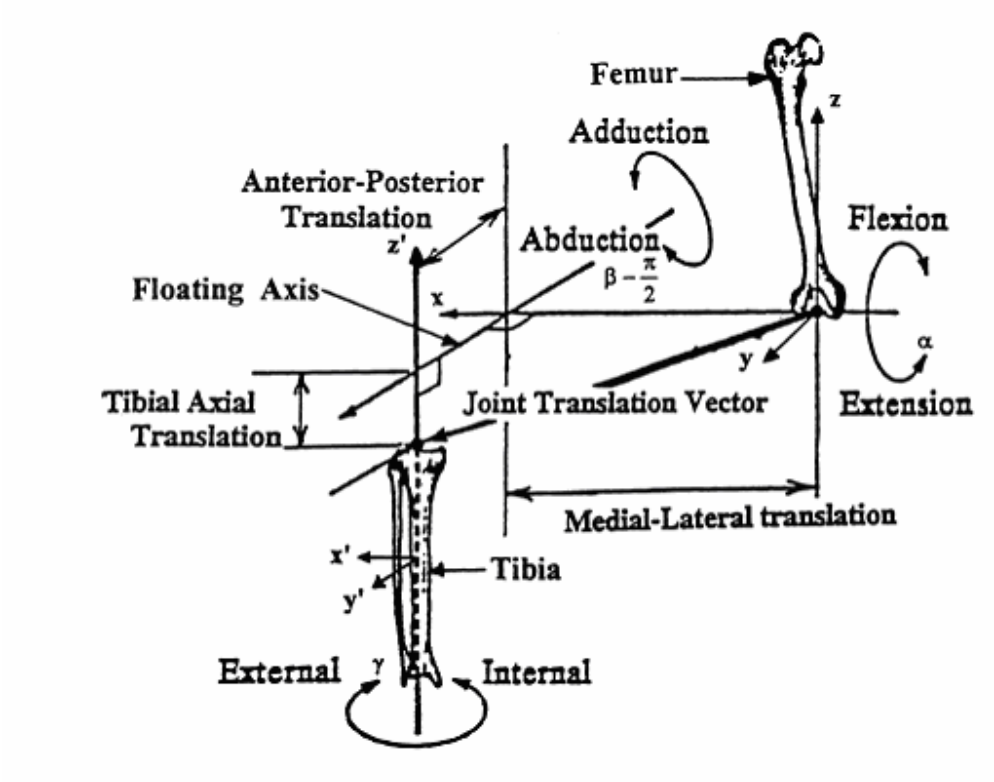

Figure 2.22 Joint rotation and translations. Adapted from [10].

2.2.2.2.1.2 Instant Centered Screw Axis Techniques

This method indicates if relative sliding, rolling distraction, or intruding is occurring in the contact region. The instant center technique describes the motion in one plane only, this method should not be used if more then 15° of rotation takes place in any plane other then the one being measured [18]

2.2.2.2.2 Models Describing Knee Kinematics

The ligaments, capsular structures and their insertion sites on the bones controls the motion between the tibia and femur. The instant center is the point where the cruciate links cross each other which can be seen in the four bar linkage model. There are two types of models to describe knee kinematies: models tracking the path of the instant center and the instantaneous screw axis, and analytical models.

Freudenstein and Woo [26] determined the path of the instant center (IC) for planar flexion motion from 0° to -90°. In this research the femoral IC path was approximated as a logarithmic spiral and the tibial IC path was taken to be a straight line parallel to the plateaus.

Blacharski *et al.* [27] and Van Dijk *et al.* [28] used photographic and sterophotogrammetric techniques to determine the screw axis for consecutive flexian angle. Using their kinematic data, Van Dijk *et al.* [28] calculated the changes in the tibio-femoral distances between markers located at the tibial and femoral insertion areas of the anterior and posterior cruciate ligaments.

Hartfel and co-workers [18] extended the instant center concept to 3-dimensions. In their model instantaneous screw axis changed continuously generating two surfaces which roll and slide relatively to each other and completely describe the relative motion of the articulating surfaces.

The analytical models describe knee kinematics using mathematical relations between motion coordinates. According to research carried by Crowninshield *et al.* [13] tibial rotation occurred about an axis located to the medial side of the knee, and varies as a function of the fifth root of flexion.

2.2.2.3 Static and Quasistatic Models

In literature, most of the static and quasistatic models have been suggested to determine the forces (ligament and joint contact forces) under equilibrium conditions. There are some models to determine the effect of the active forces such as muscle contraction. The ligaments stretch and resist the motion when the bones are displaced. Forces are transmitted through contact surface. Combined with the bone contact compressive forces, ligament and/or muscle allow transmission of moments. The reaction of the articulating surface is the sum of the individual ligament and/or muscle, and each of the two contact forces. Because the number of unknowns is greater than the number of equilibrium equations, solution of the problem is indeterminate. To get a determined system, anatomy of the joint needs to be simplified.

2.2.2.3.1 Type I-Models of Load Sharing

There several models to determine .the sharing of forces in the muscles and- ligaments. Reilly and Martens [29] presented a 2-dimensional model for the motion of leg-raise exercise where the patellar tendon force, the tibio-femoral reaction force, the weight of the limb, and the weight of an exercise boot forces were accounted for. The point of action of the joint contact force was kept constant throughout flexion.

In an extended 3-dimensional study, Morrison [30] predicted how joint structures share the external load.

2.2.2.3.2 Type II-Models of Ligament Length:

In order to understand when ligaments function, lots of experimental techniques have been used such as simple scales, photogrammetric techniques, mercury strain gages, hall effect sensors, and wire cables. Using mathematical models is another approach to study ligament function. These model can be classified as two those which study the change of ligament length with joint motion and those which study the contribution of each ligament to stiffness of the knee.

In a 3-dimensional kinematic model to determine the length of cruciate and collateral ligaments developed by Edwards *et al.* [31], the motion of the femur with respect to the tibia was represented only three components: a rotation in the transverse plane (tibial rotation), a rotation in the sagittal plane (flexion), and a translation in the proximal- distal direction-All ligaments were represented as. straight line segments; except medial collateral ligament which was divided into two straight line segments to describe wrapping around the tibia.

Crowninshield *et al.* [13] extended Edwards' model by representing the cruciate, collateral, and capsular ligaments as 13 elements. They described the motion of the femur with respect to the tibia, adding two additional motion components to the three proposed by Edwards; these were a rotation in the coronal plane (varus-valgus) and a translation in the anterior and posterior direction. Furthermore, Crowninshield *et al.* 's model predicted change of joint stiffness with flexion. This process was accomplished by incorporating into the model data on the relative cross-sectional area of the ligaments and their material properties.

In a study carried by Blankevoort *et al.* [32], the length changes of ligament fiber bundles were determined, by using the points of insertion on the tibia .and femur. The kinematic data and the insertions of the ligaments were obtained by using Roentgenostereophotogrammetry. Different fiber bundles of the anterior and posterior cruciate ligaments and the medial and lateral collateral ligaments were identified. On the basis of an assumption for the maximal strain of each ligament fiber bundle during the experiments, the minimal recruitment length and the probability of recruitment were defined and determined.

In another study, Blankevoort *et al.* [33] proposed a three-dimensional mathematical

model of the human knee to investigate the wrapping of a ligament. The bony edge was described by a curved line on which the contact point of the line element representing a ligament bundle was located. Contact was assumed to be frictionless. This model was applied to the medial collateral ligament (MCL) interacting with the bony edge of the tibia.

2.2.2.3.3 Type III-Models of Femoral-Tibial Contact Stresses

This type of mathematical models are primarily concerned with the joint contact forces and stresses. In order to understand how contact force between the medial and lateral plateaus changes, these models were developed.

In Chand *et al.*'s model [22], the tibio-femoral contact was assumed to be at two points. For solution technique, finite element methods were used.

Minns [34] proposed a model to predict the effects of anatomical variations on the medial and lateral contact forces. He included patellar tendon in his model.

In a simplified model developed by Maquet and Pelzer [35], maximum contact stress in/normal and abnormal knee joints was predicted. Contact force was assumed to be the sum of two forces. The effects of knee deformity, muscular force, location of the center of gravity and weight of the partial body was investigated. Maquet and Pelzer performed experimental measurements to obtain the geometrical data needed in their analysis.

2.2.2.3.4 Type IV-Models Including Both Ligamentous Structures and Geometric Constraints

Andriacchi *et al.* [36] and Wismans *et al.* [4] developed the most extensive 3-dimensional anatomical quasistatic knee models.

Andriacchi *et al.*'s model [36] simulated the effect of ligamentous reconstruction surgery. Ligaments were idealized as 21 linear springs, using finite element methods. The

menisci were assumed to undergo shearing, bending, and axial stiffness. In order to represent contact force, ten hydrostatic elements resisting forces perpendicular to their surfaces were selected. Also this model was used to investigate the relationship between the applied varus moment and the varus stiffness under compressive loads or constraints to coupled degrees of freedom.

Different from Andriacchi *et al.* [36] Wissmans *et al*. [4] considered the geometry of the joint surfaces in his model. However they neglected the menisci. Wissmans *et al.* represented the ligamentous and capsular structures as seven nonlinear springs and they reduced the contact areas to two contact points. However, this model was. not suitable to analyze varus-valgus motions that produce separation.

2.2.2.4 Dynamic Models

A majority of the mathematical models which have been developed studied the knee under static or quasistatic conditions. The available 2-dimensional models, considered only the sugittal motion of the knee.

Moeinzadeh *et al.* [37] developed a model which considered the relative dynamic motion of femur and tibia, the contact force and the ligament forces. Ligaments were modeled as 4 non linear spring elements. Each ligament was assumed, to be relaxed at 54.79° of flexion, and to carry force if its length was longer than the relaxed length. During the entire flexion, one point contact was assumed.

Another anatomical dynamic model which analyzed the planar motion between the femoral and tibial contact surfaces was developed by Wongchaisuwat *et al.* [38]. The tibia was considered as a pendulum that swinged about the femur. For mathematical description of gliding and rolling motions, Newton-Euler equations were used.

Three dimensional formulation of the dynamic modeling of an articulating human knee joint was introduced a decade ago. Two-dimensional version of this formulation was afterwards applied and solved. However, because of the iterative nature of the solution

technique, early 2-dimensional models could not handle impact conditions.

Engin and Tümer [39] introduced alternative solution methods which enabled investigation of the response of the human knee to impact loading on the lower leg via an anatomically based model. In addition, the classical impact theory was applied to the same model an a closed form solution is obtained. Two methods, namely the method of "Excess Differential Equation" and the method of "Minimal Differential Equations", were proposed as the alternative to the previously employed iterative technique. All shortcomings of the previous method of solution were eliminated, and capability of the alternative methods to handle impact loads of very short time duration was demonstrated. The proposed methods were quite successful in handling such cases due to their noniterative nature. Authors believed that especially the method of excess differential equations, can be employed for more complex problems such as three-dimensional formulation which remains still unsolved. The method of minimal differential equations has been applied for the solution of three-body (tibia-patella-femur) segmented planar human knee model [39].

Abdel Rahman and Hefzy [40] developed a 2-dimensional model to simulate the effect of sudden impact. They modeled the ligaments as 10 nonlinear springs. In the analysis, the joint profiles were represented by polynomials. At all times, one point contact was assumed. To transform the motion equation into a set of nonlinear algebraic equations, Newmark constant-average scheme was applied. The Newton-Raphson iteration technique was then used to obtain the solution. Abdel-Rahman and Hefzy [10] developed their model and created a 3 dimensional dynamic model to analyze contact forces and the ligament forces in the intact knee. They could succeed to produced simulate normal knee movement with this model.

Szaklar *et al.* [41] described a simple dynamic knee simulator. The tensions in two flexible cables acting as lumped muscle group equivalents were used to control the active flexion/extension motion, white their simultaneous action was used to control joint compressive force. The tensions in the cables were caused by the electrohydraulic servo, system acting under real-time microprocessor control. The performance of the system during simulation of an idealized level-walking function was evaluated.

Li *et al.* [42] constructed a 3-D finite element model of a human knee joint to predict

knee kinematics and forces in the ligaments. Their model included ligaments, modeled as nonlinear springs, bony structures, modeled as rigid bodies, cartilage, modeled as a linear elastic material, and menisci, modeled as equivalent compressive springs. Their study is limited to quasi-statics of the knee, predicting the kinematics and the role of ligaments at certain flexion angles and internal–external loads applied at the knee center.

2.2.2.4.1 Models of the Patello-Femoral Joint:

Models of the patello-femoral joint were directed towards the determination of the patello-femoral contact force and the changes in the position of the patella during knee motions. Mostly, the patella was assumed to undergo patellar tendon force, the quadriceps muscle force and a patello-femoral reaction force.

One of the model of the patello-femoral joint was a 2 dimensional model developed by Van Eijden *et al.* [43]. In this model, both movements and forces in the sagittal plane were considered. The quadriceps muscle was assumed to be a string of variable length that freely changed direction as it wrapped around the femur and the patellar ligament was assumed to be an inextensible link. The profiles of the articulating surfaces were represented by parametric functions, and a single point contact between surfaces was assumed. For a given joint position, a set of nonlinear equations were solved to obtain the position of the patellar ligament, patella and quadriceps tendon, the location of the patello- remoral contact point, and the ratios of the patellar ligament force and the quadriceps tendon force to the reaction force, respectively.

Hirokawa [44] presented another mathematical model analysis of the patello-femoral joint which includes articulating surface geometry and mechanical properties of the ligaments. In the model, a computed-aided-design theory was introduced for the solution. It has been possible to express the articular surface geometries in a mathematical formulation and hence explain the joint movement mechanic.

2.2.2.4.2 Models of The Tibio-Patello-Femoral Joints

The tibio-patello-femoral model including the three segments of the knee: tibia, patella and femur, which was developed by Tümer and Engin [45]. Model included two contact surfaces for each articulation, three muscle groups (quadriceps femoris, hamstrings, and gastrocnemius), and the primary ligaments (anterior cruciate, posterior cruciate, medial collateral, lateral collateral, and patellar ligaments). it was possible to see the effect of specified muscle actions as well as extremely-applied transient forces on the lower leg. The authors simulated the extension of the knee under the impulsive action of the quadriceps femoris muscle group. Also, tibio-femoral and patello- femoral contact forces, as well as forces in various ligaments are determined during dynamic motion of the knee.

Pandy *et al.* [46] and [47] developed a 3-D musculoskeletal model of the human knee joint to investigate the interactions between the muscles, ligaments and bones. The geometry of the femur, tibia and the patella are represented by 3-D polynomials. Their model included cartilage between tibio-femoral contact, modeled as a thin, linear, elastic layer mounted on rigid bone, the ligaments modeled as nonlinear springs. The model is actuated by musculotendinous units, each unit modeled as a three-element muscle in series with tendon.

Full lower limb FE model, developed by Beillas *et al.* [48] allows simulation of the experimental knee kinematics under impact loading during “hopping on one leg” condition, with high accuracy. Although their model is highly accurate, due to the explicit nature of the technique, the computation can be laborious. Nonlinear elastostatic finite element model including articular cartilage, menisci and four major ligaments, to investigate the coupling between anterior and posterior cruciate ligaments under anterior femoral force at different flexion angles was developed by Moglo and Shirazi-Adl [49]. Their model was quasi-static and was more focused on the role of PCL on the joint response and the coupling between cruciate ligaments under 100 N anterior force at different flexion angles.

2.3 Theory of Motion Analysis

Motion analysis is the subjective or objective analysis of human locomotion. It can be performed as taking the direct and indirect measurements. The direct measurements, goniometers and accelerometers, gives information about the instant joint angle or velocity and displacement of limb the limb segment by attaching the devices to the body. If the clinician wants to see the body movement as a whole, large number of devices is needed and movement is affected by straps and cables.

With the advance of digital image processing techniques, indirect and objective analysis of human motion became available. Depending on the type of application, 2D photography, 2D video imaging, and 3D video imaging may be utilized. Developments in video imaging and processing techniques allow us to record position-time information of each joint and limb and interpret to a high-resolution 3D coordinate frame. Markers are placed on important points of the body to measure the motion and kinematic parameters: joint angles, velocities, and accelerations. In addition, ground reaction forces are utilized in the calculation of kinetic parameters like forces, moments, and momentums.

It should be pointed out that just because a system computes the 3D coordinates of each marker, it does not mean, a priori, that 3D kinematics will be produced. To obtain true 3D motions, each body segment must be defined by at least three markers (which create a plane passing through the segment), joint centers must be defined, and Euler angles computed. Knee and ankle joint centers are either determined from width measurements or medial markers used only during a calibration ("quiet standing") test (Figure 2.23).

Link segment model is an idealization of a non-rigid body onto a rigid frame. In this model each segment of the body is defined using 3 marked points: at two nodes apart and in the middle of the limb. These markers should form a plane on the limb and the lengths in between. Those planes are used to determine:

- The center of rotation of each joint, and
- The linear and rotational position of each limb.

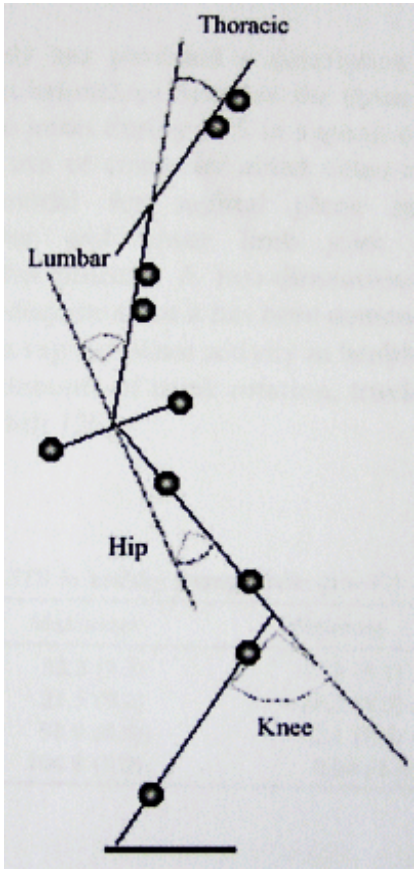

Figure 2.23 Link segment model representation.

2.3.1 Kinematics

Kinematic variables describe the movement, independent of the forces that cause the movement. They include linear displacements, *d*, speed, *s*, and velocities, *v*, and accelerations, *a*, and also angular displacement, Θ, velocities, ω, and accelerations, α [50].

Movement or motion indicates a joint action, the relative angular movement of the limbs on the distal and proximal sides of the joint [50]. By identifying the plane of motion in which direction the action takes place, motions are defined by flexion and extension occurring when movement around the transversal axes, movement around antero-posterior axes is identified by abduction (moving out from the body) and adduction (toward the body), movement around the longitudinal axes is called rotation, internal and external.

To describe the kinematics of a segment a coordinate reference system is used. Each segment can be set with an origin and a principal axis, which is usually defined along the long axis of the segment. Three dimensional imaging systems are used to detect kinematic data from a subject in a motion analysis. Three types of coordinate systems are used to derive the kinematics, the global reference system (GRS) which remains fixed in space, a technical reference system which is derived from the subject's reflective markers, and an anatomical reference system (ARS) which is attached to each body segment [51].

A moving segment's translation and rotation, are described by the segment's ARS position and orientation relative to the GRS. In two dimensional translation of a point, a, in the ARS, (x_i,y_i), relative to the GRS, (X_i, Y_i), can be written as [50]:

$$\begin{bmatrix} X \\ Y \end{bmatrix}_a = \begin{bmatrix} X \\ Y \end{bmatrix}_i + \begin{bmatrix} c & -s \\ s & c \end{bmatrix} \begin{bmatrix} x \\ y \end{bmatrix}_{ia} \qquad (2.1)$$

Where *s* is denoting sine and *c* cosine of an angle (θ).

A rigid body moving in a three dimensional system, has a possibility of translations and rotations. This implies a 3 × 3 transformation matrix, [ϕ].A common angular system used to define the angular orientation in space is the Euler system of angles. A specific definition of Euler angles will describe in which sequence the rotations take place [50]. Euler's convention contains 12 different sequences of rotations [51].

An axis system denoted by *x, y, z* will be transformed into a system denoted by *x‴, y‴, z‴* in a chosen sequence. The Cardan system, which is common in biomechanics, describes the sequence order of axes to rotate about (Equations 2.2, 2.3, 2.4 and 2.5) [50]. The first rotation, θ_1, is about the x axis to get *x′, y′, z′;* the second rotation, θ_2, is about the new y' to get *x″, y″, z″;* and the last rotation, θ_3, is about *z″* to get to *x‴, y‴, z‴*.

An assumed point in the original *x, y, z* axis system with coordinates x_0, y_0, z_0, will have coordinates x_1,x_1, x_1 in the *x′ ,y′, z′* axis system, based on rotation θ_1. The second rotation θ_2 will provide coordinates x_2,y_2,z_2 in the axis system *x″, y″ ,z″,* and the final rotation θ_3 will provide the point the coordinates x_3, y_3, z_3 in the axis system *x‴, y‴, z‴*. These rotation can be written as:

$$[\phi_1] = \begin{bmatrix} 1 & 0 & 0 \\ 0 & c_1 & s_1 \\ 0 & -s_1 & c_1 \end{bmatrix}, \tag{2.2}$$

$$[\phi_2] = \begin{bmatrix} c_2 & 0 & -s_2 \\ 0 & 1 & 0 \\ s_2 & 0 & c_2 \end{bmatrix}, \tag{2.3}$$

$$[\phi_3] = \begin{bmatrix} c_3 & s_3 & 0 \\ -s_3 & c_3 & 0 \\ 0 & 0 & 1 \end{bmatrix}. \tag{2.4}$$

Where (c_1, s_1), (c_2, s_2) and (c_3, s_3) denote ($\cos\theta_1$, $\sin\theta_1$), ($\cos\theta_2$, $\sin\theta_2$), and ($\cos\theta_3$, $\sin\theta_3$) respectively.

The transformation of the point from the axis system x, y, z to x''', y''', z''' can then be reduced to [52]:

$$\begin{bmatrix} x''' \\ y''' \\ z''' \end{bmatrix} = [\phi_3] \cdot [\phi_2] \cdot [\phi_1] \cdot \begin{bmatrix} x \\ y \\ z \end{bmatrix}. \tag{2.5}$$

2.3.2 Kinetics

Kinetics deals with the forces associated with a movement. Internal forces come from muscle activity, tendons and ligaments, and joint contact forces and external forces comes from ground reaction forces, segment weight, or applied loading on the musculoskeletal system [50]. Knowledge of the muscle forces is important for understanding the causes of movement. Kinetic quantities are evaluated from kinematics, anthropometric data and external forces, such as the ground reaction force, f_{GRF}, [50].

Newton's second law of motion (Equation 2.6) together with the Euler dynamic equation (Equation 2.7), make up the basis for the mathematical model of the limbs called

link-segment modeling using inverse dynamics, where joint forces, *R,* and joint moments, *M,* are calculated [50,53] as:

$$R = m \cdot a \tag{2.6}$$

$$M = I \cdot \alpha \tag{2.7}$$

where *m* is the mass of the object, *a* is the linear acceleration, *I*, is mass moment of inertia and α is the angular acceleration of the object.

Link-segment modeling and free body diagram of the foot- and shank segment, showing moments of inertia, I_i, masses, m_i, reaction forces, R_{yi} and R_{xi}, joint moments, M_i, i = 1,2,3. Moment and forces are calculated via inverse dynamics (Equations 2.8 and 2.9). The link-segment model is broken down at the joints into segments which are treated separately as rigid bodies, creating a free-body diagram (Figure 2.24(a)) [54]. In accordance to Newton's third law, there is an equal and opposite force acting at each joint, and moment and forces can be evaluated at any joint with a known external loading or reaction force. Modeling the limb in this way carries the assumptions that (1) each segment has a fixed mass located at its center of mass (in the center of gravity) (2) the location of each segment's center of mass (COM) remains fixed (3) joints are considered without translations (4) mass moment of inertia of each segment is constant and (5) the length of each segment is constant during movement [50].

The method of inverse dynamics is usually employed in gait analysis to compute the net joint moments, net joint powers and intersegmental forces. Evaluation starts at the foot segment (Figure 2.24(b)) with the ankle joint forces and moment (Equations 2.6 and 2.7) [54]. Establishing the forces in the y direction and the moment about the ankle, M_i:

$$\sum R_{yi} = m_i \cdot a_{yi} = f_{GRFyi} + R_{yi} - mg\,, \tag{2.8}$$

$$\sum M_i = I_i \cdot \alpha = f_{GRFyi} d_{GRF} + R_{yi} d_{yi}\,. \tag{2.9}$$

Where d_{GRF} describe the moment arm of the ground reaction force f_{GRFy} to the ankle joint and

d_y the moment arm to the reaction force R_{y1} to the ankle joint. The weight mg is located at the center of mass (COM), moment of inertia, I, is evaluated from anthropometric tables. Linear and angular acceleration, a and α, are obtained from kinematic data. From this point the knee joint moment and forces can be evaluated by applying equal and opposite reaction force on the shank segment (Figure 2.24.c) [54].

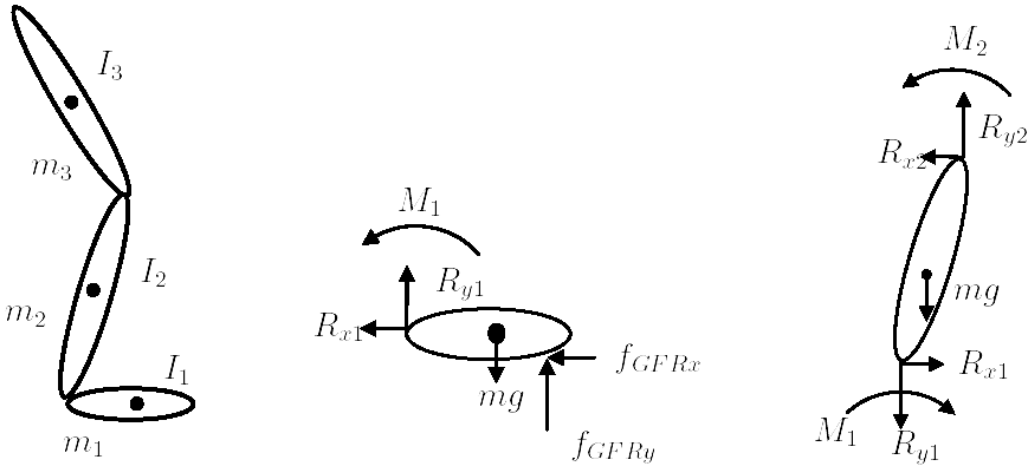

(a) Link Segment (b) Foot Segment (c) Shank Segment

Figure 2.24 Link-segment modelling and free body diagram. Adapted from [54].

2.3.3 Gait Analysis

2.3.3.1 Normal Gait

The determination of abnormal gait requires one to first have an understanding of the basic physiology and biomechanics of normal gait [50]. The gait cycle is a time interval or sequence of motion occurring from heel-strike to heel-strike of the same foot. The gait cycle has been broadly divided into two phases: stance phase and swing phase.

The stance phase is about 60 percent of the gait cycle and can be subdivided into double-leg and single-leg stance. In double-leg stance, both feet are in contact with the

ground. Single-leg stance comprises up to 40 percent of the normal gait cycle. The muscles that are active during the stance phase act to prevent buckling of the support limb (Figure 2.25) [56].

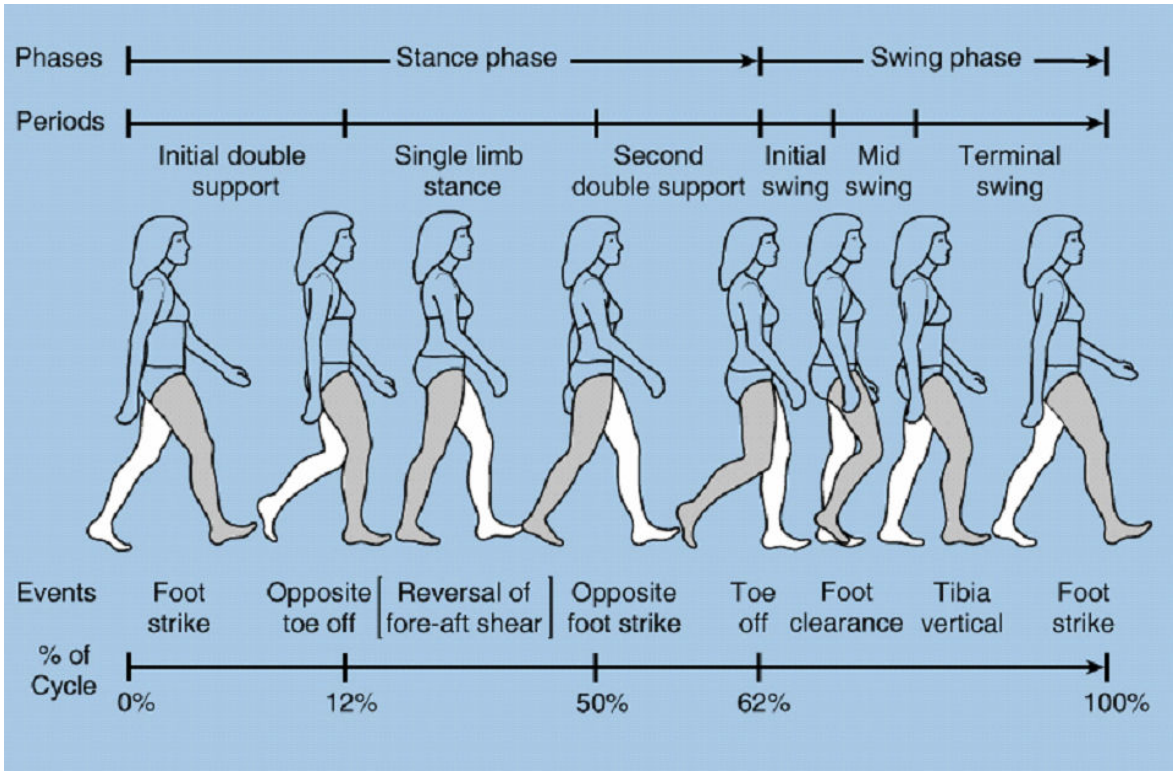

Figure 2.25 Time dimensions of the gait cycle. Adapted from [56].

The swing phase is described when the limb is not weight bearing and represents 40 percent of a single gait cycle. It is subdivided into three phases: initial swing (acceleration), midswing, and terminal swing (deceleration). Acceleration occurs as the foot is lifted from the floor and, during this time, the swing leg is rapidly accelerated forward by hip and knee flexion along with ankle dorsiflexion. Midswing occurs when the accelerating limb is aligned with the stance limb. Terminal swing then occurs as the decelerating leg prepares for contact with the floor and is controlled by the hamstring muscles [56].

2.3.3.2 Computerized Gait Analysis

The pattern of how a person walks is called the gait. The ability to walk upright is a defining characteristic of man. Gait is the manner in which walking is performed and can be normal, antalgic, or unsteady. Gait analysis is a sophisticated laboratory technique by which modern electronics are used to incorporate information from a number of inputs to illustrate and analyze the dynamics of gait (Figure2.26). It describes for the clinician (physician, surgeon, therapist) in quantitative and dynamic terms the movement of the body and its limbs and the changing relationships of one extremity to other extremities during motion (e.g.: walking, leg raising). It helps the clinician judge what are the forces resulting in a dysfunction in movement of a limb and what is the result of compensating for the dysfunction; to put it another way, what is cause and what is effect [55].

a) b)

Figure 2.26 Illustration of setting reflective markers (a) and gait analysis (b).

The 3D motion of pelvis, knee and ankle during walking is illustrated in Figure 2.27. The y axis demonstrates the anglular displacements of the joint and x axis shows the percentage of the one gait cycle (the duration of time between two heel strikes [58].

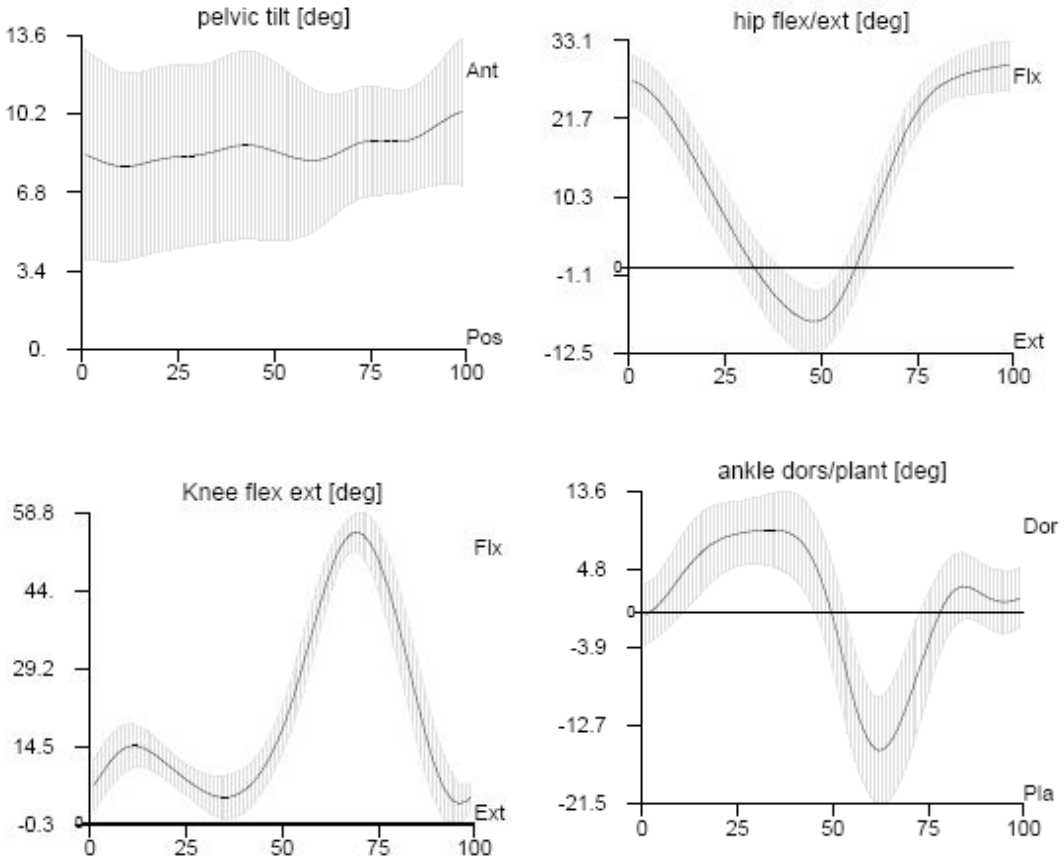

Figure 2.27 Normal kinematics of the pelvis, hip, knee, ankle during walking. Adapted from [58].

The normal kinetics during walking illustrated in Figure 2.28. The first row of the figure shows the sagittal plane kinematics of hip (left), knee (middle) and ankle (right). The second row demonstrated the normalized moment (N-m/kg) of the hip, knee and ankle. The third line illustrates normalized intersegmental power (Watts/kg) of the hip, knee and ankle.

A force signature, vector, or butterfly graph combines the three force components and center of pressure (COP) location in to one 2-D image that can be rotated to view in three dimension. A typical walking signature has two humps and often a spike immediately after initial foot contact. Figure 2.29 shows the forces from a single footfall in which the rear foot landed on one force platform and the forefoot and other, a set up used in a two segment foot model to improve accuracy in modeling the foot dynamics during walking. Also shown in the

single ground reaction force (GRF). This process enables the computation of the moments of force across the metatarsal phalageal joint, which is usually modeled as rigid body. During walking, peak forces fluctuate around the body-weight line by approximately 30% of body weight [59].

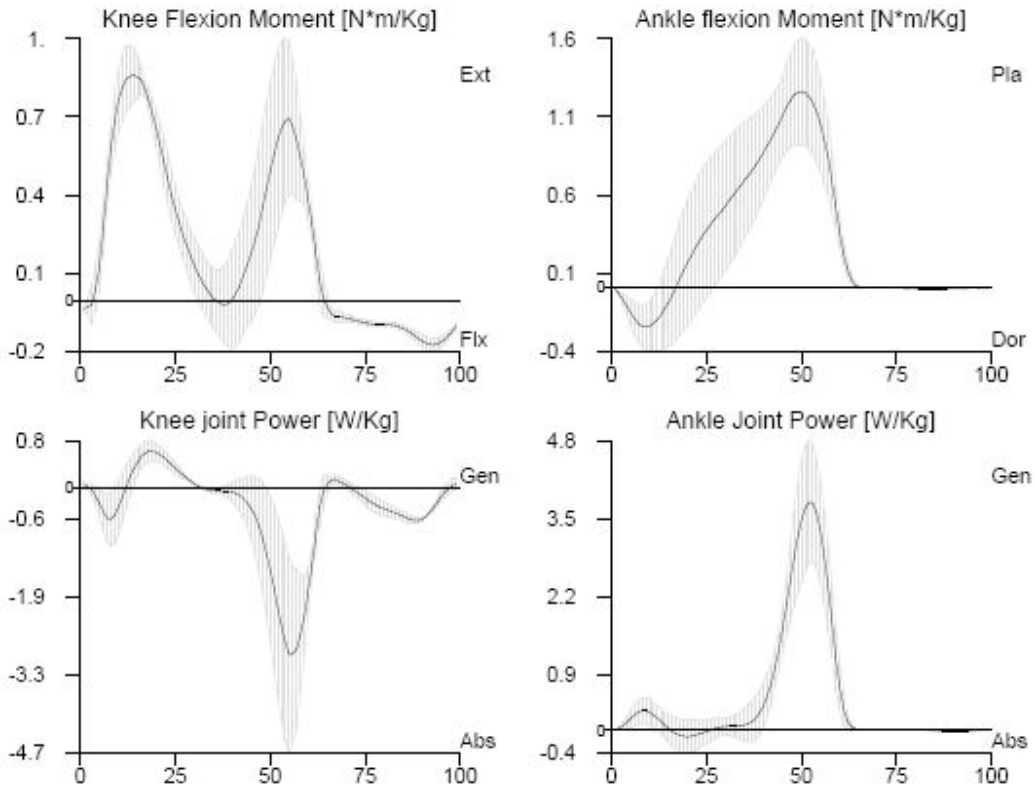

Figure 2.28 Kinetics of the joints during normal walking. Adapted from [58].

2.3.4 Gait Abnormalities

Walking or gait abnormalities are unusual and uncontrollable problems with walking. Many different types of gait abnormalities are produced unconsciously. Most, of them are due to some physical defect [14].

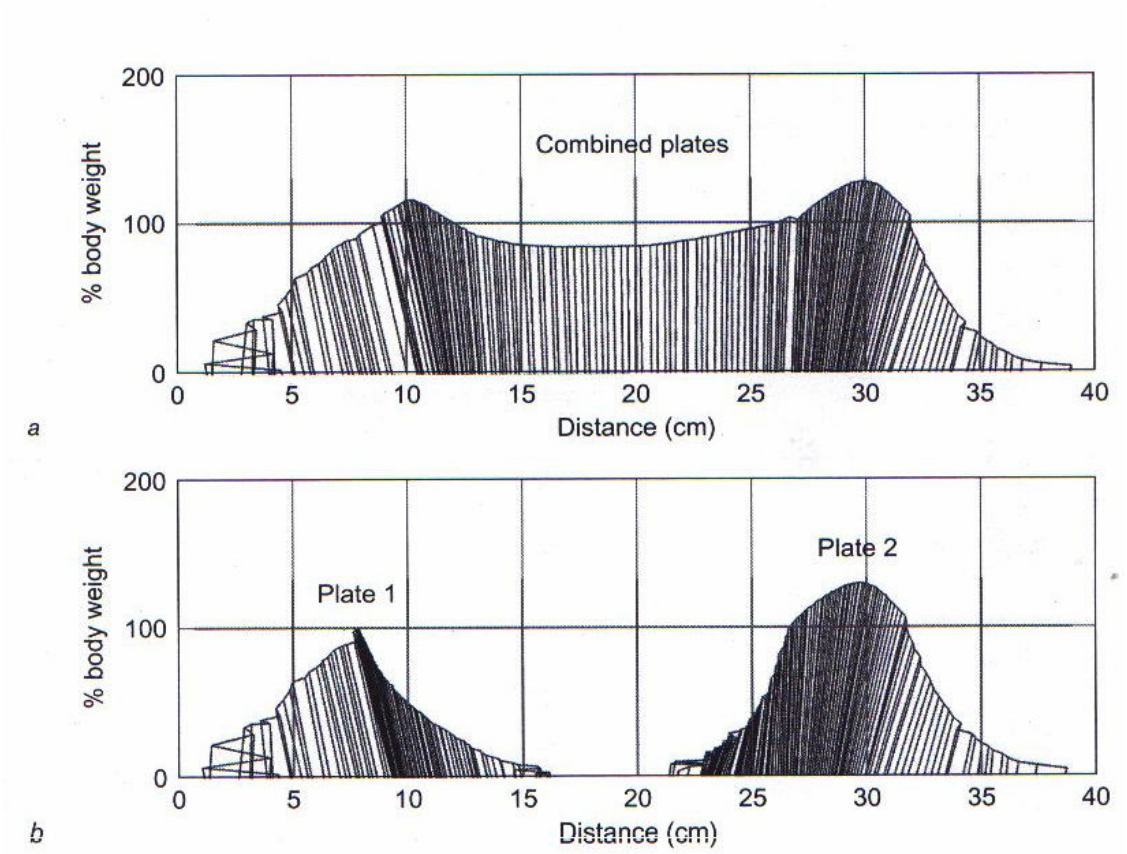

Figure 2.29 (a) Combined ground reaction force (GRF) vectors from walking. (b) Same GRF from force palteforms under rear and forefoot. The line segments indicate direction and relative magnitudes of GRFs. The lower end of the segments correspond to the location of the COP in the antero-posterior direction. Adapted from [59].

2.3.4.1 ACL Deficiency

The motions of the knee during walking are determined by the interaction between the passive constraints of the joint and the forces acting on the joint. Thus rupture of the anterior cruciate ligament (ACL), one of the four major ligaments of the knee, is likely to cause changes in the kinematics of the knee during walking. ACL provides primary anterior and rotational stability to the knee [60]. In particular, changes in the anterior–posterior (AP) translation and internal–external (IE) rotation of the ACL deficient knee can be expected during specific phases of the gait cycle if there is an anterior force or internal–external

moment acting at the knee.

The AP translation and IE rotation are particularly important for normal knee function even during routine activities such as walking. Alterations or a shift in AP translational and IE rotational motion of the knee during dynamic activities could have profound effects on secondary restraints such as the medial meniscus. Clinical reports of the presence of osteoarthritis of the knee in patients with ACL injury suggest that abnormal motion at the knee could be a cause of degenerative changes [60].

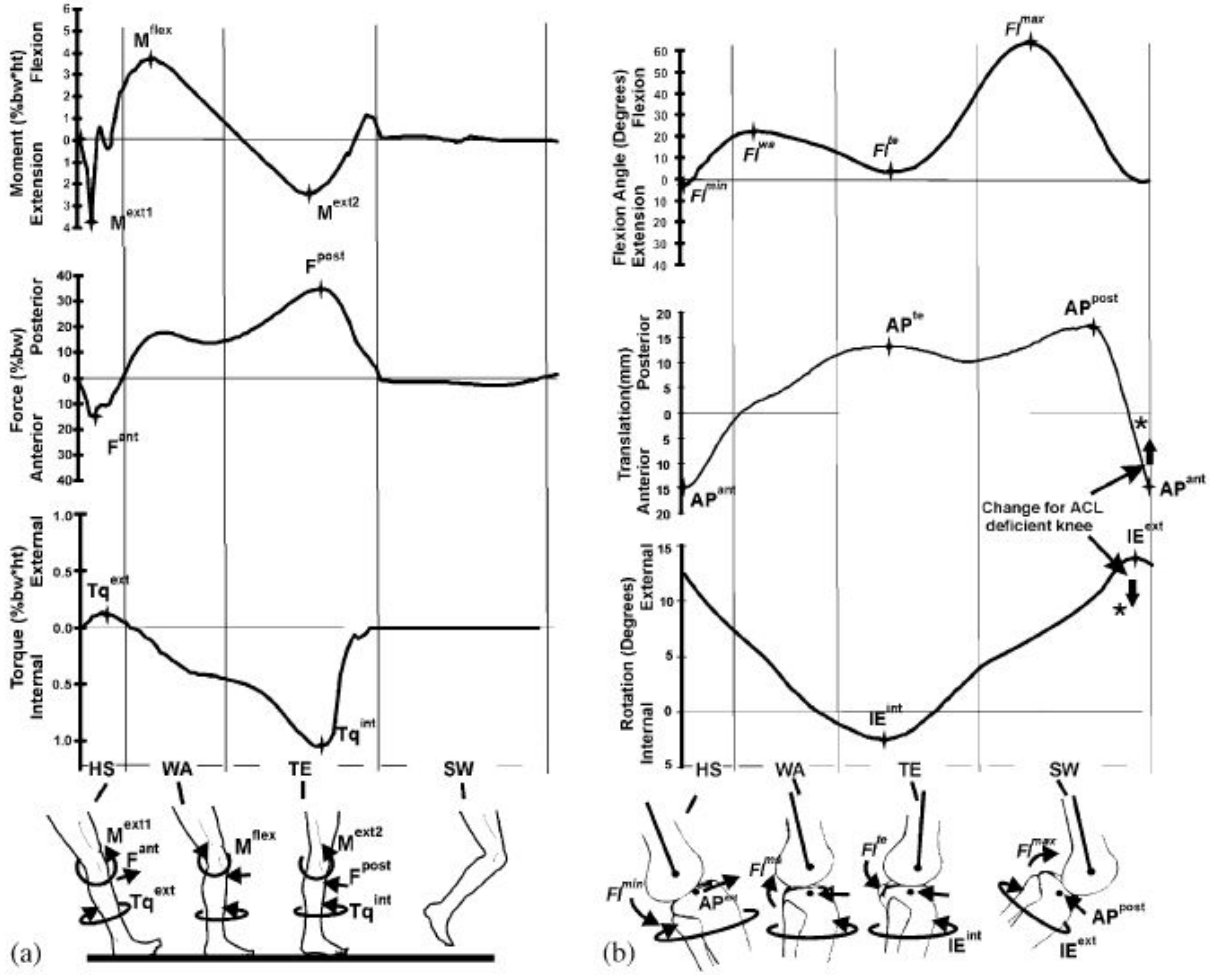

Figure 2.30 (a and b), The gait cycle divided into four phases (HA, WA, TE and SW). The extrema of intersegmental anterior–posterior force (Fant, Fpost) were in the same direction as the corresponding displacements (APant and APte) during stance phase. The extrema of intersegmental internal–external moment (Tqext and Tqint) were in the same direction as the corresponding rotations (IEext and IEint) during stance phase. The arrow_ indicates the direction of significant changes for the ACL deficient knee. Adapted from [60].

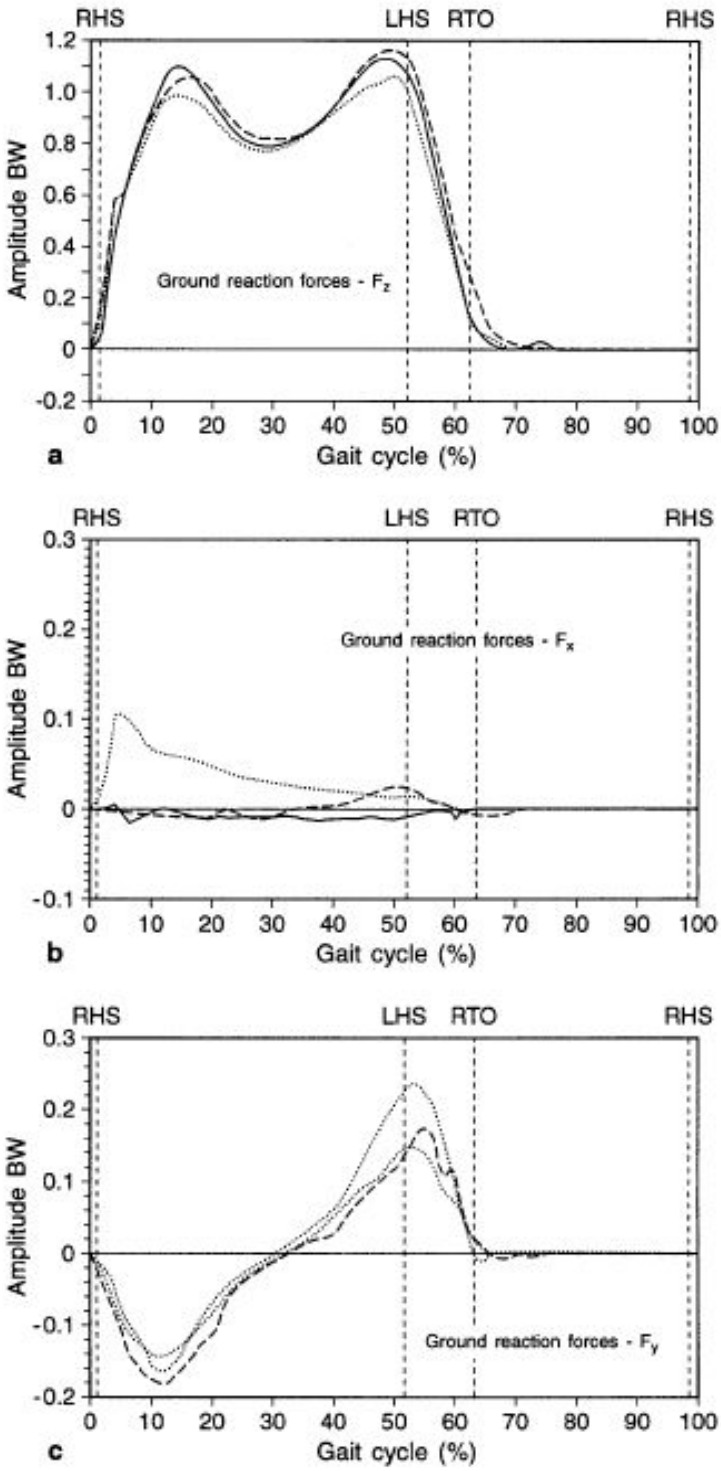

Figure 2.31 Mean values of the ground reaction forces (——— normal subjects, ····· ACL-deficient subjects, – – – ACL-reconstructed subjects). The amplitude of the force is indicated in relation to the phases of the gait cycle beginning with heel strike. Values are normalized to subject's weight. Adapted from [61].

Andriacchi *et al.* found that kinematic changes associated with complete tear of the ACL occurres primarily during the terminal portion of swing phase of the walking cycle where, for the ACL deficient knee, the tibia has reduced external rotation and anterior translation as the knee extends prior to heel strike (Figure 2.30). In particular, during swing phase, the ACL deficient knee has reduced external rotation as the tibia extended prior to heel strike, suggesting a loss of the normal screw home movement that causes maintained internal rotation in stance phase.

Bulgheroni *et al.* [61] showed for ACL-deficient subjects that the knee extension moment is significantly greater at heel strike. During the loading response, a reduction of the knee flexion moment was compensated by an increased flexion moment at the hip joint. These authors also found that both the knee and the hip show a decreased adduction moment during the entire stance phase. The ankle joint shows significant changes only in the sagittal plane: upon loading the extension moment is reduced, and during the preswing phase, the flexion moment is increased with respect to the normal control group [61].

Andriacchi *et al.* concluded that the abnormal rotational position were correlated with the magnitude of the flexion moment (balanced by a net quadriceps moment) during weight acceptance. These results suggest that adaptations to the patterns of muscle firing during walking can compensate for kinematic changes associated with the loss of the ACL.

On the other hand, the analysis of ground reaction forces (Figure 2.31) demonstrate a significant reduction of the peak values of the vertical component, an altered horizontal component at the loading response and an increased anterior force at preswing ($P < 0.05$) [61].

2.3.4.2 Anterior Drawer Test

The Drawer test is considered clinically to be the most reliable diagnosis for an anterior cruciate ligament (ACL) lesion. The patient's knee is flexed to 90°, and the hip is flexed to 45°. In this position, the anterior cruciate ligament is almost parallel to the tibial plateau. The patient's foot is held on the table by examiner's body with the examiner sitting on

the on the patient's forefoot and the foot in neutral rotation. The examiner's hand are placed around the tibia to ensure that the hamstring muscles are relaxed (Figure 2.32). The tibia is then drawn forward on the femur. The normal amount of movement that should be present is approximately 6mm. The drawer test may be applied by rotating the tibia internally and externally. Tibia slides forward anteriorlly with external rotation more than internal rotation for patient with ACL deficiency [81]. This test assesses only one plane anterior stability [17]. The difficulty of this test is determining the neutral starting position if the ligaments have been injured.

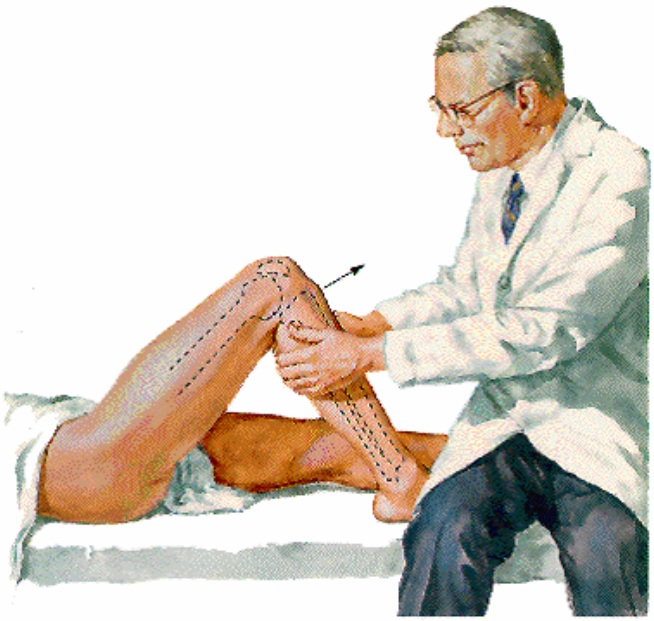

Figure 2.32 The illustration of anterior drawer test. Adapted from [17].

2.3.5 The Simulation Tool

The simulation tool which is called BRG.LifeMOD was used in the present study [62].

The resulting system is expected to provide researchers with a tool to simulate walking, calculate force and rotations at joints, pinpoint which portions of the step cycle need augmentation, and devise ways of placing less stress on muscles and bones. Each leg of the full-body model is comprised of 26 bone segments representing the femur, tibia/fibula, and the

many intricate bones in the foot. These bones are coupled with mechanical joints and bearing surface contact joints. Redundancy issues such as soft tissue spanning several joints are included in the model. Methods for handling ill-conditioned properties such as agonistic/antagonistic muscle activity are also included [62].

ADAMS Software is helping orthopedic and prosthetic device manufacturers study the behavior and mechanical performance of a variety of devices as well as simulate the surgical procedures of orthopedic implants (Figure 2.33).

Motion data from a source such as digitized video (MOCAP) can be imported to drive the passive, reacting to the forces of gravity and the environment, or active, effecting the environment though muscle/joint forces models.

BRG.LifeMOD contains a facility called "Motion Agents" which provide a method to distribute this motion data on the segments of the human model. Motion agents are mass-less parts which track the trajectories of the recorded motion. They are attached to the model using spring bushing elements so as to influence the motion of the human model, not govern it. This allows for the model to only move within the kinematic capabilities of the joints and the dynamics of the environment (i.e., the foot will not penetrate the floor).

For passive human models, the joints are built using passive force elements consisting of nonlinear stiffness, damping, friction and joint stops with hysteresis. The data curves used for the passive elements are derived from the actual Hybrid III Crash Dummy [62].

For active human models, the joints are built using PD-servo torque elements or articulate or biarticulate muscle forces. The PD-servo Joint torques are driven using an angulation history recorded from an inverse dynamics simulation, or a simulation in which the model is articulated using Motion Agents.

The muscle forces contain a series elastic and contractile element. The contractile element is driven using muscle elongation history information recorded from an inverse dynamics simulation.

For the forward dynamics simulation, the motion agents used to induce the motion for the inverse-dynamics simulation are removed from the model. The joints and/or muscles are updated to include the angulation/contractile histories and a simulation is performed with the

human model as the active element [62].

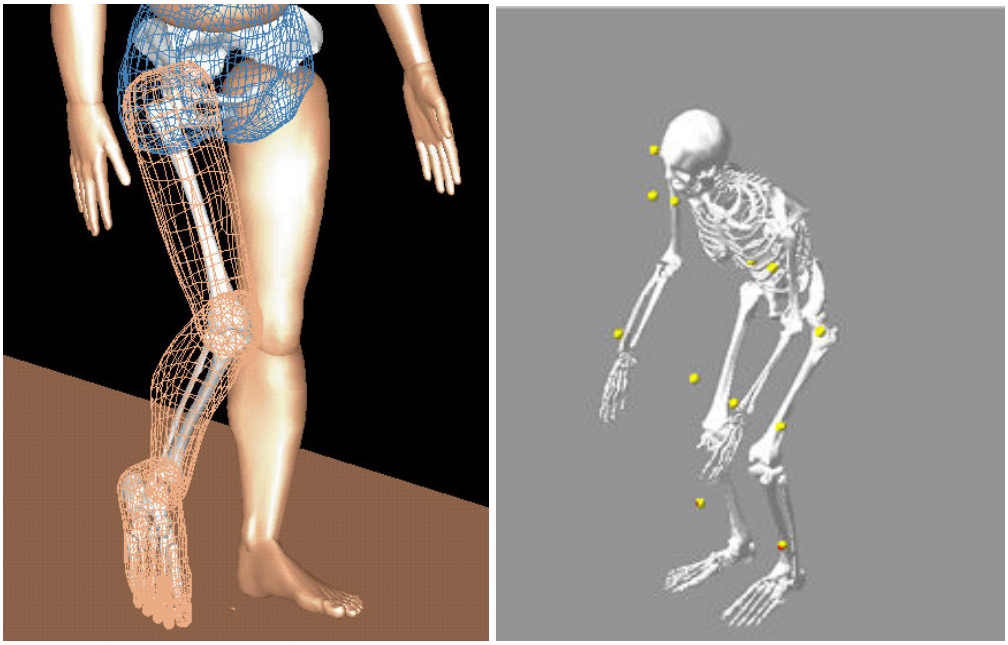

(a) (b)

Figure 2.33. Illustration of ADAMS a) and LIFEMOD b) software. Adapted from [62].

3. MATERIALS AND METHODS

The objective of this study is to illustrate the role of the ligament bundles and contact surfaces on passive knee motion. Different from the existing models in the literature we included multiple contact points, and we did not assume spherical shape for the femur condyles. To test our model, we compared the tibial rotation, translation and contact forces during passive knee flexion of a normal knee model. After the completion of the tibiofemoral model a dynamic patello-femoral joint model was created and the tibiofemoral model was integrated in to the dynamic patella-femoral model to simulate walking pattern for a person with intact knee joint and with ACL deficiency. The patello-tibio-femoral model was also tested by simulating drawer tests and knee extension exercise for medium level quadriceps contraction. The patello-tibio-femoral model was also integrated into full body musculoskeletal model in LIFEMOD software. To simulate normal and ACL deficient walking, ADAMS and LIFEMOD software [62] with a work station was used. This study was performed at Boğaziçi University, Istanbul, Turkey.

3.1 Constraint Based Model

First we modeled a three-dimensional tibia that is anatomically appropriate. It has a mass of 4kg, with the inertial parameters: I_{xx}=0.0672 kg m^2, I_{yy}= 0.0672 kg m^2, and I_{zz}= 0.005334 kgm^2 as for an average male adult described in Abdel-Rahman and Hefzy [10].

It was assumed that the tibial condyles are planar expressed as;

$$g(x, y) = my + c \tag{3.1}$$

where *m* and *c* are (0.358, 213mm) and (0.341, 212.9mm) for the medial and lateral tibial plateaus, respectively (Fig 3.1 and 3.2) [10].

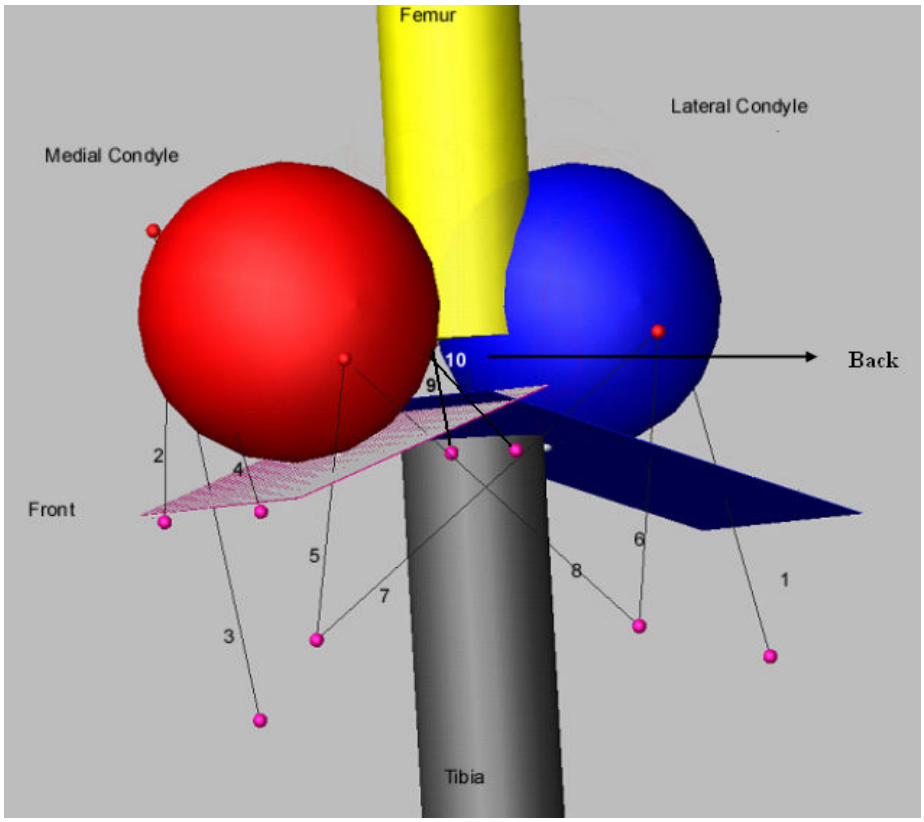

Legends:

1 LCL: Lateral Colleteral Ligament

2 aMCL: Anterior bundle of Medial Colleteral Ligament

3 dMCL: Deep bundle of Medial Colleteral Ligament

4 oMCL: Oblique bundle of Medial Colleteral Ligament

5 MCP: Medial Capsule of Popliteal ligament

6 LCP: Lateral Capsule of Popliteal ligament

7 OPL: Oblique Popliteal ligament

8 APL: Arcuate Popliteal Ligament

9 aPCL: Anterior bundle of Posterior Cruciate Ligament

10 pPCL: Posterior bundle of Posterior Cruciate Ligament

Figure 3.1 Back-oblique view of three-dimensional model of the knee joint.

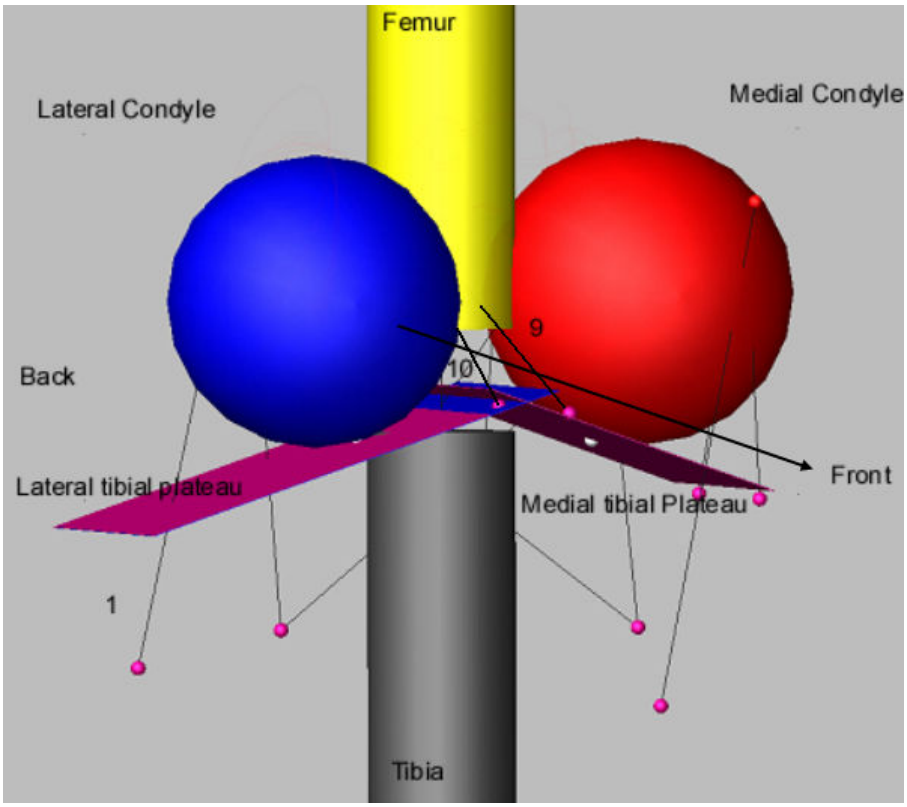

Legends:

9 aACL: Anterior bundle of Anterior Cruciate Ligament

10 pACL: Posterior bundle of Anterior Cruciate Ligament

Figure 3.2 Frontal-oblique view of three-dimensional model of the knee joint.

As an approximation, we have considered a ligament as isometric if its relative length is within ± 0.05 of its original length. As a result, anterior portion of ACL and PCL, anterior and deep fascicles of MCL become the tensile constrains during passive knee flexion [13] as illustrated in Figure 3.3.

Then the isometric ligament attachment points for aACL, aPCL, aMCL and dMCL were identified on the tibia according to reference model [10]. The corresponding attachment points of the same ligaments were identified on a rigid body representing femur. No assumption was made at this stage about the shape of the femur condyles. Four rigid links

were attached through spherical joints to the femur from one end and to the tibia on the other as in Figure 3.4. The links were attached at the ligament attachment points with the same lengths of the corresponding ligaments.

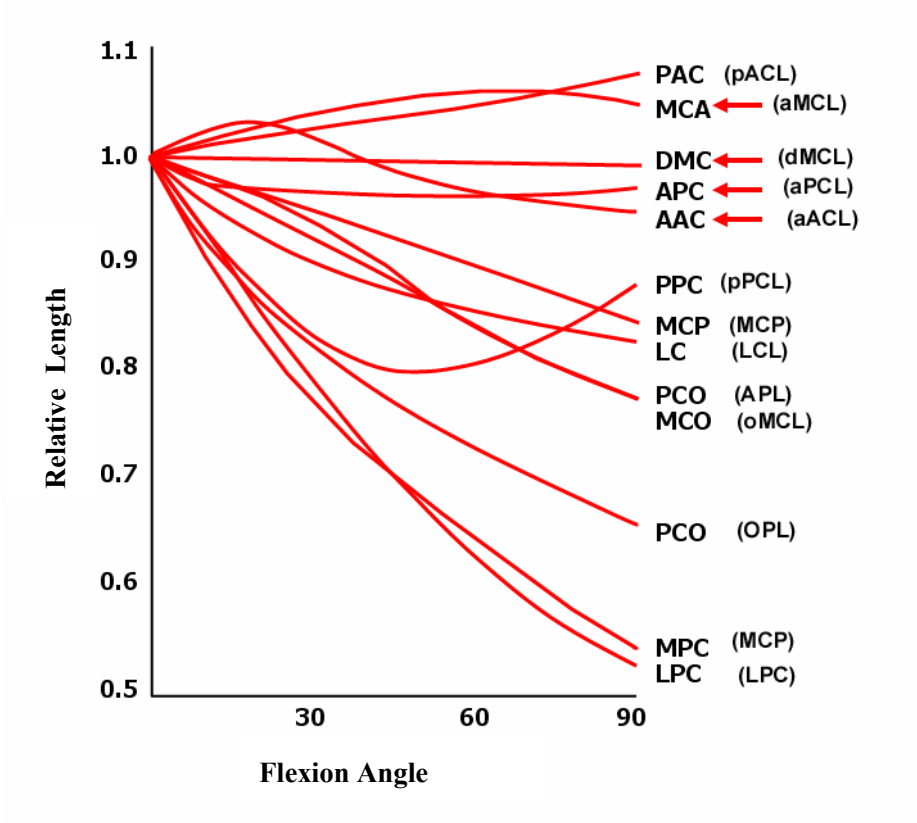

Figure 3.3 Relative ligament length during knee flexion. Closely agreed with the literature. The abbreviations in parenthesis state the ligaments in this study correspond to Crowninshield *et al.*`s representations for each ligament. Adapted from [13].

Different from the models in the literature, we adapted the contact points reported in Freeman *et al.* [3]. These contact points defined for an average male adult for passive knee flexion were transformed in to our model by matching the 0° knee flexion contact point between Freeman's representation and Abdel-Rahman and Hefzy's model at the same orientation. Ten contact points were determined on tibial plateau corresponding to sliding and rolling motion of the knee in segments as illustrated in Figure3.5, Table 3.1 [3].

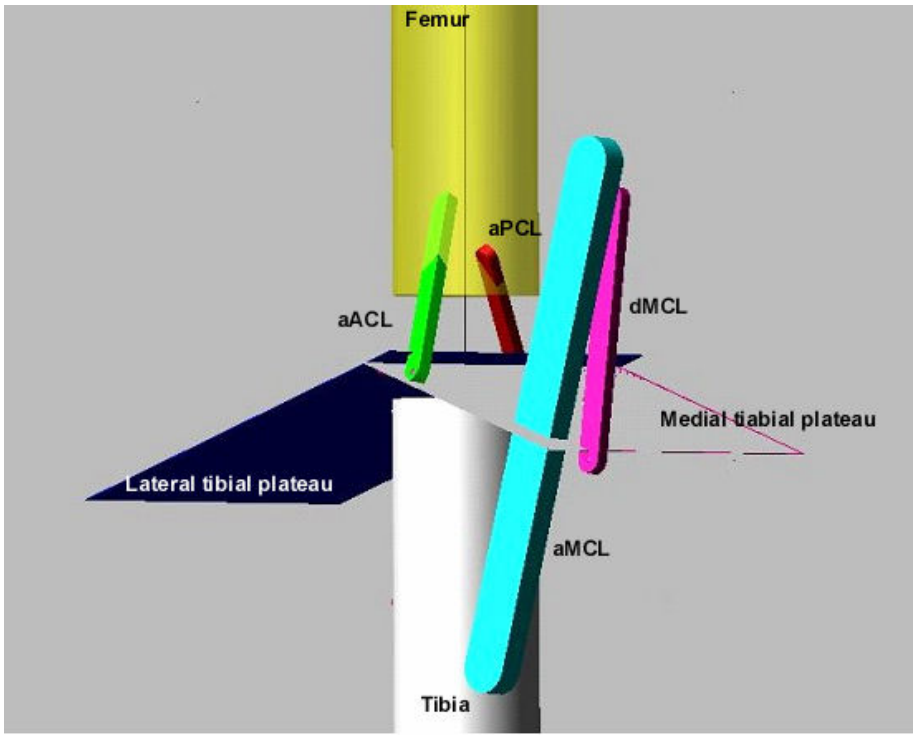

Figure 3.4 Assumption of inextensible rigid ligaments.

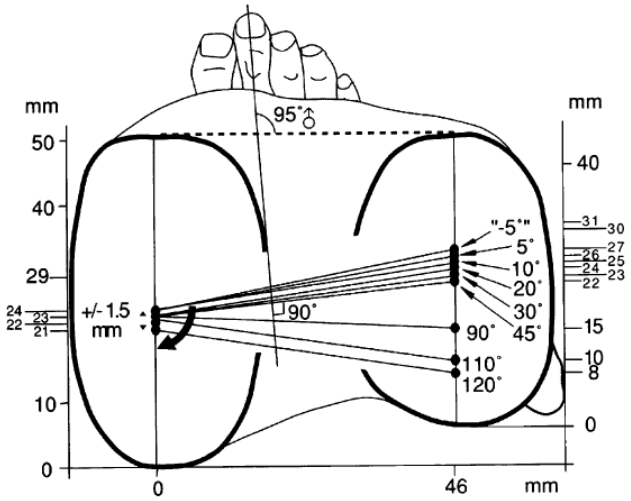

Figure 3.5 Contact points during passive knee flexion Adapted from [3].

During flexion, the contact points were clustered about the center of the medial tibial plateau, while the contact points were distinct in the lateral plateau. In our simulation knee

flexion range was 0-90° and the contact points in lateral and medial plateau were sampled from [13] and paired as in Table 3.1.

Table 3.1 Medial and lateral contact points on tibial plateau for flexion range from 0 to 110° [3].

Flexion Angle	Contact Points (mm)	
	Lateral	Medial
[0-10°)	26.5*	24
[10-20°)	25	24
[20-30°)	24	23
[30-45°)	23	23
[45-90°)	22	23
[90-110°)	15	22
[110-120]	10	21

*(Average of -5° and +5°)

Contact points defined for an average adult were mapped in to our coordinate system. Only the first six of the seven points from the lateral plateau were used due to the range of flexion. There were only three distinct contact points on medial side for the same range of motion. Consequently six contact point trajectories for the lateral and three for the medial sides were produced.

In the simulation knee was extended referred to as 0° as the initial condition. The tibio-femoral knee flexion was obtained by fixing the femur horizontally while letting the tibia fall

freely due to gravity in supine positioned knee. The simulation was ended when the knee reached at 90° flexion due to the gravity. Gravity was the only force acting on the tibia.

If the femur condyles were in place they would contact to the tibial plateau with in the proximity of the contact points identified as in Freeman *et al*. [3] for the specified range of knee flexion (Table 3.1). Therefore, the traces of these contact points during the knee flexion identify the contact surfaces on the femoral condyles. The assumption is that the rigid links together with the contact points on the tibia define a trajectory similar to femoral shape. There were 9 trajectories in total corresponding to the 9 contact points for the range of motion studied here. Each trajectory represents a span of the flexion for the range defined in Table 3.1. The trajectory segments for each compartment, medial (3 segments) and lateral (6 lateral segments), were concatenated end to end within the compartment. A smoothed transition between the seven segments in the lateral and three segments in the medial compartments yield the two femoral condyles (Figure3.6 and 3.7).

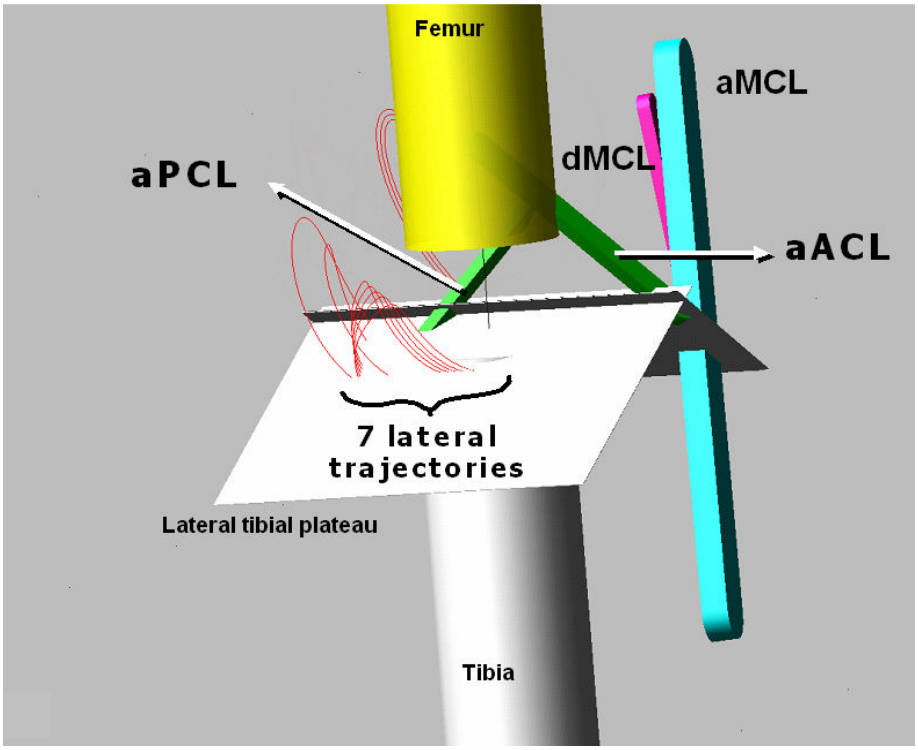

Figure 3.6 Seven lateral trajectories of the contact points after tracing the lateral contacts during knee flexion and the constraints of the model in the present study.

The compressive and tensile forces produced on the four links are the constraints of the passive knee motion in this simulation. After defining the femoral condyle shapes from the contact trajectories, the rigid links can be replaced with the above mentioned four ligaments. The tensile forces on the links are now replaced with the tensile forces on the ligaments. The compression forces on the same links will be reproduced as the compression forces at the contact points between the tibial plateau and femoral condyles. With this approach the formed femur shape was more anatomically appropriate compared to the commonly used spherical representations [10].

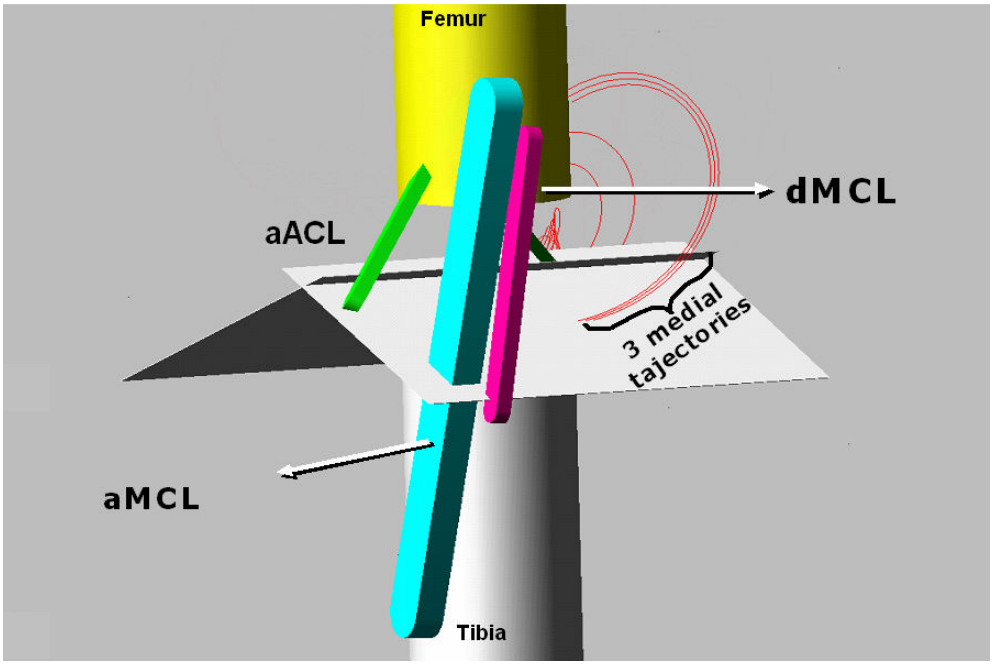

Figure 3.7 Three medial trajectories of the contact points after tracing the lateral contacts during knee flexion and the constraints of the model in the present study.

It should be noted that aACL, aPCL, aMCL and dMCL are not the only ligaments involved during passive knee flexion. In the reference model and also in this study we had to include eight more ligaments that are not isometric. Twelve ligaments were defined as; anterior, deep, oblique fiber bundles of MCL, anterior and posterior bundles of PCL and ACL, one LCL bundle, one medial, one lateral regions of the posterior capsule, one oblique, and one arcuate popliteal ligaments [1, 10, 13, 63]. The attachment points of these ligaments and the

elastic properties were obtained from elsewhere [1, 10]. A ligament is assumed to be a line element extending from the femoral origin to tibial insertion, as [10]:

$$F_j = \begin{cases} 0; & \in_j \le 0 \\ K1_j (L_j - L_{oj})^2; & 0 = \in_j \le 2 \in_j \\ K2 L_j - (1 + \in_1) L_{oj}; & \in \ge 2 \in_j \end{cases} \qquad (3.2)$$

where ϵj is the strain in the jth element, K1j and K2j are the stiffness coefficients of the jth spring element for the parabolic and linear regions, respectively and Lj and Loj are the current and slack lengths [10].

The coefficients, K1, K2, Loj were obtained from Abdel-Rahman and Hefzy [10]. The linear range threshold was specified as ϵ1 □0.03 [10, 12, 63, 64] relationship of the jth ligament exhibit two regions: a parabolic region in the initial stage and a linear region in the later stages [10].

Dynamic modeling in the simulation requires the definition of as set of reaction forces on the contact planes. In our study the reaction force between tibia and femur was formalized as:

$$F_n = k_g + step[g, 0, 0, d_{\max}, c_{\max}] \frac{dg}{dt} \qquad (3.3)$$

where, *k* (10 000 N/mm) is the stiffness coefficient, *g* is penetration dept (1 mm), d_{max} (1mm) is the penetration limit, c_{max} is the maximum damping coefficient (100 N/mm/sec), dg/dt is the penetration velocity [62]. The contact and reaction forces were created between each interacting solids. These contact properties were shown to be in agreement with the experimental studies [4, 65, 66,].

The equation defining the Step function is:

$$Step = \begin{cases} h_0; & : x \le x_0 \\ h_0 + a * \Delta(3 - 2\Delta); & : x_0 = x \le x_1 \\ h_1; & : x \ge x_1 \end{cases} \quad (3.4)$$

Where

$$a = h_1 - h_0 \quad (3.5)$$

and

$$\Delta = (x - x_0)/(x_1 - x_0) \quad (3.6)$$

where x is a real variable that specifies the independent variable (g), x_0 is value of independent variable at which the STEP function begins; defined by a real number, an expression or a design variable (0), h_0 is initial value of the step; defined by a real number, an expression, a design variable or a run-time function (0), x_1 is value of independent variable at which the STEP function ends; defined by a real number, an expression or a design variable (dmax), h_1 iss final value of the step; defined by a real number, an expression, a design variable or a run-time function (cmax) [62].

A trajectory by definition was not a solid object, making it a complex problem to define a contact force between a plane and a point on a trajectory in ADAMS software. To facilitate real time computation and simplify the problem, we have sampled the two trajectories with a set of equally spaced tiny spheres.

These spheres with 1mm radius and no weight (Fig 3.8) make it possible to define a contact point between the femur and the tibia reduces the computational demand during real time simulation.

3.2 Validation of Tibiofemoral Model

To test the validity of the simulated passive knee flexion we compared the estimated contact forces, tibial rotations and displacements with the findings reported in the literature.

For the comparison of the contact forces we used Abdel-Rahman and Hefzy's model as the reference by reconstructing their model. With the reconstructed model we could reproduced the same contact forces in the same range as reported by Abdel-Rahman and Hefzy [10].

The reconstructed reference model allows us to estimate the tibial rotations and displacements that were not available in the reference study itself [10]. These estimated motions were compared with the tibial rotation and displacement reported in Wilson *et al*. [7] Therefore we used tibial rotation and displacements from Wilson *et al.* not only to validate the proposed model, but also to validate the results of the reconstructed reference model.

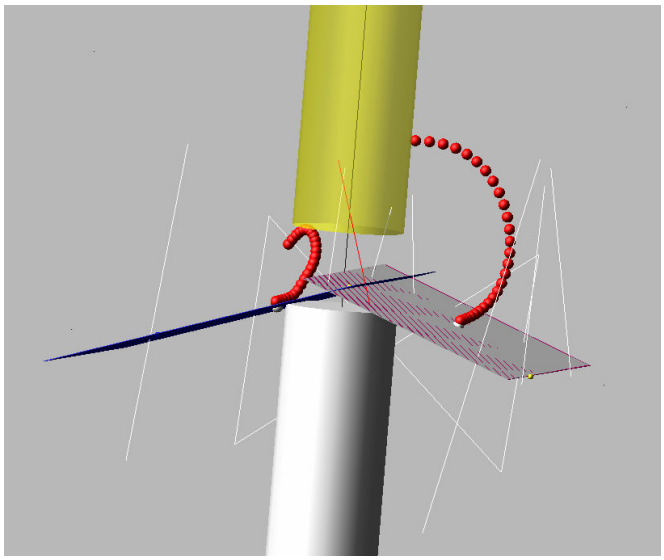

Figure 3.8 The spheres to represent distal femoral geometry in the present study.

The Bryant angle method was performed to define rotational changes during the flexion. The relative three-dimensional angles of rotation between tibia and femur were

calculated using the Cardan (or Bryant)-type Eulerian angles of rotation [67]. The tibio-femoral coordinate system was adapted from Grood and Suntay [68]. The tibial attachment of posterior bundle of ACL is selected as the reference point to describe translational displacement.

3.3 Patello-Tibio-Femoral Model

3.3.1. Modeling Femoral Geometric Shape

After validating tibiofemoral model, distal femoral geometric shape was described according to cadaver study [69, 70]. The sulcus angle, distance between trans-epicondilar line and the deepest point of trochlear groove were necessary to create the distal femoral geometric shape in ADAMS software.

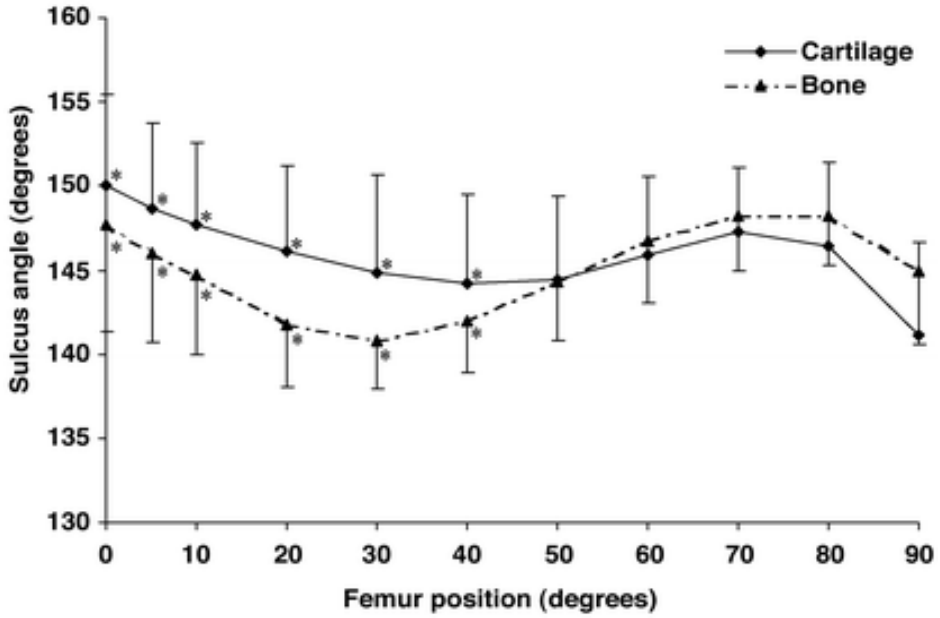

Figure 3.9 Sulcus angle in 33 cartilaginous and 29 osseous specimens, mean± SD. Error bars are shown in only one direction for clarity: those for cartilage go up, those for bone go down. Adapted from [69].

In Shih *et al*. work, mean value of the cartilage sulcus angle was described as 146.1°± 5.5. The excursion of the angle for a mean individual femur was not very high, then it can be taken as constant value (Figure 3.9). Therefore the sulcus angle was modeled as constant (146°).

The distance between trans-epicondilar line and the deepest point of trochlear groove was defined as 30.4 mm (G-H in Figure 3.10). The trans-epicondilar distance was estimated as 86.95 mm (E-F in Figure 3.10). The trans-epicondilar distance is the distance between most lateral point of the lateral sphere and most medial point of the medial sphere in Spherical Based model. Therefore the Abdel-Rahman and Hefzy's femoral spheres were relocated in to constraint based model to define the transcondylar line. The angle between the anatomical axis of the femur and the groove axis was defned as 7.5°.

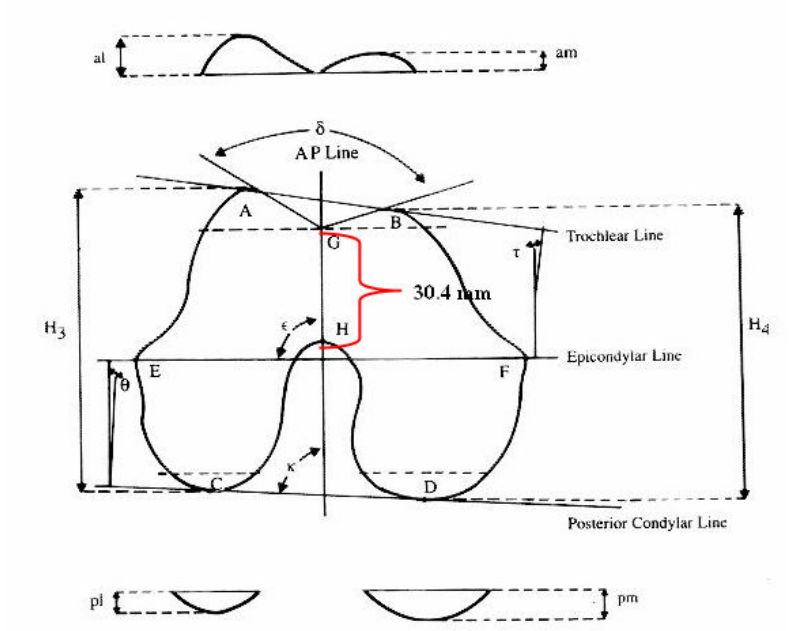

Figure 3.10 Diagram of the axial view of the distal femur. A and B = the most anterior projections of the lateral and medial femoral condyles; C and D = the most posterior projections of the lateral and medial femoral condyles; E and F = the most prominent points of the lateral and medial epicondyles; G = the deepest part of the trochlar groove; H = the center of the intercondylar notch; AB = trochlear line; EF = trans epicondylar line; CD = posterior condylar line; GH = anterior-posterior line; AGB = [sigma] = sulcus angle; [epsilon] = AP line-epicondylar line angle; [kappa] = AP line-posterior condylar line angle; [THETA] = epicondylar line-posterior condylar line angle; [tau] = trochlear line-epicondylar line angle; H3 = height of the lateral condyle; H4 = height of the medial condyle; al = anterior lateral cut; pl = posterior lateral cut; am = anterior medial cut; and pm = posterior medial cut. Adapted from [70].

The defined lengths and angles were in agreement with the literature [69, 70]. The distal femoral geometry was created by using the revolution tool of the ADAMS software (Figure 3.11).

Then it was added in to our tibiofemoral model by matching the center of the revolution and the midpoint of transepicondylar axis of Spherical Based model. Once the created femoral shape was located, the spheres were removed. The model included tibial plateaus, two contact trajectories and 12 ligaments at this stage.

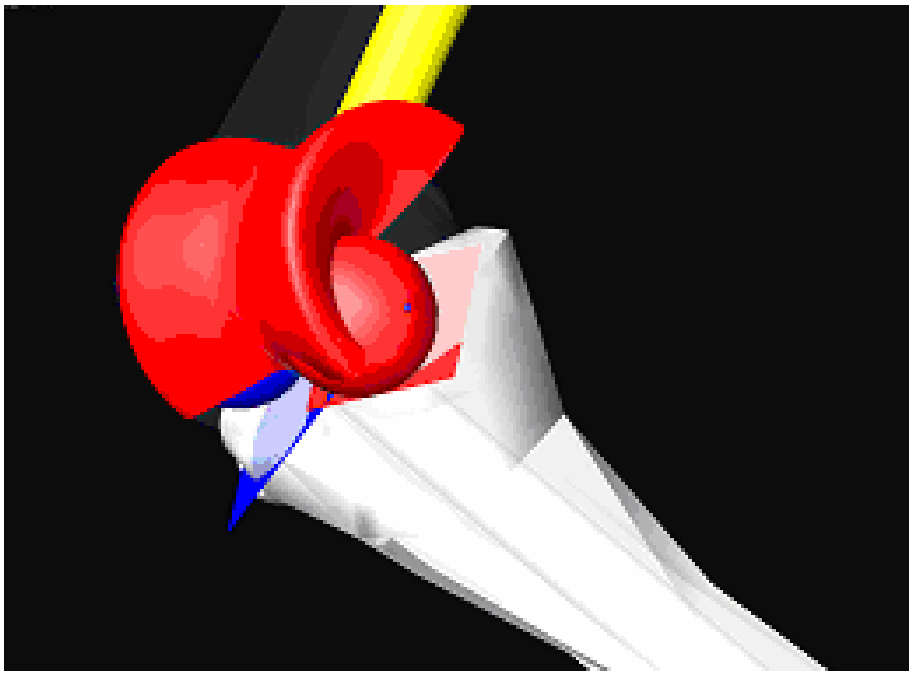

Figure 3.11 Representing distal femoral geometry in the present study.

3.3.2 Modeling Patello-Tibio-Femoral Joint

Patella femoral joint is the joint between the distal femur and patella. Patella fits the intercondylar groove and slides between medial and lateral facets as seen in Figure 3.12 and 2.19.

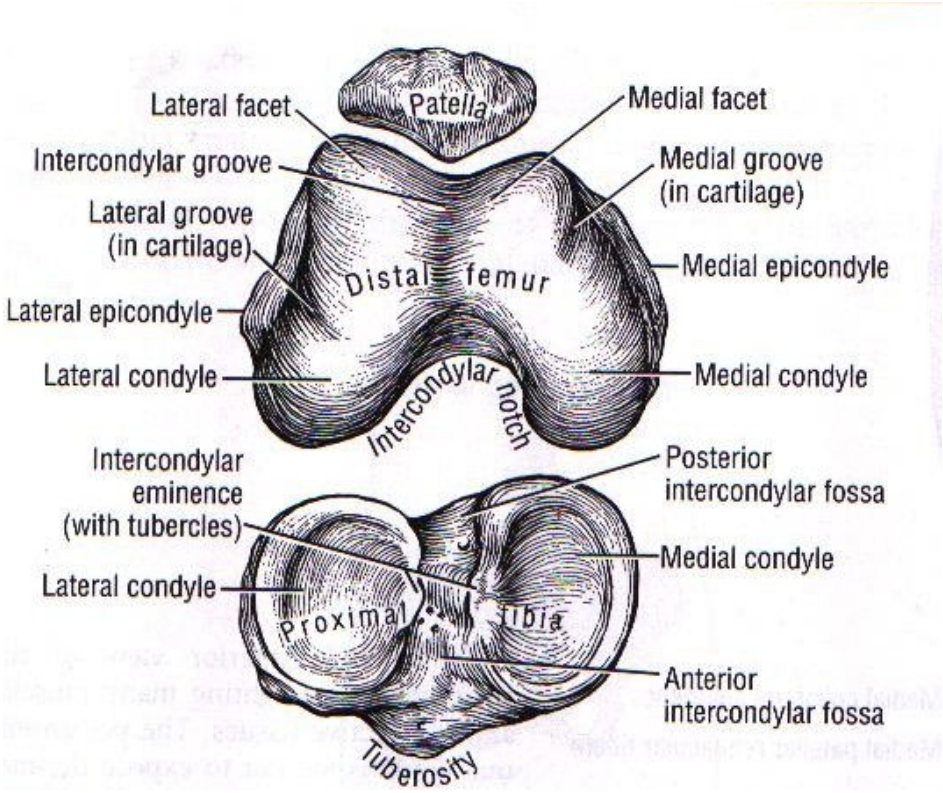

Figure 3.12 The anatomy of patella femur and the tibia. Adapted from.[17]

In the present study patella was created by using the revolution tool by pivoting the sulcus angle in ADAMS software. Revolution tool was employed by defining two axes, length and the depth of the patella, around the sulcus angle. As described in cadaver studies, 3.94 cm and 1.63 cm were defined as the length and the depth of the patella respectively [43, 71] (Figure 3.13). The inertial patellar parameters were assumed as follows: m= 0.1 kg. Ixx= 0.0000015625 kgm^2, Iyy= 0.00003125 kgm^2, Izz= 0.00001615625 kgm^2 [11].

Patellar tendon was represented by the three spring dampers as described in Caruntu *et al.*'s work [11].

The patellar tendon was formulized as;

$$F_p = k_p(L_p - L_{0p}) \tag{3.7}$$

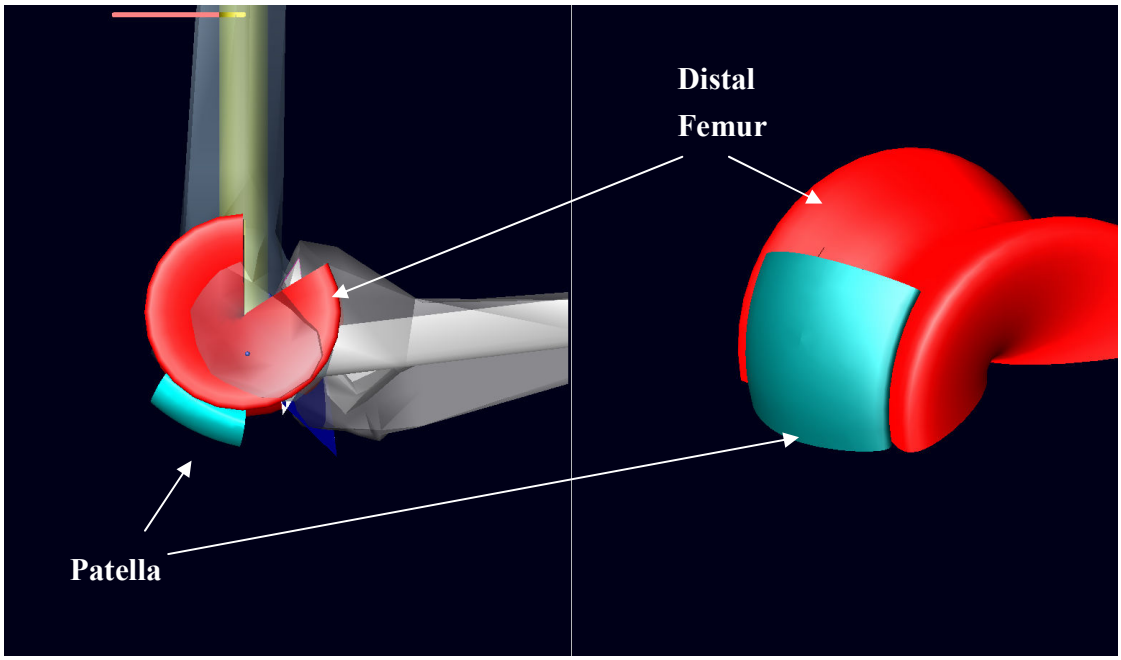

Figure 3.13 Oblique and sagittal view of the patella femoral model in the present study.

Where kp, Lp, and L0p are the stiffness, the current length and the slack length of the patellar ligament respectively [11]. The stiffness was assumed to have a value of 200 N/mm [11], the slack length L0p was specified to allow a ratio of 0.6 between the patellar ligament force and the quadriceps force at 90° knee flexion [11].

Patellar ligaments were attached to the tibial tuberosity and patella in the present model as described in cadaver study [72]. Hirokowa attached the patellar tendons and quadriceps to the tibial tuberosity, patella and femur by using large oval spares. The position of the attachment points defined by intersecting points between the line which bisect the area length (parallel to the long axis of the tibia and femur) and the two lines which trisect the area width (papendicular to the above-mentioned long axis) [72] (Figure 3.14).

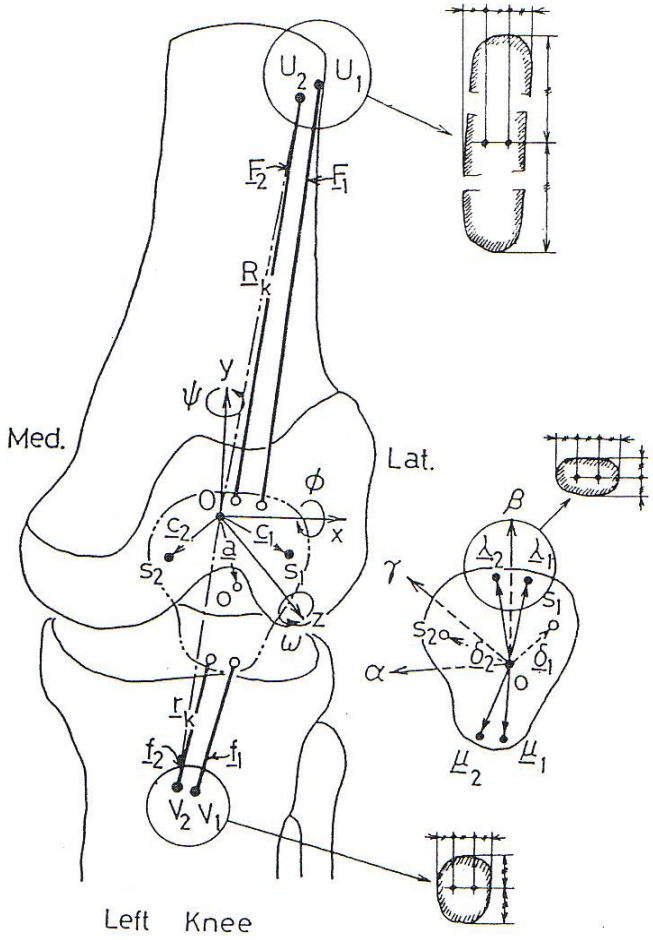

Figure 3.14 The representation of tendon attachments for patellar tendon and quadriceps. Adapted from [71].

The tibial tuberosity was identified by using tibia shell represented in LIFEMOD software. The location of patella, quadriceps and the patellar ligaments was in agreement with the literature [43]. The angle between patellar tendon and the tibial axis was 20°, the angle between longitudinal patellar axis and patellar tendon was 165°, the angle between quadriceps tendon and the normal was 10° as described in Van Eijden *et al.*'s work [43]. Patellar tendon length was assigned as 6.52 cm as described in cadaver studies [43, 71]. In this simulation, the tibia and the patella were assumed to begin their motions from rest. The initial position was defined according to the experimental data available in the literature [7, 11] by specifying the

following kinematic parameters: tibial flexion of 89.80 deg, patellar flexion of 61 deg, varus (adduction) angle of 4 deg, tibial internal rotation of 22 deg, patellar medial rotation of 0.25 deg, and patellar medial tilt of 0.2°.

The quadriceps was also assumed parallel to the femur and it was represented as a single line force which generates 400N mean force as introduced in the literature [11]. The attachment points were described as in literature [71]. The quadriceps force was defined as a simulation of knee extension exercise activity. The dynamic load was applied to the patella through the quadriceps tendon causing the tibia and patella undergoes 3-D motion while the femur fixed in horizontal position [11]. The applied force during the knee extension was shown in other study [11]. We applied the function during the knee extension exercise with medium level quadriceps force (mean: 400N) (Figure 3.15).

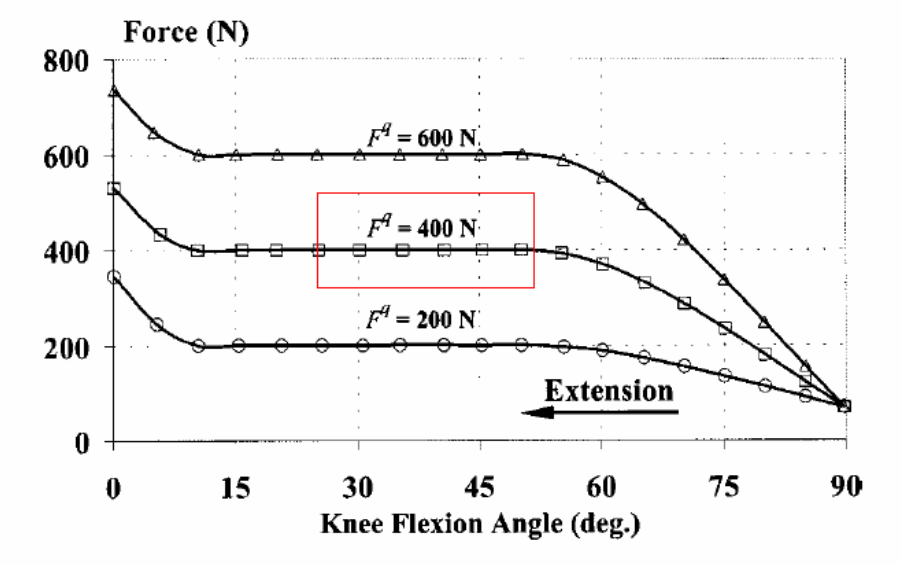

Figure 3.15 Forcing functions applied to the quardriceps tendon to simulate knee extension exercise. Adapted from [11].

Quadriceps tendon connects the quadriceps muscle to the patella and it was represented by three spring damper elements which have the same stiffness coefficients with patellar tendon.

The first contact occurs between quadriceps tendon and distal femur around 70° knee

flexion and wraps around the femoral groove beyond that flexion [11, 71, 72] (Figure 2.19). In ADAMS software, the spring dampers and the single component forces have no masses so that the contact forces can not be defined between these elements and solids. To represent the via point between quadriceps tendon and the distal femur, a cylinder which has a negligible mass was created between the quadriceps force element and the quadriceps tendon. To round the edges of the cylinder two spheres were added to the ends of this cylinder (Figure 3.16).

To test the patello-tibio-femoral model, patellar rotations, translations and tibiofemoral contact forces on the medial and lateral compartments during knee extension were compared to the literature [11, 71, 75].

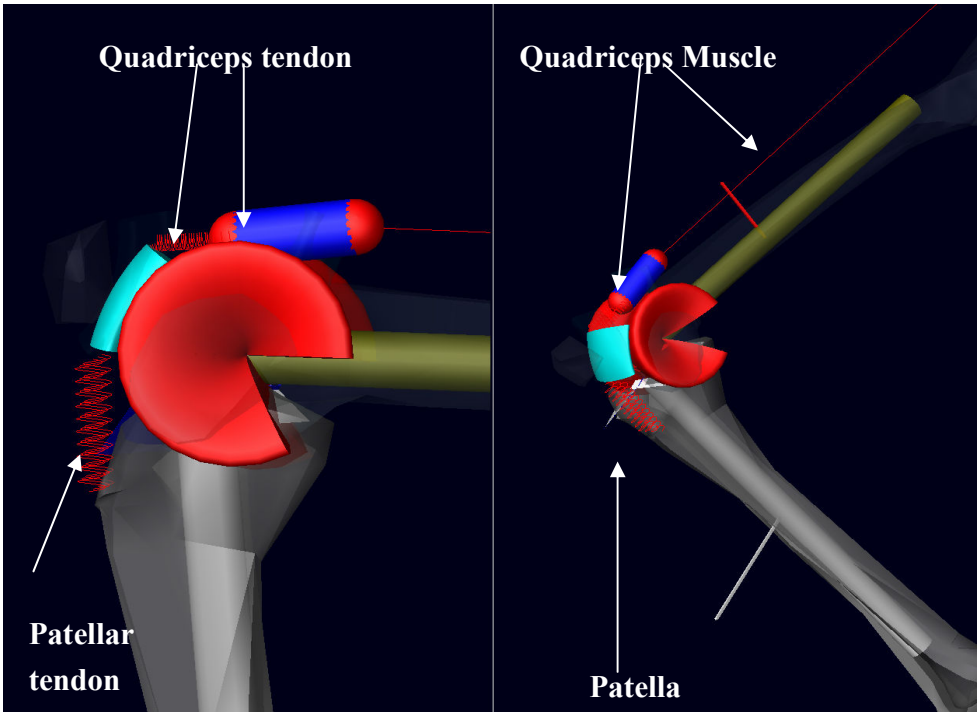

Figure 3.16 The sugittal and oblique view of patello-tibio-femoral joint in the present study.

3.3.2.1 Simulation of Anterior Drawer Test

To simulate the drawer test, force (100N) was applied from the tuberistas tibia (about 5cm below of the tibial plateau) to the 90° flexed patello-tibio-femoral model. To represent the

examiners' resistance against foot movement, a rigid link fixed to the ground was created in front of the tibia and a contact force was defined between tibia and the link (Figure 3.17). This test was repeated for 0°, 30°, 60° and 90° knee flexion angles and the anterior translation of the reference point relative to the femur was compared with the literature [81].

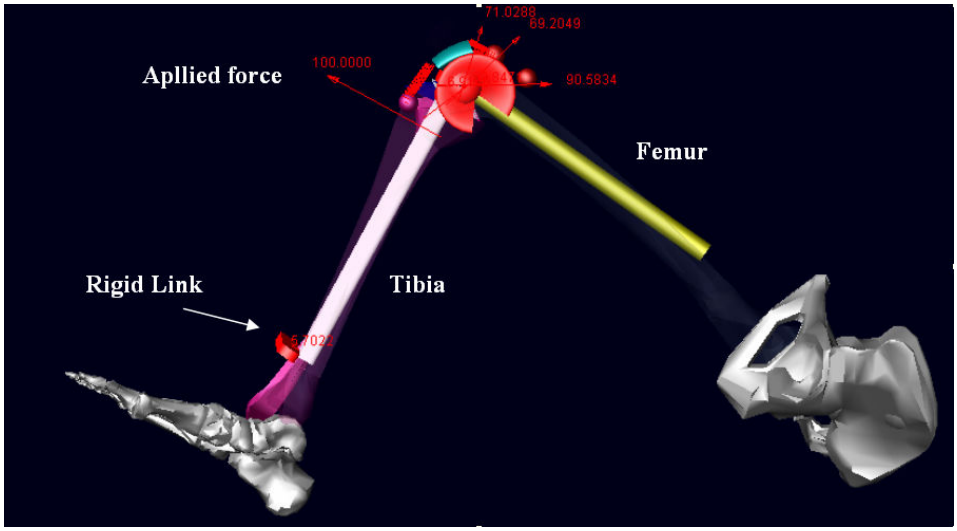

Figure 3.17 The simulation of anterior Drawer test in the present study.

Subsequently the anterior drawer test was repeated for the 90° knee flexion by applying a 200N internal and external rotational force to the center of mass of the tibia. After that anteriorly directed force (100N) was applied to the internally and externally rotated tibia. The maximum anterior translation on the tibia was recorded for both rotations. The anterior translation of the tibia is reduced when tibia rotated internally for the ACL deficient patient in clinic.

3.4 Implementing the Knee Model into the Full Body Model

The musculoskeletal model for a 1.80 m tall, 80 kg, 18 year old male human full body model was created by using LIFEMOD software. The physical properties of the segments,

muscle attachment points and joints were created by the guidance of LIFEMOD [62]. The each joint was represented as three revolute joints perpendicular to each other in the software and there is no natural sliding and rolling motions are allowed. The contact force was created between foot and the ground by using “Creating contact tool” of the software. The contact properties were assigned by the guidance of LIFEMOD [62].

After building the full body model, standing was simulated. To do that the muscles were defined as a “training element” in standing posture. The training element is a contraction recorder which records contractions when external forces are applied to the body. After the joints were fixed, the simulation was run and record muscles contraction during the standing simulation. Then forward dynamic simulation was performed by running trained muscles in standing posture with free joints. The full body model successfully stood tall on the ground (Figure 3.18).

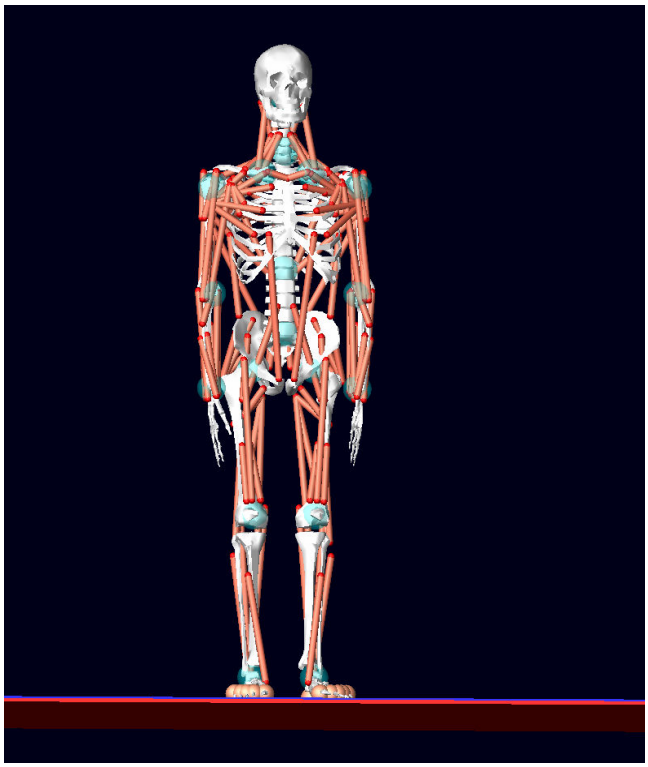

Figure 3.18 The full body model in LIFEMOD software in the present study.

After implementation of the knee model in to the full body model, normal walking was simulated. The positions of the segments during walking were imported from LIFEMOD software tutorial [62]. The imported file includes the gait analysis data obtained from a normal person. Therefore it allowed us to make the body walk normally (Inverse dynamics). The muscles were in "training element mode", so they recorded the contraction during inverse dynamic simulation of walking. Once the muscles were trained, the forward dynamic simulation was performed. A normal human walking was succeeded by the recorded muscle contraction.

Then the knee model (patello-tibio-femoral model) in the present study was imported to the full body model. The knee model was created only for the right side. Therefore only right knee were replaced with our knee model. The left knee was not changed.

The forward simulation was performed with the present knee model at the right side and normal walk was obtained (Figure 3.19).

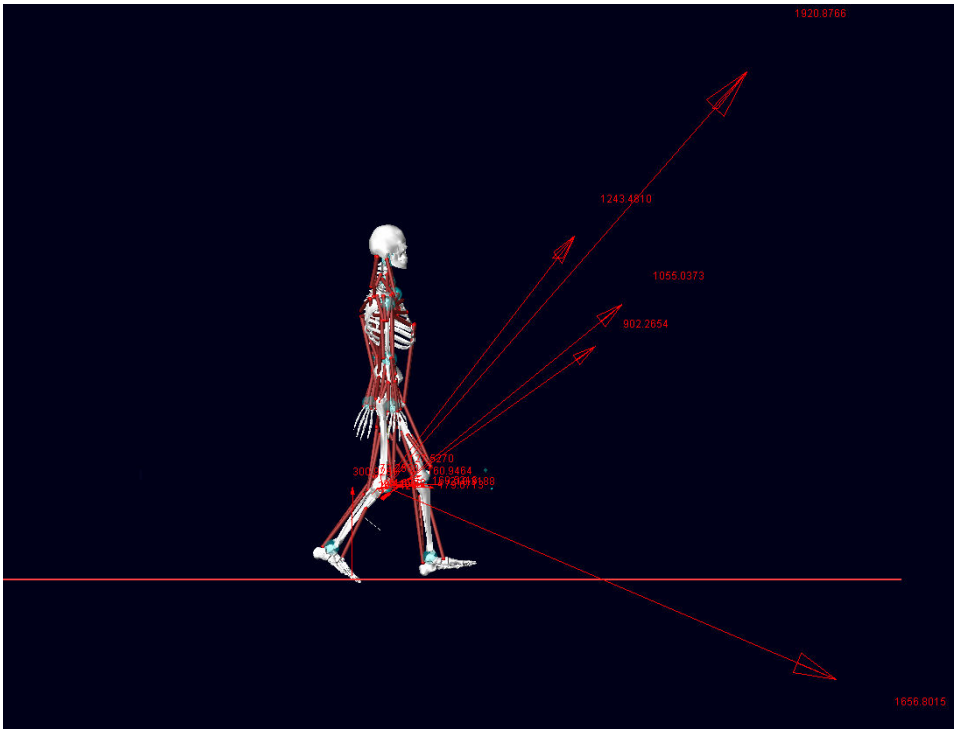

Figure 3.19 Simulation of normal walking in the present study.

After simulating normal walking, we removed the aACL bundle from the present model to simulate ACL deficient gait. The tibial translations and the vertical ground reaction forces were compared to the muscle driven normal walking simulation and to the literature [60, 61].

4. RESULTS

4.1 Constraint Based Tibiofemoral Joint Model

Passive knee flexion is characterized by internal rotation and posterior, proximal, medial displacement of the tibial attachment point of the posterior bundle of anterior cruciate ligament. In the reconstructed reference model, the tibia rotates and moves in normal range compared to the experimental data [73] as shown in Figure 4.1. Although passive knee motion always involves internal rotation with flexion, there are no consistent patterns of abduction or adduction [73].

The only external force applied in Abdel-Rahman and Hefzy's model [10] is kept perpendicular to the tibial plateau. There is no ground reaction force or muscular contraction. As a result with no projection of the applied force on the contact points, one might expect the same contact force profile at different external forces. This condition was illustrated in Figure 4.2 for 60 N, 100N, 140N, producing the same contact force behavior [10]. In our model similar contact force behavior during passive knee flexion was expected, since there was no muscular contraction and additional external force. This expectation was confirmed for the simulated contact forces of the normal knee (Figure 4.3).

The tibia rotated internally with the knee flexion in the Constraint Based Model as in the Spherical Model with peak values 24° and 27° respectively. The behavior of the abduction / adduction graph of the tibia was quite similar for both models. The peak adduction was -1.2° and -3.2° in constraint based and spherical models respectively (Figure 4.4).

We found that the motion of the reference point, agreed with the literature [7, 49, 73] (Figure 4.5).

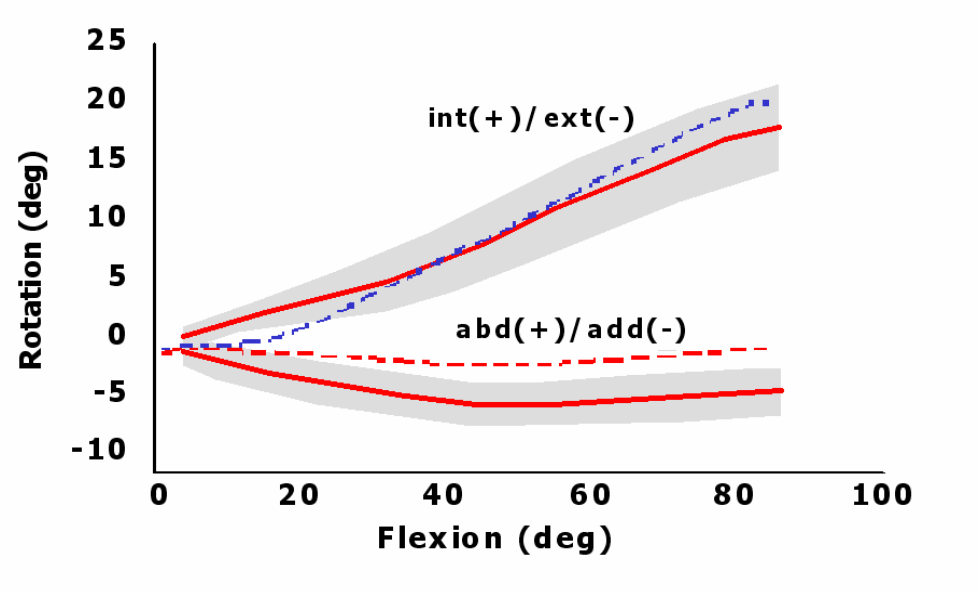

Figure 4.1 Tibial rotations of the present study (dashed lines) and rotations from Wilson *et al*, 2000 (Solid lines and gray ranges).

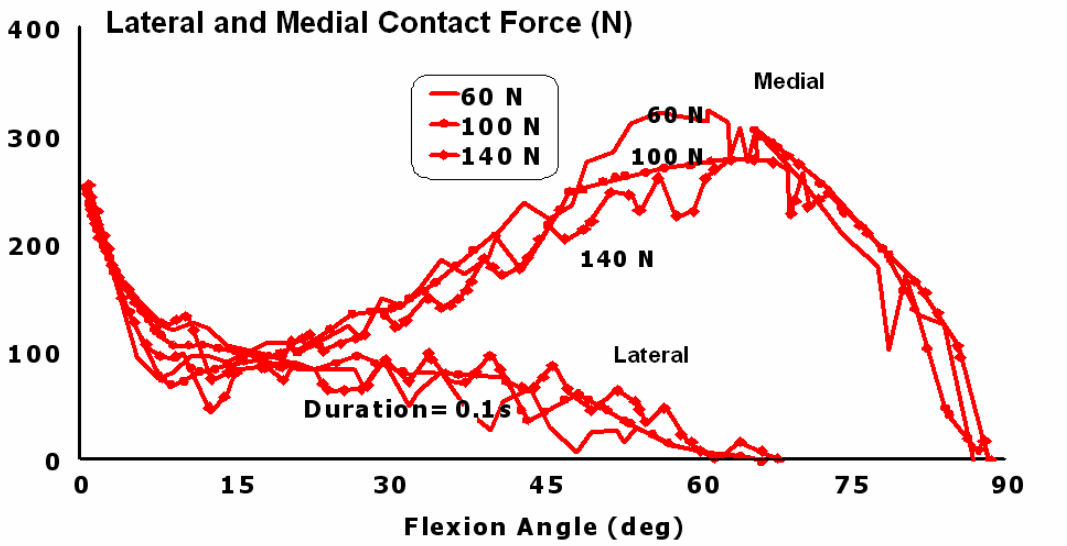

Figure 4.2 Medial and lateral contact forces of the tibiofemoral joint Adapted from [10].

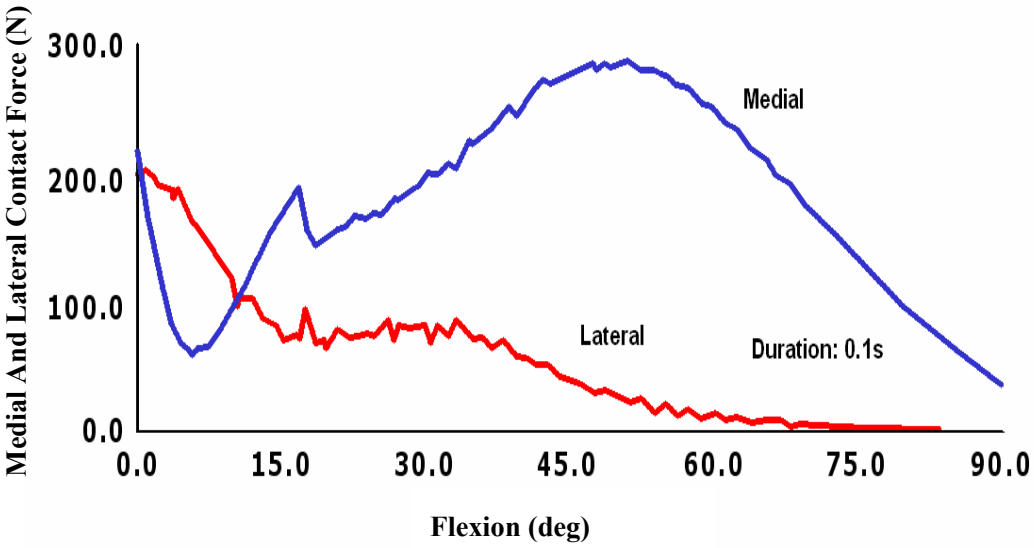

Figure 4.3 Medial lateral contact force in the present study.

Figure 4.6 illustrates that medial and lateral contact forces decreased in Constraint Based Model relative to Spherical Model during knee flexion. Although the lateral contact force in Constraint Model was higher than Spherical Model for the first 13° knee flexion, it was lower than the Spherical Model after 13°. The medial contact force was smaller than the Spherical Based model during the entire knee flexion.

The maximum contact force was 205 N for both models which was the value at the 0° knee flexion. The lateral contact reached zero earlier (at 32° flexion) for the Constraint Based model. As a result Constraint Based Model could produce acceptable normal kinematics for the knee flexion [1, 73, 74].

4.2 Patello-Tibio-Femoral Joint Model

The patellar rotations, patellar shift and medio-lateral tibiofemoral contact force results

during the simulation of knee extension exercise were compared with the literature [11, 72]. The findings were found to be in agreement with the literature as shown in Figure 4.7, 4.8. Patella extended, rotated medially, tilted laterally during extension within the normal range.

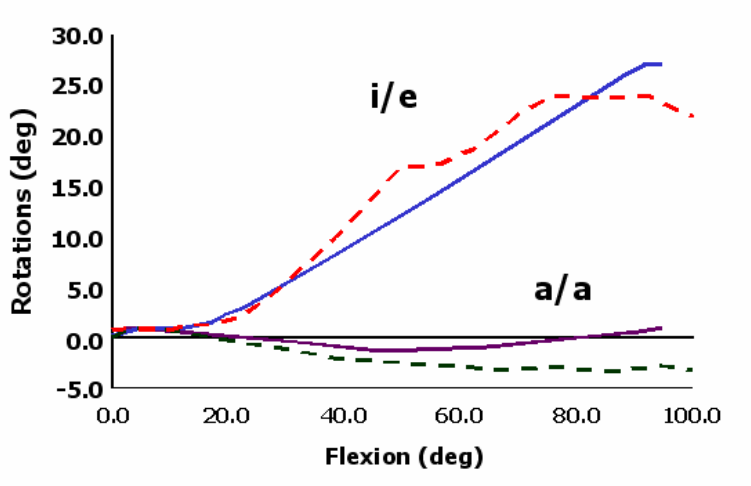

Figure 4.4 The dashed lines indicate constraint based simulation results and the solid lines demonstrate simulation of spherical model. Internal/external rotation (i/e) and abduction / adduction (a/a).

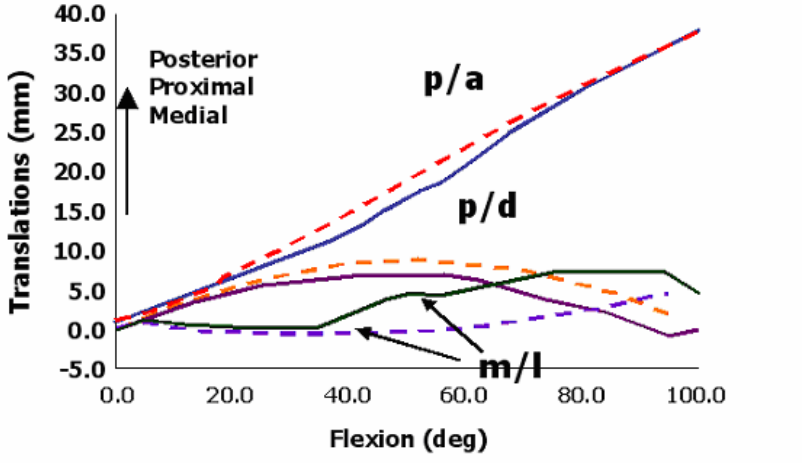

Figure 4.5 The dashed lines indicate constraint based simulation results and the solid lines demonstrate simulation of spherical model . Antero/posterior (p/a), proximo/distal (p/d) and medio/lateral (m/l) translations. Adapted from [72].

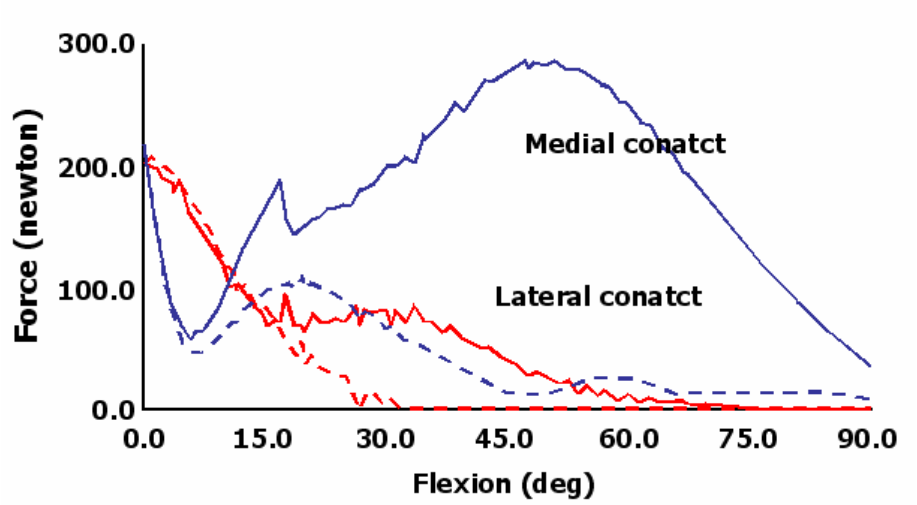

Figure 4.6 Comparison of the medial (black lines) and the lateral (red lines) contact forces for constraint based (dashed lines) and Spherical Model (solid lines) with tibio-femoral flexion.

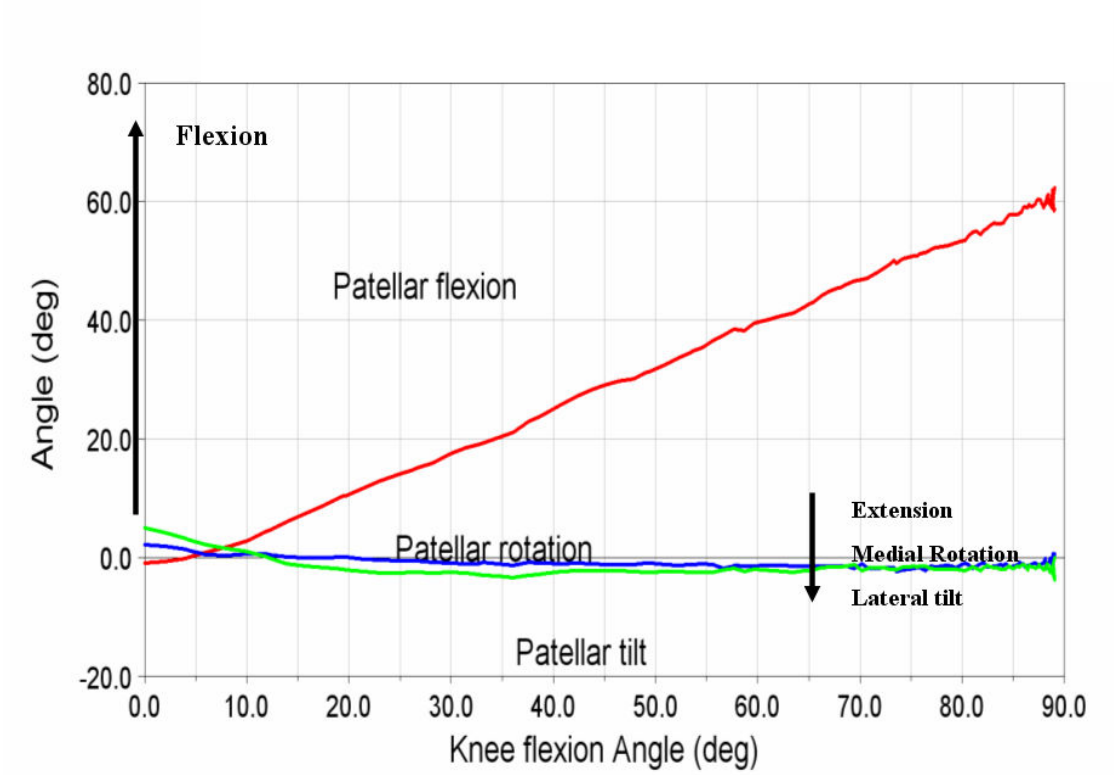

Figure 4.7 Illustration of the patellar rotations in the present study.

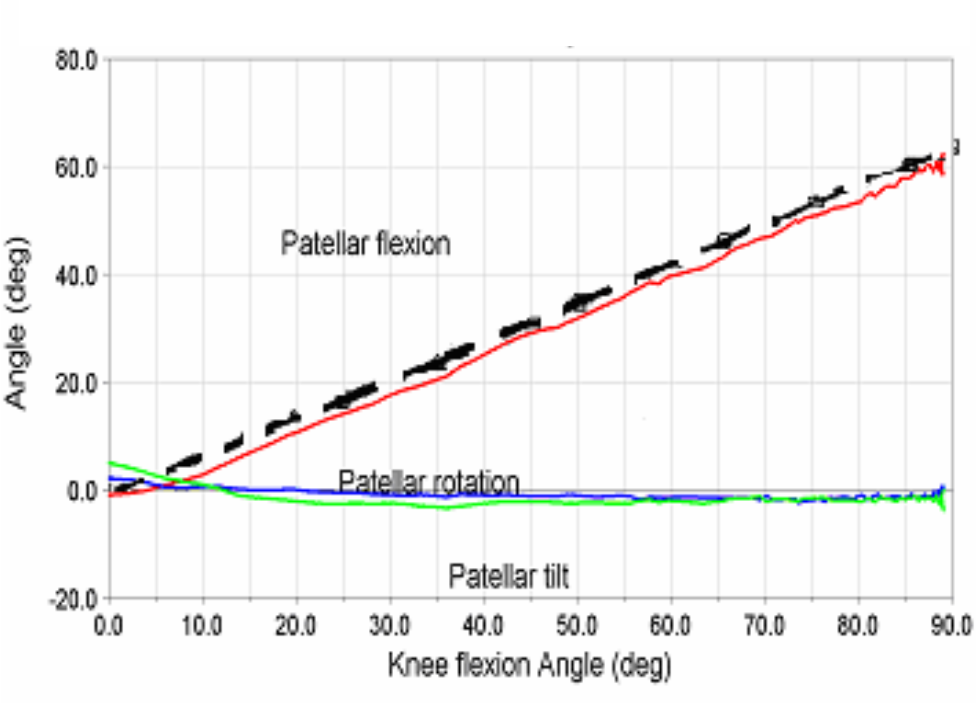

Figure 4.8 The comparison of patellar rotations during knee extension with the literature (dashed black line for plantar flexion) [11].

The patellar displacements during knee extension were compared with the literature [75] (Figure 4.9). Patella translated laterally, proximally and posteriorly in agreement with the literature [75]. 63°, 4°, 2.5° were the peak patellar flexion, patellar rotation and patellar tilt values respectively in the present study.

The contact forces of medial and lateral compartments on the tibial plateau were also compared with the literature [11]. It was found that the medial compartment of the tibio-femoral contact force was larger than the lateral compartment. However the magnitudes of the contact forces were smaller than the only data available in literature [11]. The peak forces were 500N and 200N in the present study although around they are around 600 N and 352N in Caruntu *et al.*'s work for medial and lateral compartments respectively. Even though the some differences between the present study and the Caruntu *et al*'s work, the double force on the medial component relative to the lateral during at least 30° of knee extension was achieved as

mentioned in the literature [11].

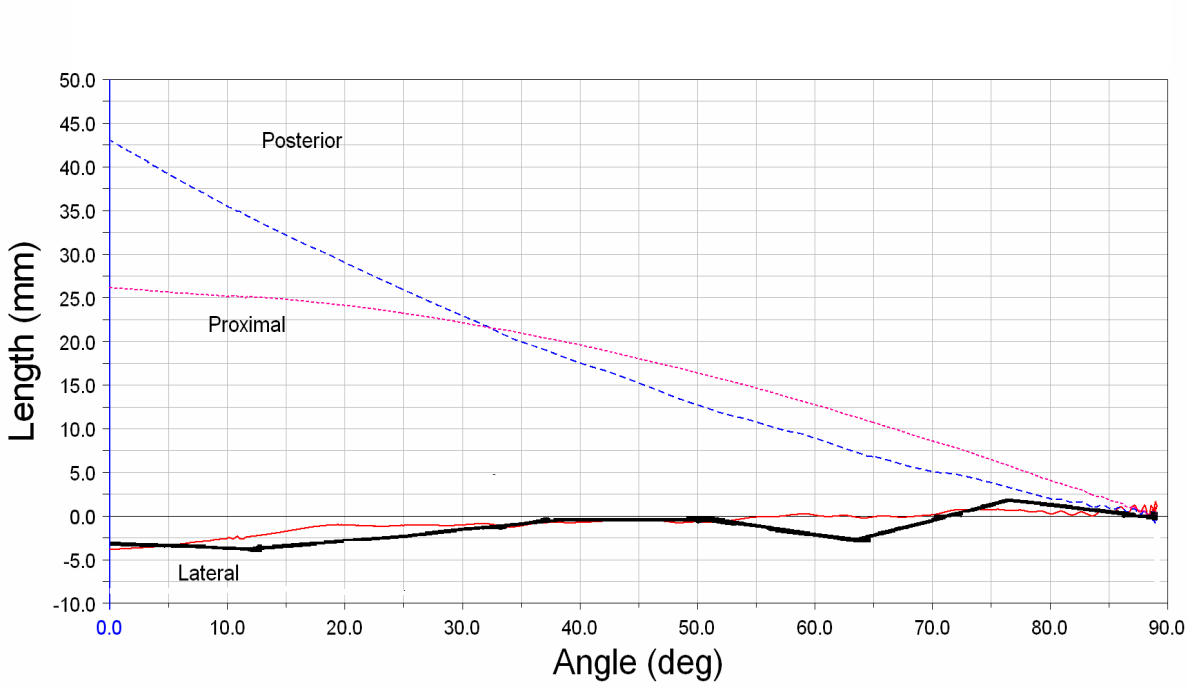

Figure 4.9 Patellar lateral (solid red line), proximal (dashed pink line), posterior (dashed blue line) translations during knee extension in the present study compared with the literature (solid black line for lateral tilt) [75].

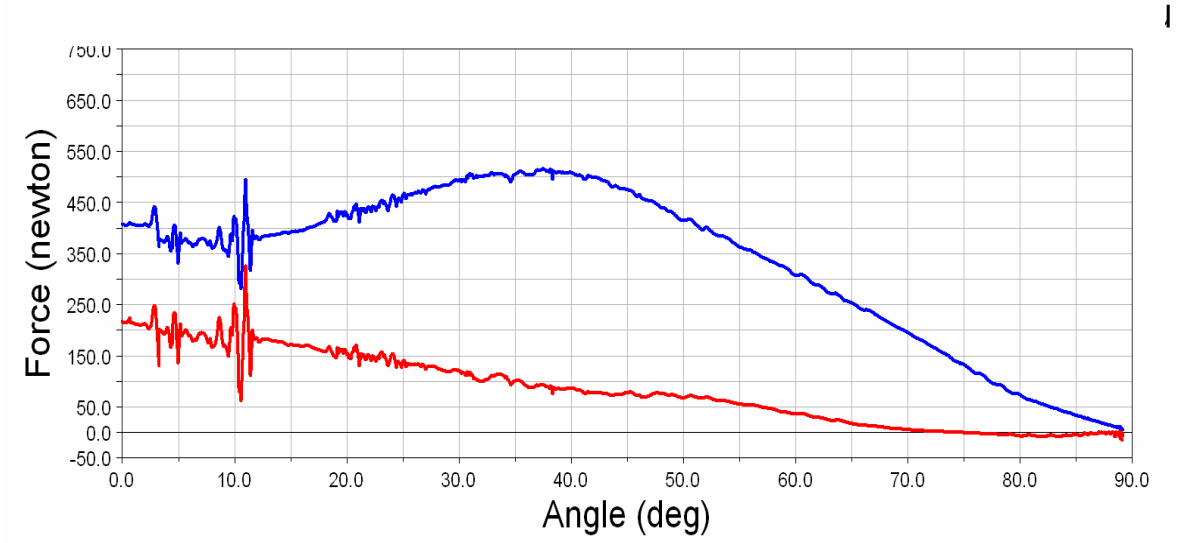

Figure 4.10 Illustration of contacts force on medio-lateral compartments of the tibia during knee extension.

4.3 Simulation of Drawer Test

A single component force (100N) was applied to the tibia and the anterior translation of the reference point, tibial attachment point of the posterior cruciate ligament, relative to the femur was measured for 0°, 30°, 60°, 90° knee flexion angles. 0.9mm, 3.2mm, 2.9mm, 2.1mm were the anterior translations of the tibia for the 0°, 30°, 60°, 90° intact knee flexion respectively. The translations were agreed with the in vitro data for the intact knee [81].

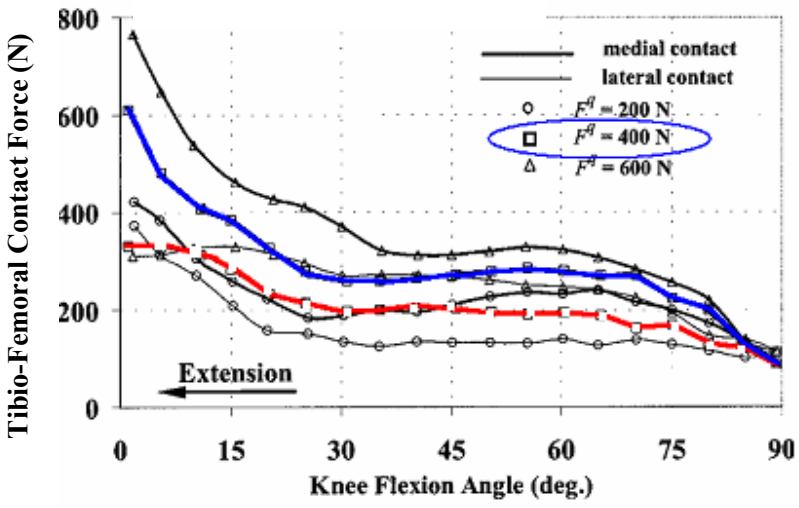

Figure 4.11 Contact forces on medial (Solid blue line) and lateral (Dashed red line) compartments from the literature[11].

The test was repeated by removing aACL, and pACL ligaments from the model to simulate positive drawer test which is usually seen for patients with ACL deficiency. Anterior tibial translation results of the no ACL model compared with the literature [81] (Figure 4.13).

The anterior translation of the tibia was larger in the ACL deficiency simulation as revealed in the literature [81]. The anterior translations of the tibia were 5.1mm, 9mm, 7.3mm, 8.1mm for the 0°, 30°, 60°, and 90° knee flexion respectively in the patello-tibio-femoral model with no- ACL.

The anterior drawer test was repeated for the 90° with the rotational force applied to the center of mass point of the tibia. The results showed that the anterior translation of the tibia

reduced with the internal force and increased with the external rotational force for the no-ACL model as revealed in the literature [82] (Figure 4.14).

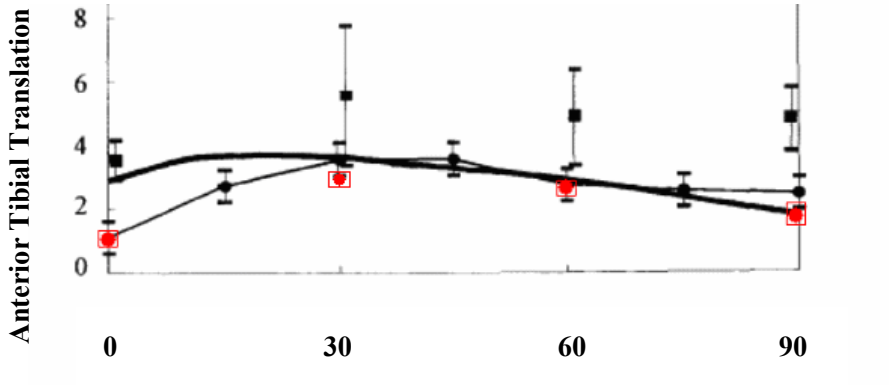

Figure 4.12 Anterior displacement of the tibia during drawer test simulation in the present study for intact knee (red spheres) and the literatures (vertical and solid lines) [81].

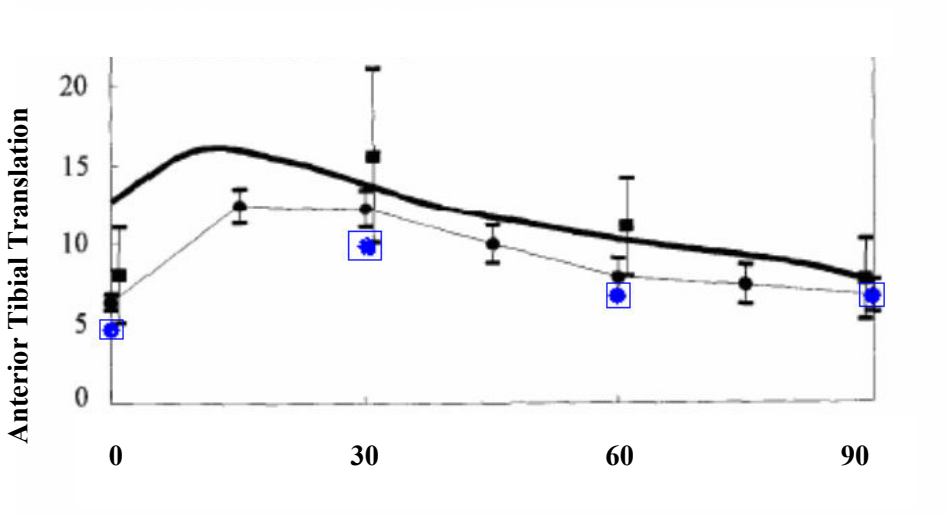

Figure 4.13 Anterior displacement of the tibia during simulation of drawer test in the present study (blue sphere), for ACL deficient knee and the literatures (vertical and solid lines) [81].

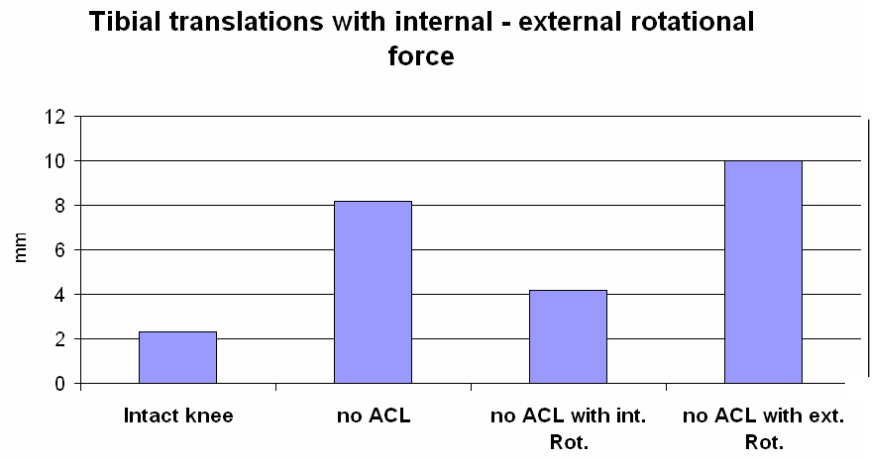

Figure 4.14 The anterior translation of the tibia during anterior drawer test with internal-external rotational force for intact and no-ACL model in the present study.

4.4 Full Body Model

After the training period of muscles during normal walking forward dynamic simulation which has only for revaluate joint representations, the hip, knee and ankle kinematics were observed that they were quite normal. However a decreased excursion of the knee,and ankle in sugittal plane was noticed.

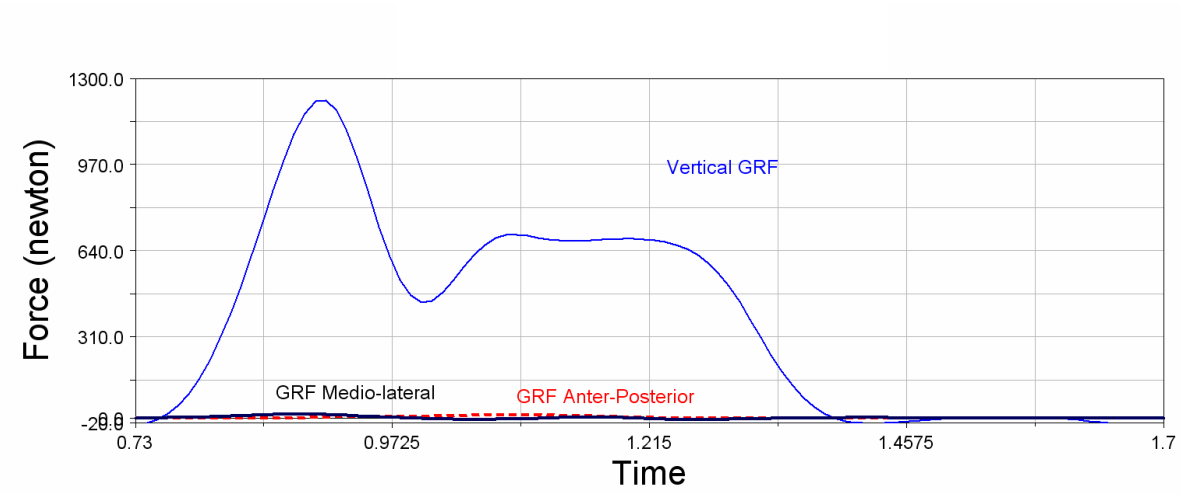

Figure 4.15 GRF during the muscle driven forward dynamics of normal walking simulation in present study.

The GRF for the right side was illustrated in Figure 4.15. The peak value of the first peak was 1210 N, and the second peak was 701 N. The second peak was smaller than normal (Figure 2.29).

After the simulation of walking with our patello-tibio-femoral joint model, we found the peak GRF during the stance phase of the gait cycle as 2238N and 1834N for the first and second peak of GRF respectively which agreed to the literature (Figure 2.29 and 4.16) [59].

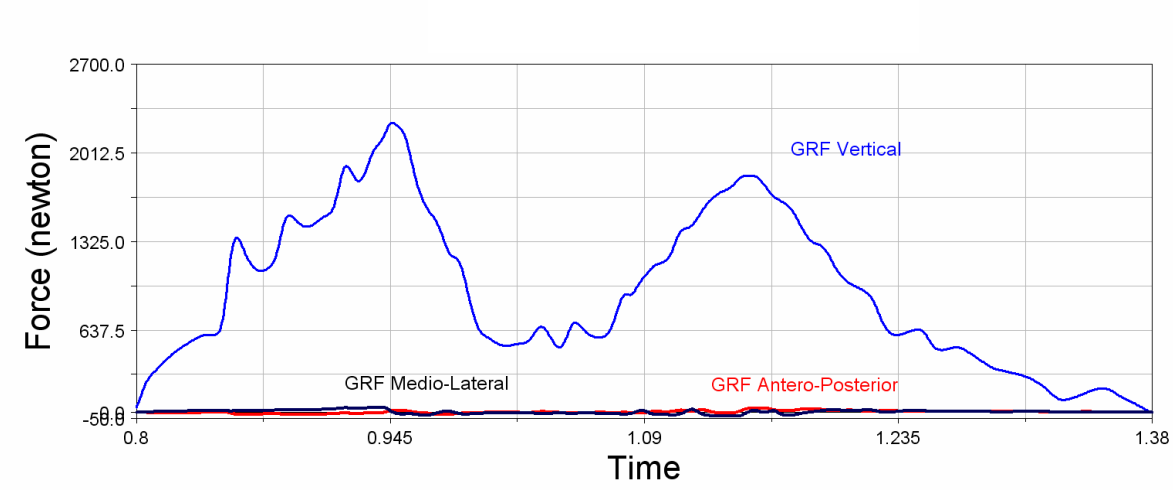

Figure 4.16 The GRF illustration of muscle driven forward dynamic simulation of normal walking with the patello-tibio-femoral joint in the present study.

When the aACL and pACL (All portions of ACL) were removed from the model to represent the ACL complete rupture, the contact forces was reduced remarkably (Figure 4.17).

When the anterior portion of ACL was removed and the posterior part of the ACL was stayed intact, the first and the second peak of the GRF were reduced as literature (Figure 2.31, 4.18, and 4.19).

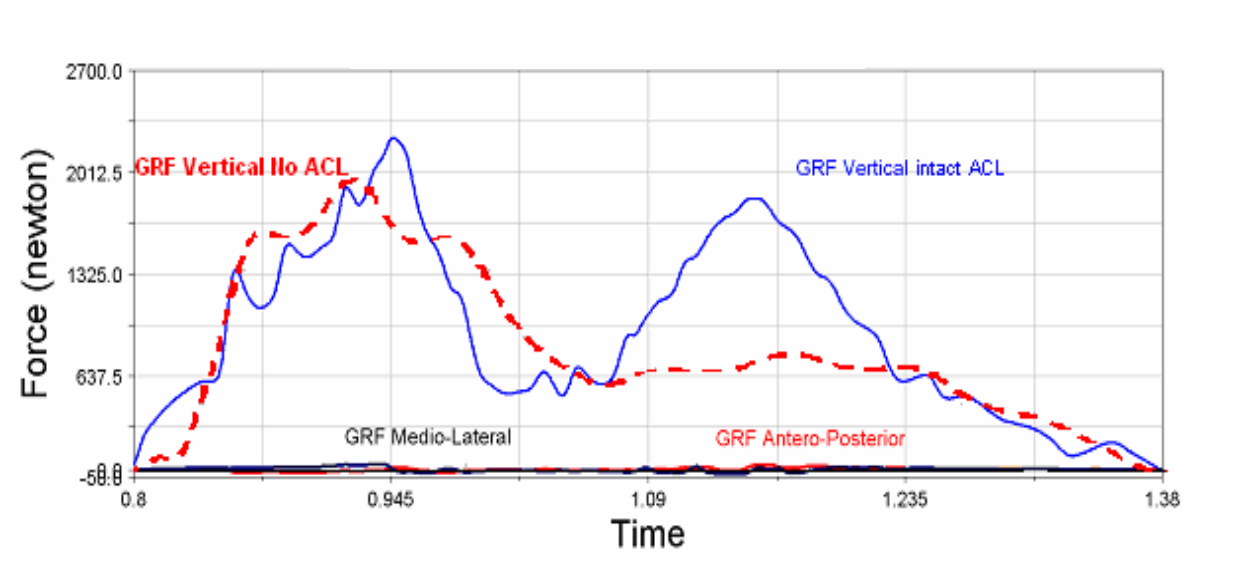

Figure 4.17 The comparison of GRF for the intact knee model (blue solid line) and model with no ACL (dashed red line) for the right side in the present study.

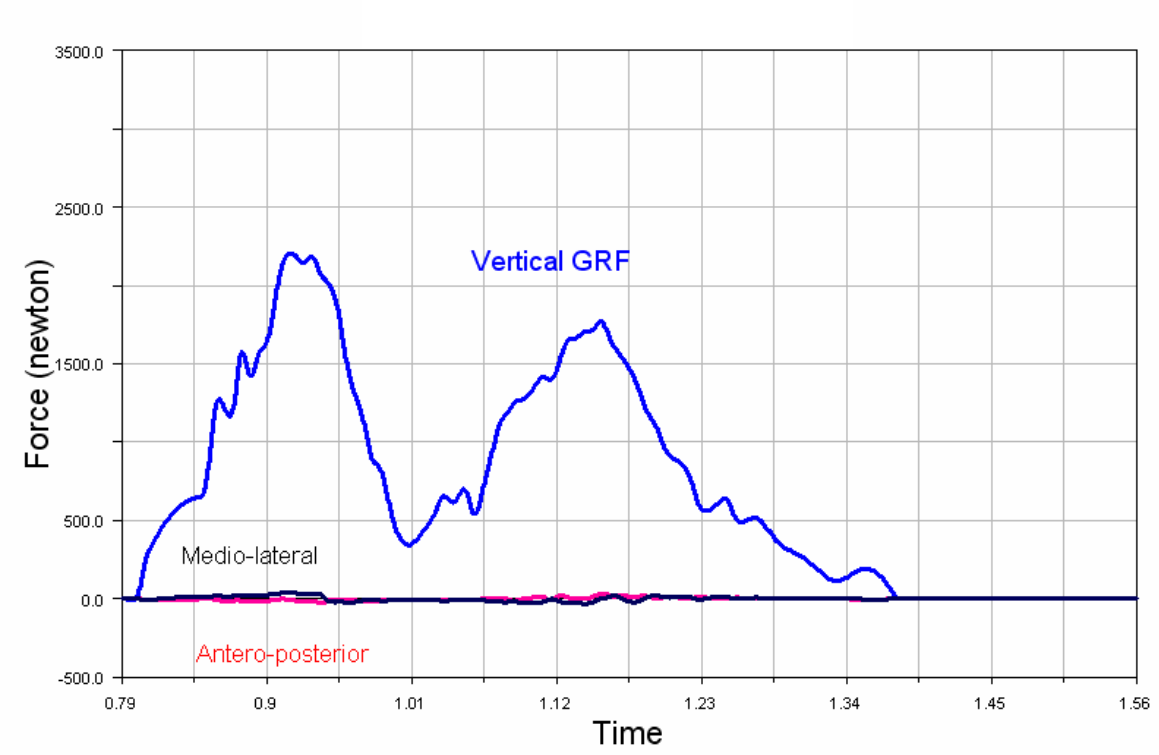

Figure 4.18 The GRF for the model with no aACL in the present study.

The peaks of the GRF were found as 2201N, 1771N for the first and the second peak. respectively.

The peak values of the vertical GRF decreased as mentioned in the literature for the model with no aACL compared to the intact knee model [61] (Figure 2.31).

The anterior translation and external rotations of the tibia at the end of the swing phase were compared for two models (with and without aACL). The anterior tibial translation was -5.5mm and 5.13mm (The difference was 10.83 mm) for the intact and no-aACL model at terminal swing period of gait respectively (Figure 4.20 and 4.21). The findings revealed that, in no aACL model, the tibia translated anteriorly more than in the intact knee model. The external rotation was 22° and 15.67° for the intact and no-aACL model at swing phase.

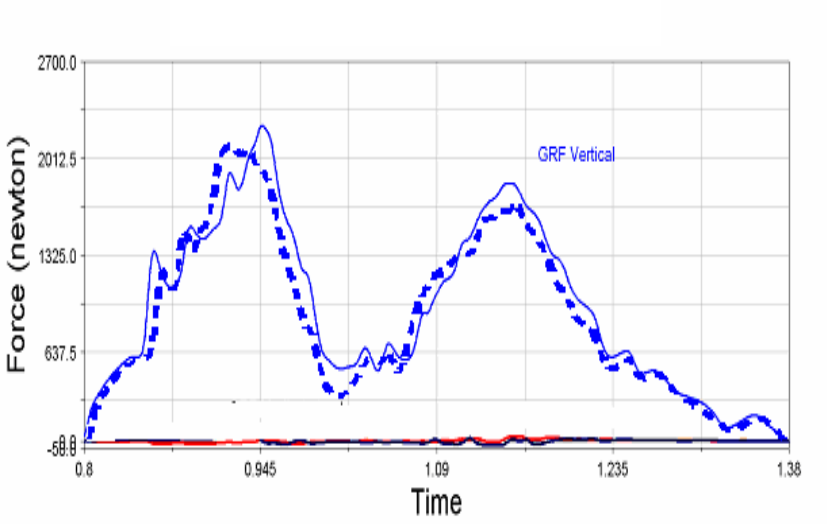

Figure 4.19 The comparison of the knee model with aACL (solid line) and without aACL (dashed line) in the present study.

The findings about the tibial rotation show that in no-aACL model, tibial external rotation was less than intact knee model at the end of the swing phase of gait cycle. The tibial translation and rotation results were not in agreement with the literature [61].

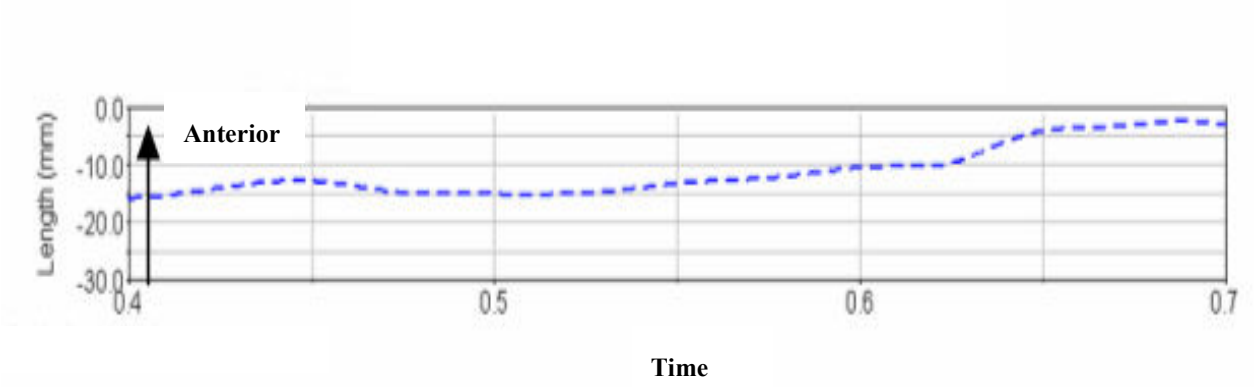

Figure 4.20 Tibial translation relative to the femur during swing phase of gait for the intact knee model in the present study.

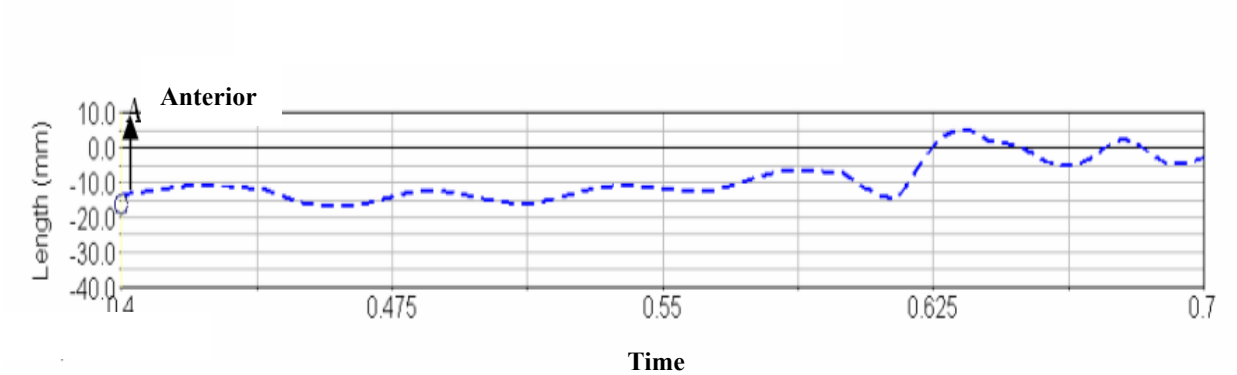

Figure 4.21 Tibial translation relative to the femur (dashed line) and tibial internal/external rotation during swing phase of gait for the model with no aACL in the present study.

5. DISCUSSION AND CONCLUSION

The hypothesis that the anterior portions of ACL (aACL) and PCL (aPCL) and anterior (aMCL)-medial (dMCL) fascicles of MCL primarily guide the passive knee flexion movement was tested. The tibiofemoral joint was represented as a three-dimensional dynamic anatomical model [10] and the results were compared with constraint based model and the findings from literature. The patello-tibio-femoral model was also created and the translations and rotations of the patella during active knee extension was analyzed and compared with the literature [49, 72, 75]. The present model was integrated successfully in to the full body model to simulate ACL deficient gait.

We argue that ligaments not only define the dynamics and kinematics of the knee motion, but also either they shape the bone structures or comply with these shapes to act together as the constraints of the joint motion.

The alignments of the ligaments, the geometries and the mechanical properties of the joint structures are changed in surgical procedures [24]. For instance the original insertion points of the ACL will change when it is replaced with a graft.

Different from the earlier studies no underlying shape was assumed for the femoral condyles in this study. We argued the lengths of inextensible ligament bundles ACL, PCL, MCL and their contact points must be in agreement with the femur shape. To achieve this, the ligament bundles were initially replaced by a set of rods connecting femur and tibia through ball joints during the contact point trajectory generation. The translational motions of the multiple contact points for each condyle were calculated at every increment of the flexion angle to constitute medial and lateral femoral condyle geometry. The rods that were extended to represent the fascicles of the ligaments were then removed with string like structures representing the ligaments. This approach allowed us to produce femur shapes and ligament attachments that constraint the knee motion, but did not contradict with isometric ligaments. With this approach we aim to enable analyzes of deviations from normal passive knee flexion

as a result of changes in the ligament lengths and their attachment points, which has been reported as a problem in the literature [3, 10, 63]. We expected a more accurate simulation of abnormalities due to the representation of several contact points, irregularly shape femoral condyle in the present model. However, before studying the abnormalities we had to demonstrate the capability of simulating normal passive knee flexion. For this purpose the motions were compared by analyzing peak tibial internal rotation, tibial translation, and contact forces of medial and lateral compartments.

We have found the peak rotation during the knee flexion as 24°. The rotational and translational motion of the tibia were compared with the reference model (Abdel-rahman and Hefzy [1]) and with the literature [10, 7, 66, 74]. The maximum internal rotation for the constraint based model was found as slightly lower than spherical model. Even though the peak internal rotation was in the normal range showed in the literature [73, 76], it was observed higher than some previous studies [77, 65, 74, 78]. Peak rotation during the knee flexion has been reported in a wide range [8.5° (Markolf *et al*. [77]), 10° (Shoemaker *et al*. [78]), 14.5° (Biden *et al*. [79]), 20° (Patrick F.D.P [74]), and 37° (Trent *et al*. [76]), Wilson *et al*.[73]]. The large variation is likely due to different test rigs, different conventions for representing knee rotations (Woltring [80]) and different definitions of coordinate systems (Blankevoort *et al*., 1996).

The tibial adduction in Constraint Based Model is relatively flat with a maximum reaching to 3.2° around 90° flexion, is also anatomically in normal range. The maximum abduction/adduction varies from 9° adduction to 9° abduction for an intact knee in the literature [73].

The posterior shift of the reference point, distal attachment of posterior bundle of ACL, during flexion was 34.4 mm which was the same value for spherical model as well. Even though the proximal displacement of the tibia was perfectly predicted, it was slightly higher than the proximal value described in Wilson *et al*. [73] (34 mm). However it was within the normal range revealed in Moglo and Shirazi –Adl [49] (~39 mm).

The proximal shift was 8.7 mm for constraint based model which was in the normal range according to the literature [7]. The maximum proximal displacement was 2 mm lesser

than the Spherical Model, however, it was in the normal limits defined as 6-24 mm in Wilson *et al*. [7], and ~9 mm in Moglo and Shirazi –Adl. [49].

The maximum medial shift was 4.6 mm which was in the normal range described in the literature (2-9 mm medially) [73]. The medial displacement was slightly lower than spherical model. Although the existence some small differences between the two models, the constrained based model behaved within the normal range during the passive tibio-femoral flexion.

As alternative configuration; the posterior portion of ACL (pACL) could be added to the model as another constraint. The relative length characteristic of pACL seemed to be another appropriate bundle for our aim which does not elongate much during flexion [13]. However this bundle had the highest relative length range between the selected bundle which was close the 0.9 according to Crowninshield *et al.* [13]. The simulation, with rigid pACL bundle link, stuck before 90° knee flexion. So that the most suspended of nonisometric bundle, pACL, was removed from the system then the simulation completed without any problem. The aPCL, aACL, aMCL, dMCL configuration resembled the rotation and translation characteristics of the natural knee.

Wilson *et al*. [73], Rovick *et al*. [14] revealed that the other bundle which has a similar isometric fascicle character is posterior bundle of PCL (pPCL). However the relative length of pPCL was very high (0.8) in Crowninshield *et al.*'s [13] work. So that it was not included in to model as another constraint. Addition of pPCL bundle might give another configuration to predict the passive knee motion for the future work.

In this study instead of using spherical shapes or mechanical joints, we proposed to use a constraint formed femur shape and a number of ligaments to simulate the knee motion during flexion. We could illustrate that the proposed knee model resembles not only the well-accepted knee models, but also anatomical findings based on cadaver studies. With this study we intend to get one step closer to understand the effects of surgical alterations in a virtual environment, by actually modifying anatomically meaningful parameters, such as the lengths of the ligaments, extension or removal of bony tissue. Changes in the knee anatomy, due to various external effects ligament rupture caused by an injury or other diseases, alter the

lengths and locations of the related ligaments and may demolish natural constraints and force behavior of the articular structures leading in to unnatural states and may cause pain, discomfort and unnatural gait patterns. With the proposed study, we aim to imitate similar changes in our model with one to one correspondence with the anatomy for the motion under the study.

Neglecting frictional forces between tibia and femur because of the extremely low coefficient of friction in synovia [10, 3] was a limitation of the model. Lack of meniscus and joint capsules because of their complex structures [63] was also a limitation. The MCL was modeled as a straight-line segment connecting to the femoral and the tibial attachments, while the natural MCL wraps around the tibial plateau [63]. The MCL ligament fascicle might be anisometric because wrapping point on the tibial condyle changes during flexion [7].

Although the natural MCL was modeled as a straight-line segment connecting to the femoral and the tibial attachments, it is in effect not isometric because the wrapping (contact) point on the tibial condyle changes during flexion [7]. To cope with the bending of MCL during knee flexion, the isometric fascicles can be segmented.

Patella-tibio-femoral joint motion was also modeled successfully to simulate the knee extension exercise under moderate level quadriceps contraction (400N) and anterior drawer tests [11, 72, 75, 81, 82].

Initial patellar flexion was 63° which was so close to Caruntu *et al.*'s study 65° [11]. Although we assumed that the sulcus angle is constant (146°), the patellar displacements and the rotation (patellar rotation, tilt and flexion) were in agreement with the literature [11, 72, 75]. The excursion of the sulcus angle for an individual adult cadaver is revealed as around 5° which is a quite constant and negligible value [69].

We assumed that height of the medial and lateral condyles are equal (Figure 3.10), although lateral height is longer than medial condyle around 1.1 mm [69]. We neglected only 1.1mm differences between the condylar heights for analyzing the ACL deficient gait but it should be considered if the one focuses on medio-lateral stability of the patella or to analyze the patellar subluxation in different knee flexion angle.

During the simulation of the knee extension exercise the quadriceps was loaded by

considering the force-angle description of the literature [11]. To represent the quadriceps force, 7 sample points of Caruntu *et al.*'s force-angle graph (Figure 3.15) was deployed by using 6th order curve fit of Matlab tool. The reason of using curve fitting method was the absence of more detailed data in the literature.

The quadriceps and patellar tendon was represented by 3 spring dampers in the present study. We defined the attachment points of these tendons as in Hirokowa's work [72]. Hirokowa attached the tendons by using oval spheres which was represented the anatomically specific locations. In Hirokowa's study, the oval spheres trisected parallel to the long axis of the tibia and femur. Therefore 3 points can be easily used for the attachments points of tendons. The patellar and quadriceps tendons are strap shaped structures [72], so that the 3 spring damper elements description was a better representation for tendons then the single element.

We used LIFEMOD software to place Harikova's oval spheres to the specific areas of the segments. To locate Harikova's spheres, we created a lower leg model which has the same physical properties as height, weight, age and sex by using the "segment creation tool" of lifemod. Then the oval spheres were easily placed on to the bone segments with the visual guidance the software.

The contact forces were lower than the literature [11] on the medial and the lateral compartments of tibial plateau during the simulation of knee extension exercise. Caruntu *et al.* created the patello-tibio-femoral model based on Abdel-Rahman and Hefzy's tibiofemoral model. The contact forces were found smaller in our tibiofemoral model than Abdel-Rahman and Hefzy's work [10]. Therefore it is natural that the contact forces of the medio-lateral compartments of the tibial plateau are lower than Caruntu *et al.*'s work. Although there is a difference of contact forces between our model and the reference model (Spherical Based Model) [10], the natural kinematics were obtained in the Constraint based model.

The relationship of the contact force between medial and the lateral compartments during knee extension was also agreed with the literature [11]. The medial contact force was larger then the lateral side and the medial contact force doubled relative to the lateral side as revealed in the literature [11].

The ACL is the primary restraint to anterior draw in the intact knee. Anterior laxity increases at all flexion angles when the ACL is removed. The calculations were consistent with published in vitro data which show that anterior laxity was greatest at 30 ° of flexion in the intact and ACL-deficient knee [81] (Figure 4.12 and 4.13). This was also consistent with the clinical observation that loss of the ACL is more readily detected by the Lachman Test which is performed at 20 °- 30° of flexion than the Drawer Test which is done at 90 °. Maximum values of anterior tibial translation were around 3 mm for the intact knee and increase by as much as 7 mm when the ACL is removed (Figure 4.12 and 4.13).

The rotational anterior drawer test was also agreed with the literature [17]. When the tibia is rotated internally the tension on the PCL becomes higher and the anterior translation decreases at the 90° knee flexion. Contrary, when the tibia is rotated externally the PCL slacks and tibial anterior translation increases for the patients with ACL injury. When the tibia externally rotated, it translated anteriorly 2.1 mm longer than the anterior drawer test in the ACL free model. The anterior translation decreased around 6 mm relative to the externally rotated tibia in no-ACL knee. The rotational force was chosen arbitrary because of the absence of the literature about the force that the examiners are applied to the patient's tibia in the clinic. We did not rotate the tibia manually not to lose the natural behavior of axial tibial rotation. We applied the anterior force, after the rotational force succeeds to rotate the tibia as much as it could (around 30°rotation at 90° knee flexion).

The full body model was created by the guidance of LIFEMOD manual [62]. The normal human model was constructed by selecting the height as 1800mm, the weight as 80kg and the age as 360 months (18 years old) in the "Create Base Set" tool. This tool constructs the segments (bones), joints (revolute joints), soft tissues (Mucles; as single force line elements) and positions by scaling them about the physical conditions that the user selected. The anatomic locations of the segments, the locations of the revolute joints, the range of motions of each joint and the attachment points of the muscles were defined automatically by the LIFEMOD software. The software is used very commonly to analyze human motion and the validation tests were performed by the software builders [83]. Unfortunately the full body model does not include the ligaments and tendons.

The gait analysis data recorded from normal person was obtained from the LIFEMOD

tutorial [62] which is used for demonstration of normal walking. The data has imported to the full body model to simulate normal walking. The walking pattern was checked and noticed that the knee and ankle excursions in suggital plane was little lower than normal but it can be interpreted as the lower limit of the normal excursion.

During the inverse dynamic simulation (walking by the guidance of data from gait analysis laboratory), the soft tissue elements (muscles) were trained by recording the length changes and external forces applied to the segments that they connected. During the forward dynamic simulation of walking (Muscle driven simulation of walking), the soft tissue elements were applied what they recorded during inverse dynamic simulation.

The muscles are characterized as single line force elements which are equal to resultant forces of the musculotendon structures in the software. Therefore the muscle in the software only represents the line of action of the related muscle in the real human body. The via points and the wrapping around the bones actions of the tendons were neglected by the software.

The importation of our model in to the full body model was performed without any difficulty. We created the full body model with the same properties such as weight, height, age and sex as we built the tibiofemoral model. Because of the femoral and the tibial properties were the same, we could easily import our patello-tibio-femoral model in the full body and replaced the right knee joint of LIFEMOD with our model. The right knee has now the sliding and rolling motions.

The vertical component of GRF of the muscle driven forward simulation of walking was compared with the inverse dynamic simulation results and the literature [59]. It was found that the second peak in the full body model (the model has revolute joints only) was quite lower than the first peak. The second peak of GRF was lower than dynamic simulation also. The revolute joint representation seemed affecting the force that the body applies to the ground.

The vertical component of the GRF for the right side was found quite normal but the peak amplitudes were higher then the literature [59]. The definition of the contact force between the ground and the foot segment of the model might have played in important role. For both simulations the first peaks of the GRF were larger then %130 of the body weight.

The LIFEMOD software assigns a trajectory marker, located at the center of mass point of pelvis, to prevent the full body model falls during the inverse dynamic simulation. The force is defined between the trajectory marker and its trace by the software like a weak rubber. The marker records its trajectory during the inverse dynamic simulation and applies the weak resistance force if there is a difference with large magnitudes between the inverse and forward dynamic simulations. The location of the ground may be different in gait analysis laboratory that the data is obtained originally and in our simulation. The trajectory marker may have applied a force to bring the body in to original ground level. This may affect results of the simulations but the conditions were the same during every simulation so that the comparison results were still reliable.

The muscle driven forward dynamic walking simulation was repeated by removing the anterior portion of anterior cruciate ligaments to simulate the ACL deficient walking. The tibial translations and rotations and the vertical components of GRF were compared the data available in the literature [60, 61]. The vertical GRF data was closely agreed with the literature (Figure 4.18 and 2.31) [61]. The first and the second peaks of the vertical GRF were decreased as revealed in Bulghari *et al.*'s work. The similar changes was occurred in the simulation with no ACL (The both parts of the ACL were removed). The second peak of the vertical GRF was reduced significantly.

Although the expected changes were achieved for the GRF, the tibial rotations and translations seemed as disagreed with the Andriacchi's work. Andriacchi revealed that the anterior translation and external rotation of the tibia were reduced at the end of the swing phase of gait for the patients with ACL deficiency [60]. However Andriacchi emphasized the importance of the compensations of muscle firing also. The reason of the opposite findings with literature may be cause of the normal firing representation of the muscles during the no ACL deficient patient's simulation. The muscles acted as they trained during the inverse dynamic simulation which was normal. Therefore the compensatory muscle firing was not represented in the simulations. The experimental studies which shows the tibial rotational and translations for the patients with ACL deficiency without compensatory muscle firing was absence.

Actually the anterior drawer test simulation results supported our dynamics findings. The anterior drawer test showed that, increased anterior tibial translation was expected for the patients with no compensatory muscle contractions. The rotational anterior drawer test was also demonstrated that internal rotation of the tibia reduces the anterior displacement of the tibia which supports the findings of our ACL deficiency simulation. The tibia rotates externally and the patients may want to reduce the external rotation and the anterior displacement of the tibia at the end of the swing by increased muscle contarctios. It was proven that the increased firing of quadriceps muscle was chosen as the adaptation for the patient with ACL deficiency to decreases the anterior translation and internally rotation of the tibia. Andriacchi emphasised that, the correlation between offsets from the AP and IE positions with flexion moment (balanced by a net quadriceps moment), indicated that adaptations to the patterns of muscle firing could compensate for the loss of the ACL. The offset from normal of the tibiofemoral position increased with an increase in the magnitude of the flexion moment. Thus by adapting a gait pattern with a lower flexion moment during weight acceptance (Mflex) the ACL deficient patient can achieve a more normal tibiofemoral position during walking [61]. Our model may demonstrate the real behavior of the knee without compensatory changes for the patient with ACL injury.

This study demonstrated that the specific bundles of the ligaments and articular surfaces guide the passive knee flexion motion. The patello-tibio-femoral model can be used to analyze static and dynamic behaviors of the knee joint for patients with ACL injuries.

The aACL, aPCL, aMCL, dMCL bundles and the medial-lateral articular surfaces might play a primary role to give the nature of distal femoral sphere like shape. The clinical significance of the work is that anything which changes the lengths and locations of the related ligaments may demolish natural constraints and force the articular structures in to unnatural shape which may make the knee to change contact behavior on the articular surface and may cause pain. The surgical treatments must be accurate enough to provide both ligament bundle geometries and articular geometry to achieve a problem free knee kinematics after the surgery.

6. REFERENCES

1. Yu, C.H., Walker, P.S., Dewar E.M., 2001, The effect of design variables of condylar total knees on the joint forces in step climbing based on a computer model. Journal of Biomechanics 34,1011- 1021.
2. Li, G., DeFrate, L.E., Park, S.E., Gill, T.J., Rubash, H.E., 2005. In vivo articular cartilage contact kinematics of the knee: an investigation using dual-orthogonal fluoroscopy and magnetic resonance image-based computer models. American Journal of Sports Medicine 33, 102-7.
3. Freeman, M.A.R., Pinskerava, V., 2005. The movement of the normal tibio-femoral joint. Journal of Biomechanics 38(2), 197-208.
4. Wismans, J., Veldpaus, F., Jansen, J.Huson, A.,Strulen, P.,1980. A three-dimensional mathematical model of the knee joint. Journal of Biomechanics 13, 677-85.
5. Li, G., Suggs, J., Hanson, G., Durbhakula, S., Johnson, T., Freiberg, A., 2006. Three-dimensional tibio-femoral articular contact kinematics of a cruciate-retaining total knee arthroplasty. Journal of Bone and Joint Surgery (Am) 88: 395-402.
6. Feikes, J.D., O'Connor J.J., Zavatsky, A.B., 2003. A constrint-based approach to modeling the mobility of the human knee joint. Journal of Biomechanics 36, 125-129.
7. Wilson, D.R., Feikes, J., O'Connor, J.J., 1998. Ligaments and articular surfaces guide passive knee flexion. Journal of Biomechanics 31, 1127-1136.
8. Meyer, H., 1853. Die mechanik des kniegelinks. Archiv fur Anatomie Physiologie 497-547.
9. Weber, W.E., Weber, E.F.W., 1836. Mechanik der menschlichen Gehwerkzeuge. in der Dietrichschen Buchhandlung, Gottingen.
10. Abdel-Rahman, E.M., Hefzy, M.S., 1998. Three-dimensional dynamic behavior of the human knee joint under impact loading. Journal of Biomechanics 20, 276-90.
11. Caruntu, D.I. Hefzy M.S., 2004. 3-D anatomically dynamic modeling of the human knee to include tibio-femoral and patello-femoral joints. Journal of Biomechanical Engineering 126 (1), 44-53.
12. Amis, A.A., Zavras, T.D., 1995 Isometry and graft placement during anterior cruciate ligament reconstruction. Knee 2 (1), 5-17.
13. Crowninshield, R. Pope, H., Johnson, R.J., 1976. An analytical model of the knee. Journal of Biomechanics 9, 397- 405.
14. Rovick, J.S., Reuben, J.D., Schrager, R.J., Walker, P.S., 1991. Relation between knee motion and ligament length patterns. Clinical Biomechanics 6 (4), 213-220.
15. Randale Sechrest, 2006. Body1 Inc., Cambridge MA, Available in www.knee1.com/reference/previewcategory.cfm/11.
16. Stuart Schneller, 2001. Knee anatomy, Montana Spine & Pain Center, Missoula MT, Available at http://www.eorthopod.com.

17. Neumann, D.A., 2002. Knee. In Neumann, D.A.,. Kinesiology of the musculoskeletal systems. Mosby Inc., St. Louis, 1st ed., page: 434-476.

18. Küçük, H., 1995. A two dimensional dynamic model simulation of human knee joint. M.Sc. thesis., Boğaziçi University.

19. Hefzy, M., S., Grood, E., S., 1988. Review of Knee Models, Appl Mech Rev. 41(1), 1-13.

20. Huson, A., 1974. Biomechanische probleme des kniegelenks, Orthopaede, 3, 119- 126.

21. Bandi, W., 1972. Chondromalacia patellae und femoro-patellare artlırose, Helv Chirc Acta, Suppl. 11, 1-70.

22. Chand, R., Haug, E., Rim, K., 1976. Stress in the human knee joint, J Biomech, 9, 417-422.

23. Hight, T. K, Piziali, R. L., and Nagel, D. A., 1993. A Dynamic, Nonlinear Finite-Element Model of a Human Leg, J Biomechanical Engineering, 101(6),176-184.

24. Moffat, C. A, Harris, E. H., and Haslam, E. T., 1969. An Experimental and Analytical Study of the Dynamic Properties of the Human Leg, J Biomech, 2, 373-387.

25. Pope, M.H., Crowninshield, R., Jhonson, R., 1976. The static and dynamic behavior of the human knee in vivo, J Biomech, 9, 449-452.

26. Freudenstein, F., and Woo, S.L, 1969. Kinematies of the Human Knee Joint. Bull Math Biophys. 31.

27. Blacharski, P.A., Somerset, J. H, and Murray, D.G., 1975. A Three-Dimensional Study of the Kinematics of the Human Knee, J Biomech, 8, 375-384.

28. Van Dijk, R, Huiskes, R, and Selvik, G., 1979. Roentgen stereophotogrammetric. methods for the evaluation of the three dimensional kinematic behavior and cruciate ligament length patterns of the human knee joint. J Biomech. 8, 727-31.

29. Reilly, D.T., and Martens, M., 1972. Experimental analysis of the quadriceps muscle force and patello-femoral joint reaction, force for various activities, Acta Orthoped Scand., 43, 126-137.

30. Morrison, J.B., 1970. The mechanics of the knee joint in relation to normal walking. J Biomech, 3, 51-61.

31. Edwards, R G, Lafferty, J F, and Lange, K O, 1970. Ligament strain in the human knee joint, J Basic Eng. 92,131-136. 8.

32. Blankevoort, L., Huiskes, R., De Lange, A., 1991. Recruitment of the knee joint ligaments. ASME Journal of Biomechanical Engineering 113(1), 94-103.

33. Blankevoort, L., Huiskes, R., 1991. Ligament-bone interaction in a three- dimensional model of the knee, J Biomechanical Engineering, 113, 263-269.

34. Minns, R.J., 1981. Forces at the knee joint: Anatomical considerations, J Biomech. 14, 633-43.

35. Maquet, P.G., Pelzer, G.A, 1977. Evolution of the maximum stress in osteoarthritis of the knee. J Biomech. 16 (1), 107-117.

36. Andriacchi, T.P, Mikosz, R.P, Hampton, S.J., Galante, J.O., 1983. Model studies of the stiffness characteristics of the human knee joint, J Biomech, 16(1), 23-9.

37. Moeinzadeh, M.H., Engin, A.E., Akkas, N., 1983. Two-dimensional dynamic of human knee joint. J Biomech.16 (4), 253-64.

38. Wongchaisuwat, C., Hemami, H., and Buchner, H.J., 1984. Control of sliding and rolling at natural joints, J Biomechanical Engineering, 106, 368-375.

39. Engin, A.E., Tümer, S.T., 1993. Improved dynamic model of the human knee joint and its response to impact loading on the lower leg, J Biomechanical Engineering, 115, 137-143.

40. Abdel-Rahman, E., Hefzy, M.S., 1993. A Two-dimensional dynamic anatomical model of the human knee joint, J Biomechanical Engineering, 115, 357-65.

41. Szaklar, O., Ahmed, A.M.,1987. A simple unconstrained dynamic knee simulator, J Biomechanical Engineering, 109, 247-251.

42. Li, G., Kanamori, A., Woo, Y., 1999. A validated three-dimensional computational model of a human knee joint, J. Biomech. Eng. 121, 657–662.

43. Van Eijden, T.M.G.J., Kouwenhoven, E., Verburg, J., Weijs, W.A., 1986. A mathematical model of the patello-femoral joint, J Biomech , 19(3), 219-29.

44. Hirokawa, S., 1991. Three-dimensional mathematical model analysis of the patello-femoral Joint, J Biomech., 24(8), 659-671.

45. Tümer, S.T., Engin, A.E., 1993. Three-body segment dynamic model of the human knee, J Biomechanical Engineering, 115, 350-356.

46. Pandy, M.G., Sasaki, K., Kim, S., 1997. A three-dimensional musculoskeletal model of the human knee joint. Part 1 theoretical construction, Comput. Methods Biomech. Biomed. Eng. 1, 87–108.

47. Pandy, M.G., Sasaki, K., Kim, S., 1998. A three-dimensional musculoskeletal model of the human knee joint. Part 2 analysis of ligament function, Comput. Methods Biomech. Biomed. Eng., 265–283.

48. P. Beillas, P., Papaioannou, G., Tashman, S., Yang, K.H., 2004. A new method to investigate in vivo knee behavior using a finite element model of the lower limb, J. Biomech., 37, 1019–1030.

49. Moglo, K.E, Shirazi-Adl, A., 2003. On the coupling between anterior and posterior cruciate ligaments, and knee joint response under anterior femoral drawer in flexion a finite element study, Clin. Biomech. 18, 751–759.

50. Winter, D. 2005, The biomechanics and motor control of human gait, Waterloo: University of Waterloo Press, 3rd ed., Canada,.

51. Gage, J. R., 2004. The Treatment of Gait Problems in Cerebral Palsy. London: Mac Keith Press, United Kingdom.

52. Zatsiorsky, V. M., 1998. Kinematics of Human Motion, Champaign: Human Kinetics Publishers, 1st ed., USA.

53. Zatsiorsky, V. M., 2002. Kinetics of Human Motion, Champaign: Human Kinetics Publishers, 1st ed., USA.

54. Kirtley, C. 1992. Gait Analysis: Normal and Pathological Function, London: Slack Incorporated, 1st ed., Elsevier, UK.

55. Saunders J.B., Inman, V.T., Eberhart H.D., 1953 The major determinants in normal and pathological gait. J Bone Joint Surg. 35A, 543-58.

56. Murrey M.M., Bernard A., Kory R.C., 1964. Walking Patterns of Normal Men. Journal of Bone and Joint Surgery 64(2), 335-60.

57. “Gait Abnormalities” , 2001. Orthoteers, the guiding light in orthopaedic education. Available at http://www.orthoteers.co.uk.

58. Kirtly C., 2007, CGA normative gait data base. Available at www.univie.ac.at/cga/data/index.html

59. Caldwell, G.E., Robertson, G.E., Whittlesey S.N., 2004.Forces and their measurements. In Robertson, G.E., Caldwell, G.E., Hamil, J., Kamen, G., Whittlesey S.N., Human Kinetics, pp:73-102.

60. Andriacchi, T. Dyby, C.O., 2005. Interactions between kinematics during walking for the normal and ACL deficient knee. J Biomech. 38, 293-298.

61. Bulgheroni, P., Bulgheroni, M. V., Andrini, L., Guffanti, P., Giughello, A., 1997. Gait patterns after anterior cruciate ligament reconstraction. Knee Surg, Sports Traumatol, Arthroscopy 5,14-21.

62. Biomechanics Research Group, Inc., Lifemod TM, 2005, available at: www.biomechanicsresearchgroup/Downloads/LM_Manual.pdf.

63. Blankevoort, L., Huiskes, R., 1996. Validation of a three-dimensional model of the knee. Journal of Biomechanics 29, 955-961.

64. Moglo, K.E., Shirazi-Adl, A., 2005. Cruciate coupling and screw home mechanism in passive knee joint during extension-flexion. Journal of Biomechanics 38 (5), 1075-83. 18.

65. Li, J., Wyss, U.P., Costigan, P.A., Deluzio, K.J., 1993. An integrated procedure to assess knee-joint kinematics and kinetics during gait using an optoelectronic system and standardized X-rays. Journal of Biomedical Engineering, 392–400.

66. Walker, P.S., 1988. Bearing surface design in total knee replacement. Engineering in Medicine 17, 149.

67. Goldstien, H., 1981.Classical Mechanics, Addison-Wesley Publishing Co., Reading Mass, 2nd. ed.

68. Grood E.S, Suntay WJ., 1983. A joint coordinate system for the clinical description of three dimensional motions: application to the knee. ASME Journal of Biomechanical Engineering 105, 136–44.

69. Shih, Y.F., Bull, AMJ., Amis, AA., 2004. The cartilaginous and geometry of the femoral trochlear groove. Knee Surgery, Sports Troumatology, Artroscopy 12, 300-306.

70. Poilvache,P.L., Insall, J.N., Scuderi, G.R., Rodrigez, D.E.F.,1996. Rotational landmarks and sizing of the distal femur in total knee arthrolpasty. Clin Orthop, V 331, 35-46.

71. Neyret, P., Robinson, A.H.N, Le Coultre, B., Lapra, C., Chambat, P. 2002. Patellar tendon legth- the factor in patellar instability?. The Knee 9, 3-6.

72. Hirokawa, S.,1991. Three-dimensional mathematical model analysis of the patellafemoral joint. Journal of Biomechanics 24, 8, 659-71.

73. Wilson, D. R., Feikes, J.D., Zavatsky, A.B., O’Connor J.J., 2000. The components of passive movement are coupled to flexion angle. Journal of Biomechanics 33, 465-73.

74. Patrick, F.D.P., 1989. Mechanics of the knee joint. D.Phil. Thesis, University of Oxford.

75. Chew, J.T.H, Strewart N.J., Hanssen A.D., Luo, P.Z., Rand J.A., An K.N., 1997. Differences in patellar tracking and knee kinematics among three different total knee designs. Clinical Orthopaedics and Related Research 345, 87-98.

76. Trent, P.S., Walker, P.S., Wolf, B., 1976. Ligament length patterns, strength and rotational axes of the knee joint. Clinical Orthopaedics 117, 263-270.

77. Markolf, K.L., Mensch, J.S., Amstutz, H.C., 1976. Stiffness and laxity of the knee the contributions of the supporting structures. A quantitative in-vitro study. Journal of Bone and Joint Surgery [American] 58-A, 583-593.

78. Shoemaker, S.C., Adams, D., Daniel, D.M., Woo, S.L-Y., 1993. Quadriceps/ anterior cruciate graft interaction: an in vitro study of joint kinematics and anterior cruciate ligament graft tension. Clinical Orthopaedics 294, 379-390.

79. Biden, E., O'Connor, J., Goodfellow, J., 1984. Tibial rotation in the cadaver knee. In: Transactions of the 30th Meeting of the Orthopaedic Research Society, 30.

80. Woltring, H.J., 1994. 3-D attitude representation of human joints: a standardization proposal. Journal of Biomechanics 13, 677-685.

81. Pandy, M.G., Shelburne, K.B. Theoretical analysis of ligament and extensor-mechanism function in the ACL-deficient knee. Clin Biomech.13(2), 98-111

82. Müller, W., 1988. The knee:form, fuction, and ligament reconstruction, Newyork, Springer-Verlog.

83. Publications of Biomechanics Research Group, Inc., Lifemod TM, 2005, available at: http://www.lifemodeler.com/.